INTERIM REPORT

Accession No. LTR 141-118

Contract Program or Project Title: LOFT PROGRAM

Subject of this Document: (Title) "Feasibility Transient Test of a Correlation Type Transit Time Flowmeter in the LTSF Blowdown Facility"

Type of Document: Experimental Data

Author(s): A. G. Baker

Date of Document: February 1980

Responsible NRC Individual and NRC Office or Division: G. D. McPherson

This document was prepared primarily for preliminary or internal use. It has not received full review and approval. Since there may be substantive changes, this document should not be considered final.

Prepared for
U.S. Nuclear Regulatory Commission
Washington, D.C. 20555

INTERIM REPORT

EG&G Idaho

INTEROFFICE CORRESPONDENCE

R-5416

date FEB 29 1980

to DISTRIBUTION

from LOFT CDCS, TAN 602, Ext. 6177 J K Hathaway

subject DOCUMENT TRANSMITTAL

The following documents released by LOFT CDCS, are hereby transmitted for your use and information:

DOCUMENT NO.	REV	CHG	DATE
LTR 141-118	Ø		2-26-80
"Feasibility Transient Test of a Correlation Type Transit Time Flowmeter in the LTSF Blowdown Facility" A. G. Baker			

REMARKS: The recommended work has been accomplished and is documented in LTR 141-119.

DISTRIBUTION

M. Akimoto - 2
W. Amidei w/o Att.
B. O. Anderson
E. C. Anderson w/o Att.
J. G. Arendts
B. L. Chamberlain w/o Att.
G. A. Dinneen
D. B. Engelman
B. L. Freed-Orig.+7
R. T. French
R. C. Gottula
R. C. Guenzler
J. C. Haire
J. Hansen
S. W. Hills
G. L. Hunt w/o Att.
F. K. Hyer w/o Att.
N. C. Kaufman w/o Att.
S. T. Kelppe
J. L. Liebenthal
A. S. Lockhart
J. H. Linebarger
D. W. Marshall w/o Att.
S. Matovich
G. D. McPherson
J. C. Morrow
S. A. Naff
N. E. Pace w/o Att.
T. F. Pointer
G. Rieger
P. Schally
D. G. Satterwhite w/o Att.
W. A. Spencer
J. C. Stachew w/o Att.
K. C. Sumpter
R. E. Tiller
S. R. Wagoner w/o Att.
G. Weimann
L. Winters
B. J. Yohn
A. G. Baker
R. E. Ford RC
D. J. Hanson
J. R. Fincke
G. D. Lassahn
D. B. Jarrell

FORM EG&G-954
(Rev. 2-77)

EG&G Idaho, Inc.

(LTR)

Report No. 141-118

Date: February 26, 1980

RELEASED BY LOFT CDCS

USNRC-P-394

INTERNAL TECHNICAL REPORT

Title: FEASIBILITY TRANSIENT TEST OF A CORRELATION TYPE TRANSIT TIME FLOWMETER IN THE LTSF BLOWDOWN FACILITY

Organization: ADVANCED INSTRUMENTATION

Author: A. G. Baker

Checked By: R. E. Ford/D. J. Hanson

Approved By: S. A. Naff

[redacted]

EG&G Idaho, Inc.

LOFT TECHNICAL REPORT
LOFT PROGRAM

FORM EG&G-229
(Rev. 06-79)

TITLE	REPORT NO.
Feasibility Transient Test of a Correlation Type Transit Time Flowmeter in the LTSF Blowdown Facility	LTR 141-118

AUTHOR	Charge Number
A. G. Baker per for A. L. Baker	
PERFORMING ORGANIZATION	DATE RELEASED BY LOFT CDCS
LOFT APPROVAL R. T. Ford S. A. Raff	February 26, 1980

PSE LEMB Mgr. LEPD Mgr.

DISPOSITION OF RECOMMENDATIONS

The recommended work has been accomplished and is documented in LTR 141-119.

LTR 141-118

FEASIBILITY TRANSIENT TEST OF A CORRELATION TYPE TRANSIT TIME FLOWMETER IN THE LTSF BLOWDOWN FACILITY

BY

ALAN G. BAKER

February 1980

THIS REPORT IS INTENDED TO BE
PUBLISHED AS LTR-141-118

TABLE OF CONTENTS

TABLE OF CONTENTS (Cont.)

TABLE OF CONTENTS (Cont.)

ACKNOWLEDGEMENTS

M. W. Dacus, V. A. Deason, I. Marot, and J. L. Morrison, Jr. made significant contributions to the design and construction of the hardware necessary for this test. C. L. Jeffery was indispensible in the performance of this test and recording of the data. Thanks also are due to many Instrumentation Division personnel and technicians for their assembly of apparatus. Finally, many thanks to Gordon D. Lassahn for his many enlightening discussions and kind assistance on the entire project and on the data analysis and interpretation.

This work was performed by EG&G Idaho, Inc. at the Idaho National Engineering Laboratory on behalf of the Loss of Fluid Test (LOFT) Program.

ABSTRACT

A feasibility test was made in September 1977 to determine the suitability of various transducer types as sensors for a cross-correlation type transit time flowmeter. The sensor types tested were single beam gamma densitometers, conductivity probes and passive thermocouples. Three forms of signal conditioning were applied to the thermocouple signals: bandpass amplification, frequency compensation and signal compression. The gamma densitometer was the most successful, the conductivity probe less successful and the thermocouple least successful. Further work is recommended.

FIGURE LISTING

FIGURE LISTING (Contd)

FIGURE LISTING (Contd)

TABLE LISTING

FEASIBILITY TRANSIENT TEST OF A CORRELATION TYPE TRANSIT TIME FLOWMETER IN THE LTSF BLOWDOWN FACILITY

1. INTRODUCTION

Transit time flowmeters are being considered as an alternative to turbine flowmeters for velocity measurement in LOFT blowdown experiments. A transit time flowmeter (TTF) consists of two basic parts: a pair of sensors and a data analysis system. The sensors are located one downstream from the other. They sense naturally occurring random fluctuations in some fluid property, such as temperature or density, for which the fluctuations move with the fluid rather than propagate through the fluid. The data analysis system is some device, traditionally a correlator, that determines the relative time delay between the signals from the two sensors. A correlator, for example, generates a curve of correlation magnitude versus delay time. This curve hopefully has one dominant peak indicative of an average or dominant delay time between the two signals. This delay time is interpreted as the (average or dominant) transit time of the fluid between the two sensors, and the velocity is trivially obtained by dividing the spacing between the two sensors by this transit time.

There are several potential advantages of transit time flowmeters over turbine flowmeters:

1. TTFs may disturb the fluid flow much less than turbine flowmeters, depending on the size and type of sensor used.

2. The hardware inside the pipe is usually much simpler and more reliable than a turbine, depending on the type of sensor used.

3. In principle, no calibration is required with a TTF. Even if calibration is necessary, the calibration problems are much less severe than with turbines.

4. In principle, a TTF can indicate the distribution of flow velocities present in the measurement region. In two-phase flow with slip for example, an ideal TTF could give separate indications of the gas velocity, the liquid velocity, and the interface velocity. (In fact, this idea is far removed from the present state-of-the-art.)

Transit time flowmeters offer a potential for either very localized or global velocity measurements, including the potential for determining both the average velocity and velocity probability density function.

2. TRANSIT TIME FLOWMETER DESCRIPTION

2.1 Sensors and Electronics

The sensor types used in this feasibility test were single-beam gamma densitometers, passive thermocouples, conductivity probes and drag screens. Two sensors of each type were employed in cross-correlation to determine the transit time.

By its design a TTF must be sensitive to changes or fluctuations in a fluid property. Therefore, the 0 Hz (dc) level signal is considered to be relatively unimportant and, hence, in most cases was discarded. Since the fluctuation signals may be expected to be of a lesser magnitude than the change in the dc level over the course of a blowdown experiment, discarding the dc level permited additional amplification of that signal portion of particular interest to a TTF measurement.

2.1.1 Single-Beam Gamma Densitometer

2.1.1.1 Sensor

Each single-beam gamma densitometer sensor consisted of a gamma source, a lead collimator and a detector cask. The source cask, collimator and detector cask were bolted to a 1.3 m long piece of 4-in wide channel iron which was welded into the gamma densitometer transducer support

frame. The transducer support frame (see Figure 1) held the densitometer beams fixed at an angle of 45 degrees to the vertical and was adjustable for interbeam separations between 270 and 1200 mm.

The two sources used were each 10 Ci Cs-137 sources, registered as S-59 in cask T-5063 and S-64 in cask T-5068. The cylindrical source casks were made of lead 20 cm in diameter by 27 cm high and had a 4.1 cm diameter shuttered beam port. The collimators were made of lead 88.9 mm thick with 9.5 mm diameter collimation holes drilled into removable inserts as shown in Figure 2. The detector casks were a stainless steel shell containing additional lead (about 5.0 cm thick on the face and 4.6 cm thick cylindrically around) for further shielding from stray and natural background radiation.

2.1.1.2 Electronics

The scintillation detectors were commercially available Harshaw 4S8/1.5 NaI(Tl) detectors. The NaI crystals are 1-in diameter by 1.5-in long integrally mounted on RCA 6199 photomultiplier tubes. The tube socket was modified as shown in Figure 3 to use only eight of the ten available tube dynodes and to operate the tube in the current mode. In this mode the anode is grounded and the cathode and, hence, also the tube unit case are floated at the negative high voltage potential, thus requiring additional insulation between the tube unit case and any nearby metal pieces or conductors and also requiring extra caution on the part of personnel. The extra insulation was 16 mm of flexible polystyrene foam around the tube sides and 29 mm at the tube face between the tube and the detector cask.

The signal conditioning and filtering electronics for each gamma densitometer channel are shown schematically in Figure 4. The schematic of the shop-built preamplifier are shown in Figure 5. The preamplifier consists of a current-to-voltage converter followed by an amplification stage. The entire unit was designed to provide a 1 volt output for a 1 nanoampere current input with a frequency response from 0 Hz (dc) to 74 Hz. Each unit was provided with its own power supply.

The preamplifier was connected to the photomultiplier tube by means of a 32-in RG174/U short coaxial cable. The output of the preamplifier was connected to two parallel channels: one in which the dc level was discarded (called the TTF channel) and the other in which the dc level was retained (called the density channel). The latter channels was deemed advisable so that some estimate of the fluid density in the pipe could be made since the test facilities three-beam gamma densitometer would not be available for the TTF tests.

For the TTF channels the output of the preamplifier was connected via a 25 m coaxial cable to the input of a Princeton Applied Research Corp. (PAR) Model 114/116 signal conditioning amplifier. This amplifier was set at a gain of 10 and a band-pass from 0.3 to 1000 Hz. The output of the PAR amplifier was connected to the appropriate tape recorder channel.

The frequency response of the two TTF channels was verified by a white noise signal injection and analysis to have a flat frequency response up to the 73 Hz break-point frequency and to have a single-pole roll-off from thereon.

For the density channels the signal from the preamplifier was connected to a Krohn-Hite Active (8-Pole) Filter which was set at maximum flat in the low pass mode with a -3db roll-off frequency of 200 Hz. The output of the Krohn-Hite (8-Pole) filter was connected to a unity gain amplifier for zero-level control and adjustment prior to each test. The output of the zero-level control amplifier was connected to the appropriate tape recorder channel.

For the TTF tests there were two gamma densitometer beams and, hence, there were four tape channels of gamma densitometer signals recorded.

2.1.2 Thermocouple

2.1.2.1 Sensor

The sensors in the thermocouple (TC) TTF tests were chromel/alumel, magnesium oxide insulated, stainless steel sheathed TCs. The TCs had a nominal outside diameter of 0.64 mm (0.025 inch) with a taper to about 0.36 mm (0.014 inch) diameter at the tip where the grounded junction was formed. The 0.36 mm taper was as small as this cable was able to be swaged without splitting the sheath. Small junctions with high frequency response are desired for TTF work.

The response times for the TCs were matched to within 1 ms by the procedure given in TREE-NUREG-1011, Appendix A. The response times for a 0 to 63% response to a step function temperature change in water was about 12.4 ms which corresponds to a roll-off frequency of about 13 Hz.

2.1.2.2 Electronics

The signals from each of the two TCs were recorded as processed by three parallel channels as shown in Figure 6. The first pair of TC channels involved merely amplifying the basic TC signal before recording; the second involved amplification plus a frequency compensating circuit before recording; the third channel pair involved amplification, additional filtering and a signal compression circuit before recording.

2.1.2.2.1 Amplifiers and Filters

The amplifiers used were PAR Model 114/116 low noise, ac, high common-mode rejection, differential amplifiers. They were connected to the TCs through approximately 25 m of RG58/U coaxial cable. The filters were Krohn-Hite 8-pole Active Filters with maximum flat amplitude response and the gain set at unity.

2.1.2.2.2 Frequency Compensation Circuit

The TCs used in this system acted as single-pole, low-pass filters for the temperature signals with a cut-off frequency near 13 Hz (as described in Section 2.1.2.1). As long as the frequency response characteristics of the TC are well-defined and constant it is possible in principle to electronically compensate for the TC's filtering and increase the frequency response range of the TC. The only practical limit to this technique is that the increasing high-frequency gain of the circuit also amplifies the high frequency noise to an intolerable level if the frequency range is extended too far. The circuit used is shown schematically in Figure 7a along with its idealized frequency response in Figure 7b.

2.1.2.2.3 Signal Compression Circuit

The signal compression amplifier characteristics are indicated in Figure 8. This circuit was to provide high gain for small amplitude signals without overdriving the tape recorder with larger amplitude signals. The difficulty with this circuit is that low level signals mixed in with higher level signals are effectively attenuated because the high amplitude "base" signal forces the total signal up into the high-amplitude non-linearly amplified region of the circuit.

2.1.3 Conductivity Probe

2.1.3.1 Sensor

The conductivity sensors were standard pin-electrode assemblies as used in the LOFT liquid level transducer. The center electrode was shortened from 25.4 mm (1 inch) (as used in the liquid level transducer) to 9.5 mm (0.375 inch) in order to increase its sensitivity to smaller bubbles and droplets.

2.1.3.2 Electronics

The electronics for the conductivity probes were configured as shown in Figure 9. The conductivity probe stimulating source, signal detector and signal conditioner were constructed as a single unit which is described in Appendix A. The probe was stimulated by a dual-polarity square-wave current source and the voltage signal developed by the probe impedance was synchronously detected, demodulated and sampled during the positive polarity phase of the driving square-wave just prior to the polarity reversal. The sampled signal was amplified to a suitable level for tape recording.

The signal conditioning electronics has an essentially flat frequency response from 0 Hz (dc) up to some cut-off frequency f_c determined by the sampling frequency. This was verified by a white noise signal injection analysis. In single polarity sampling $f_c = f_{ref}/20$, where "f_{ref}" is the frequency of the external reference oscillator. For sampling during both polarities $f_c = f_{ref}/10$. For the tests at LTSF the external reference oscillator was set at 4 KHz and the sampling mode set in positive polarity which would set the cut-off frequency f_c at 200 Hz.

2.1.4 Drag Screen

2.1.4.1 Sensor

The drag screen transducers were RAMAPO Instrument Company Mark V 2PRBD strain gauge flowmeters modified with a flow shield for the deflector beam as shown in Figure 10. A drag screen (see Figure 11) 5.12 mm in diameter and 77% open was mounted on the end of each deflector beam. The transducer plus the drag screen had a room temperature resonance of approximately 84 Hz in water and 88 Hz in air. The RAMAPO transducer alone had a mechanical resonance at 170 Hz in both air and water. The transducer was rated at 1.2 mV/V at full scale deflection. Its designed range was 2×10^3 to 2×10^5 lb/ft sec^2 with an equivalent target of diameter 0.422 inch to 0.451 inch.

2.1.4.2 Electronics

The RAMAPO transducer is a full bridge strain gauge. The electronics configuration is shown schematically in Figure 12. 5-V dc was used as the excitation to the bridge. The bridge output was fed into a differential amplifier set to bandpass 1 Hz to 100 Hz with a gain of 2000. The signal was further filtered with a Krohn-Hite 8-pole Active Filter which was set to low pass in the maximum flat mode with the -3db break frequency set at 35 Hz.

2.2.1 Spool Piece

The spool piece for the transient high pressure and temperature tests was made of 316 stainless steel Schedule 160 pipe and 1500 lb fittings, and is shown in Figure 13. The main run section was made of a 5-in nominal diameter pipe approximately 1.5 m long. A 5-in 1500 lb weldneck flange was welded to each end of the pipe for installation of the spool piece in the test facility.

The main run pipe had three 3-in diameter side bosses welded along its length to provide instrument penetrations. Each side boss consisted of a 3x5 weldolet adapter and a 3-in diameter 1500 lb weldneck flange welded together. The side bosses were positioned in the horizontal plane so as to provide separations of 279, 940 and 1219 mm between their locations as shown in Figure 13.

2.2.2 Instrumented Insert

Two instrumented inserts were designed which would hold one each of the conductivity, drag screen and thermocouple sensors. The inserts consisted of a 3-in 1500 lb blind flange to which was attached a cylindrical piece of 316 stainless steel which served principally to displace water from the volume of the 3-in diameter side boss in order to prevent any side boss blowdown from interferring with the flow in the main channel.

The sensors were configured identically on the two inserts (see Figure 14) so that no sensor on the upstream insert would directly

shadow a sensor of a different type on the downstream insert. In spite of this precaution the drag screen was considered to be too severely perturbative to the flow through the pipe for valid simultaneous measurements to be made with both the drag screens and either the conductivity or thermocouple sensors. Consequently, a blank plug was designed so that the drag screen transducers could be removed, its penetration blocked off, and further testing could proceed with the conductivity and thermocouple sensors. The instrumented inserts and close-up of the sensored end are shown in Figures 15 and 16 with the drag screen penetration plugs mounted in place of the drag screen transducers.

2.2.3 Blank Insert

To occupy the side boss volume of the third (non-instrumented) side boss position, a blank insert was designed and manufactured using a 3-in 1500 lb blind flange and is shown in Figure 17.

All three inserts, the two instrumented and one blank, were interchangeably mountable in any of the three side bosses.

2.3 Data Acquisition System

The signals from the various sensors were recorded on an AMPEX Model PR-2200 14 channel FM tape recorder. The sensor and signal conditioning configurations were as given previously in Section 2.1 and shown in Figures 4, 6, 9, and 12. Care was exercised to assign sensor pairs which were to be cross-correlated for analysis to adjacent channels of the same record head of the tape recorder, i.e., either on the odd-channel head or the even channel head. This was to eliminate the possibility of accidentally introducing into the actual transit delay time an artificial component due to possible stretching of the tape or due to non-identical interhead separations between different tape recorders. The detailed assignment of sensors to tape recorder channels will be given in Section 3.2.3.

2.4 Data Analysis System

The primary form of data analysis employed a General Radio Time/Data TDA-33 Signal Analysis System. The TDA-33 is a PDP 11/34 microcomputer system which will accept two channels of analog signals, digitize them, perform a fast Fourier transform (FFT) on the signals, and store the information in its memory in the form of auto- and cross-spectra. The digitization rate, data frame length, number of data frames averaged and many other parameters pertinent to the analysis are user selected and may be easily changed at will subject to the overall constraint of the available memory space. The signal acquisition by the computer for processing can be initiated either in a free-run mode or by an external trigger signal as from an IRIG time code translator.

A secondary form of data analysis was a PAR Model 101A Correlator. This correlator is a hand-wired unit which accepts two channels of analog signals and performs the cross-correlation calculation in real time directly on the continuously incoming signals. The correlation time range and exponential averaging time constant are user selectable, although the latter may be changed only by removing ten internal printed circuit boards and changing ten resistors on each board.

The PAR Correlator is extremely ill-suited to the analysis of transient phenomena because the internal noise-to-signal ratio from within the instrument increases as the exponential averaging time constant is decreased. A practical lower limit to the exponential averaging time constant has been found by lab tests to be $\tau_{av} \cong 3$ sec which has the consequence of limiting the transient time resolution to conditions changing in a time scale greater than about $3\ \tau_{av}$ or about 10 sec minimum resolution.

With either method of performing the cross-correlation, the output of the process is a "cross-correlogram", i.e., a graphical display of the magnitude of the correlation between the two signals versus the computationally introduced delay time. The transit time τ, is taken as that delay time at which the cross-correlation is a maximum. A further

minimum requirement is that the anticipated delay time must be less than either one half of the frame length in the TDA-33 analysis or less than the delay range in the PAR correlation analysis. In fact it is much better if the delay time is less than 1/5th times this minimum requirement.

3. TRANSIENT TESTS

3.1 Objective

The objective of these tests was to determine the feasibility of using various types of sensors as TTF transducers under transient conditions and secondly to assess the effect of different intersensor separations on the TTF performance.

3.2 Installation

3.2.1 Spool Piece

The spool piece was installed in the blowdown leg of the Blowdown Facility (BF) of the LOFT Technical Support Facility (LTSF) just upstream of the quick-opening valve (see Figure 18). The spool piece was mounted with the three side bosscs in the horizontal plane.

3.2.2 Instrumented Inserts

Initially, the two instrumented inserts were installed at side boss positions A and B (see Figure 13) with the blank insert at C. Later, the inserts were moved around to change the intersensor separation. A listing of the instrumented insert locations and intersensor separations for the various tests and sensor types is given in Table I.

During a pre-blowdown leak check of the BF system, one of the RAMAPO drag screen transducers was blown out of its fitting and damaged beyond use. Since no replacement transducer was available, the drag screen sensor type was eliminated from the testing.

3.2.3 Data Acquisition System

The TTF signal conditioning and data acquisition system (see Figures 19 and 20) was set up in the access hallway on the south side of the BF test cell. This location was chosen in order to minimize any r-f noise pick-up through the long TTF signal cables.

The TTF channel assignments and comments on signal conditioning are given in Table II. In addition to the signal conditioning configurations discussed in Sections 2.1.1.2, 2.1.2.2, 2.1.3.2 and 2.1.4.2 (Figures 4, 6, 9 and 12, respectively), a connection was made to the LTSF IRIG time code generator and this signal was direct-recorded on tape channel 14. This signal was to serve as a synchronization between the BF and TTF recorded tapes and as a triggering reference signal for the TTF cross-correlation analysis procedure. A visual inspection of the IRIG signal showed a signal which appeared to be an IRIG signal. At that time no time code translator was available to verify the quality of the time code signal. It was only during the playback of the data tapes for the cross-correlation analysis that it was discovered that the recorded IRIG signal did not decode. Thus, synchronization between the BF and TTF tapes was lost.

3.3 Initial Conditions and Test Durations

A blowdown is the release of stored energy in a high pressure and high temperature system containing some appropriate working medium, in this case water, well above its normal (atmospheric pressure) boiling temperature. A blowdown is initiated by the sudden venting of the system to atmospheric pressure as through a rupture disc or a quick opening valve.

A series of partial and full blowdown transients were conducted for the TTF feasibility study in September 1977. A blowdown of the entire 0.36 m^3 BF system volume constituted a full blowdown, while a partial blowdown was that of only the 0.049 m^3 volume of the blowdown leg piping between the BF remotely actuated valves and the quick opening blowdown valve.

Four partial and three full blowdowns were performed in the following order:

1) Partial, Number P-28-01
2) Partial, Number P-28-02
3) Full, Number F-28-01
4) Partial, Number P-29-01
5) Full, Number F-29-01
6) Partial, Number P-30-01
7) Full Number F-30-01

All blowdowns were made from the same initial conditions of:

Temperature	257°C ± 1°C
Pressure	10.3 MPa ± 0.1 MPa

at the pressure vessel and a temperature of 232°C at the nozzle (quick-opening valve).

Only the full blowdowns were intended for TTF cross-correlation analysis. The small blowdowns were used solely to verify transducer and data acquisition functioning and to adjust the gains and, signal levels of the various TTF channels for recording. The signals from the TTF transducers were recorded for approximately 120 seconds from the start of a full blowdown and 40 seconds from the start of a partial blowdown.

3.4 Blowdown Facility Reference Instrumentation

The BF data acquisition system monitored and recorded many temperatures, pressures and turbine outputs within the BF system during the tests. Those channels which were of interest to the TTF task were only the initial water temperature and pressure at the BF pressure vessel, the water temperature at the location of the nozzle or quick-opening valve, and the output of the 5-in. full-bore turbine located in the blowdown leg just upstream of the TTE test section.

The primary interest was in the blowdown leg full-bore turbine as this was the only BF instrumentation capable of measuring a fluid flow velocity during a blowdown test. This output was to be the primary comparison to the TTF indicated velocity.

Unfortunately, the BF 3-beam gamma densitometer was not installed on the BF system at the time of the TTF testing and a suitable replacement was not available. Hence, it was decided to use the TTF single-beam gamma densitometer signals in place of the 3-beam signals in the post-test analyses. However, as noted in Section 3.2.3, it was discovered after the test that the IRIG time code recorded did not decode. Thus the intertape synchronization was lost and code calculations were no longer possible.

4. DATA ANALYSIS AND RESULTS

4.1 Definition of Cross-Correlation[1)]

The mathematical definition of cross-correlation as applied to the analysis of finite signals is

$$R_{xy}(\tau) = \lim_{T\to\infty} \frac{1}{T} \int_{t=t_1}^{t_1+T} x(t-\tau)\, y(t) \qquad (1)$$

where "x(t)" and "y(t)" are the two signals, "τ" is the computational delay time between the two signals, "t_1" is the starting data time of the analysis, and "T" is the length of the data analyzed (or the data frame length). It is more common to consider a normalized cross-correlation function

$$\rho_{xy}(\tau) \equiv \frac{R_{xy}(\tau)}{\sqrt{R_{xx}(0)\, R_{yy}(0)}} \qquad (2)$$

where "$R_{xx}(0)$" and "$R_{yy}(0)$" are the values of the auto-correlation functions of x(t) and y(t), respectively, defined from

$$R_{xx}(\tau) = \lim_{T\to\infty} \frac{1}{T} \int_{t=t_1}^{t_1+T} x(t-\tau)\, x(t)\, dt \qquad (3)$$

The exact shape of $\rho_{xy}(\tau)$, and $R_{xy}(\tau)$ as well, can be predicted from a knowledge of the frequency spectra of the signals, but all theory agrees in that the $\rho_{xy}(\tau)$ will be peaked at a value of τ equal to the delay in real time between the two signals. The width of the cross-correlation peak is an inverse function of the bandwidth of the signals, and the magnitude of the peak is a function of the signal-to-noise ratio, where the "noise" is considered to be that part of the signal y(t) which has no coherence with respect to x(t).

Various computational schemes approximate the definitions in equations (1) and (3) in different ways. The PAR Correlator described in Section 2.4 performs the cross-correlation on the incoming signals in a direct fashion updating its memory storage continuously and allowing the stored signals to decay at a rate controlled by an RC time constant. The resultant cross-correlation function as obtained from the PAR is

$$R_{xy}(\tau,t) = \frac{1}{\tau}\int_{u=t_o}^{t} x(u-\tau)\, y(u)\, e^{-(t-u)/\tau_{av}}\, du \qquad (4)$$

where "t" is the real time at which the cross-correlation is observed, "τ_o" is the computational delay time, "t_o" is the time at which the correlation process was started, "u" is the real time of the signal and "τ_{av}" is the RC decay time of the correlator.

Computer methods of approximating equations (1) and (3) eliminate the restrictions of the exponential averaging in the PAR Correlator and are able to weight the data in any fashion desired by the programmer. However, the direct cross-correlation process is not computationally efficient and requires a great deal of time. A faster method is to perform a fast Fourier transform (FFT) of finite record (or portion of the signals) and compute the auto- and cross-spectra of the two signals. The cross-correlation function obtains as the inverse Fourier transform of the complex cross-spectra between the two signals:

$$R_{xy}(\tau) = \int_{0}^{\infty} G_{xy}(f)\, e^{j2\pi f\tau}\, df \qquad (5)$$

where "$G_{xy}(f)$" is the one-sided cross-spectrum, "f" is the frequency, and "j" is $\sqrt{-1}$. The Time/Data TDA-33 Signal Analyzer utilizes this approach to compute the cross-correlation function.

4.2 Other Relevant Functions to Cross-Correlation Analysis

Other functions revelant to a transit time determination by cross-correlation on a computer system are:

a) The Spectral Density Function.

The two-sided spectral density function is mathematically defined as

$$S_{xy}(f,T,k) = \frac{1}{T} X_k^*(f,T)\, Y_k(f,T) \qquad (6)$$

where "f" is the frequency, "T" is the frame length, "k" is a subscript denoting the data frame, the "(*)" denotes the complex conjugate operation and "X" and "Y" are the finite Fourier transforms of the data frames $x_k(t)$ and $y_k(t)$, respectively. The finite Fourier transform is defined by

$$X_k(f,T) = \int_0^T x_k(t)\, e^{-j2\pi ft}\, dt \qquad (7)$$

If $x_k(t)$ and $y_k(t)$ are signals from two different data channels, the spectral density is properly called the cross-spectral density; otherwise, $x_k(t)$ and $y_k(t)$ are the same data signals and the spectral density is an auto-spectral density.

The two-sided spectral density functions are defined over the frequency range $-\infty \leq f \leq +\infty$. Since a real Fourier transform measures only positive frequencies, it is customary to define corresponding one-sided spectral density functions by

$$G_{xy}(f,T,k) = 2\, S_{xy}(f,T,k) \qquad (8)$$

The utility of the cross-spectral density function has already been discussed in Section 4.1. The shape of the auto-spectral density indicates the relative magnitudes of the contribution of various frequencies to the total signal as processed by the sensor and its signal conditioning. If the frequency response of the sensor were known, then the actual frequency content of the driving signals could be determined.

The estimates of the spectral quantities from a number of "N" of frames is obtained by averaging

$$G_{xy}(f,T) = \frac{1}{N} \sum_{k=1}^{N} G_{xy}(f,T,k) \qquad (9)$$

using the cross-spectrum as an example.

b) The Phase Function.

The phase function of the cross-spectrum contains the information on the relative time delay between the two signals. The complex cross-spectrum can be expressed as a magnitude and a phase factor

$$G_{xy}(f) = | G_{xy}(f) | e^{-j2\pi\phi(f)} \qquad (10)$$

For the ideal of two completely coherent signals with a time delay between them of "ΔT", the phase relationship can be expressed as

$$\phi(f) = \Delta T\, f. \qquad (11)$$

Thus, the slope of a plot of the phase function versus frequency is the delay time.

This relationship provides an alternate method (compared to using the cross-correlation function) of obtaining the transit time. However, in practice and particularly for data records of a small number of data frames (where "small" is less than 100), the statistical fluctuations

in the phase angle make it very difficult to determine the value of the slope and, hence, the cross-correlation function was preferable to use in determining the transit times of this investigation.

c) The Coherence Function.

The coherence function is mathemetically defined as

$$Co(f) \equiv \frac{| G_{xy}(f) |^2}{G_{xx}(f)\, G_{yy}(f)} \qquad (12)$$

The function essentially gives the fraction of information at any given frequency which is involved constructively in the cross-correlation or, alternatively, the fraction that is not associated with any random noise in the signals. The coherence function is alsways within the limits

$$0 \leq Co(f) \leq 1.$$

4.3 TTF Cross-Correlation Analysis

In spite of the loss of the test IRIG time code signal and the consequent loss of intertape syncronization for post-test code calculations, it was still possible to proceed with the TTF cross-correlation analysis procedure since all of the TTF transducer signals were recorded on the same 14-channel tape. It was only necessary to duplicate the original data tape with an "artificial" but decodable IRIG signal impressed onto the IRIG channel, channel 14. However, the time of the start of each blowdown (t = 0) could not be determined with certainty and could only be approximately located.

4.3.1 TDA-33 Computer Analyses and Results

Since flow conditions during a blowdown transient change quite rapidly and often dramatically, it is not appropriate to analyze the entire two minutes of a full blowdown as a single data record. Rather, the entire two minutes must be broken down into smaller sequential

records to form a "time sequence", and each of the smaller records analyzed alone to obtain its characteristic transit time. The results of such time sequence analyses will be discussed according to sensor types.

All computer analyses were performed with a digital block size of 512. The frame time length was varied by selecting the appropriate sampling frequency according to the prescription

$$f_s T = \text{Block size} \qquad (13)$$

where "T" is the frame length and "f_s" the sampling frequency.

A selectable internal 8-pole anti-aliasing filter was set such that the filter break frequency was less than or equal to $f_s/2$.

A zero-insertion option was sometimes employed to assess and correct for the "wrap-around" effect in the digital computations. This option is explicitly noted when it is used, otherwise it is assumed to not be selected.
As long as the dominant cross-correlation peak was located at a $\tau < T/4$, the use of zero-insertion was found to have little effect on the transit time.

4.3.1.1 Single-Beam Gamma Densitometer

Several time sequences at various time resolutions were made of the signals from the full blowdowns. Figures 21, 22, and 23 show the TTF velocity time sequences for test F-28-01, F-29-01 and F-30-01, respectively, made using single frame data records with a 1 sec frame length and stepping the data tape in 1 sec time increments. A few typical cross-correllograms are shown in Figures 24 and 25 from the time sequence for F-28-01.

Figures 26, 27, and 28 show the velocity time sequences for test F-28-01, F-29-01 and F-30-01, respectively, made using two frame records with each frame 0.5 sec in length and stepping through the data in 0.5 sec time increments.

Figure 29 shows a time sequence of test F-29-01 using the zero-insertion option and was made using single-frame records with a 1 sec frame length and 0.5 sec time increments.

During the post-test analysis it was observed that there was a single-pole roll-off starting at about 73 Hz in the auto-and cross-spectra. This was due to a 2200 pf capacitance in the current-to-voltage converter stage of the preamplifier (see Figure 5). This was not thought to be a serious limitation because 1) a single-pole roll-off is not as rapid as the 8-pole roll-off filters used elsewhere in the signal conditioning and analysis and 2) because a coherence function examination never showed significant coherence between the two channels for frequencies above about 40 Hz and usually above not about 25 Hz (see Figures 30 and 31). However, in order to be certain of the effect of eliminating the higher frequencies, the densitometers were played back and re-recorded through a frequency compensation circuit similar to that shown in Figure 7a, but with the input pole set at $f = (2\pi RC)^{-1} =$ 73.5 Hz and the feedback impedance pole set at $f = (2\pi RC)^{-1} = 780$ Hz. A time sequence (see Figure 32) made on the frequency compensated data using zero-insertion, single frame records, 0.5 sec frame lengths, and 0.5 sec time increments. No significant improvement was obtained.

The time sequences made at different frame lengths and sampling formats appear to be essentially the same among themselves for each test (Figures 21 and 26 for test F-28-01, Figures 22, 27, 29 and 32 for F-29-01, and Figures 23 and 28 for F-30-01). Test F-29-01, having the shortest (292 mm) intersensor separation between the densitometer beams, exhibits the least comparison differences.

All of the TTF velocity time sequences appear to read consistently higher by about 50% when compared to the BF full-bore turbine readings for the same test (see Figures 47, 48 and 49). The reason for this systematic deviation is not known at this time. It is most likely due to the two-phase flow rather than attributable to either the signal conditioning or the cross-correlation process.

4.3.1.2 Conductivity Probe

A time sequence was made from the signals from the conductivity probes for test F-28-01, which corresponds to the minimum intersensor separation of 279 mm. This time sequence (see Figure 33) was made using single frame records, 1 sec record lengths and 1 sec time increments.

A second time sequence using single frame records, a 2 sec frame length, 1 sec time increments and zero-insertion was generated and is shown in Figure 34. The 2 sec frame lengths do provide a somewhat "better" velocity time sequence than the 1 sec frame lengths.

The tests F-29-01 and F-30-01 gave no significant cross-correlation results for the conductivity probe signals.

4.3.1.3 Thermocouple

The thermocouple signals were analyzed with time sequences for all three forms of signal conditioning: bandpass amplification alone (see Figure 35), plus frequency compensation (see Figure 36), and plus signal compression amplification (see Figure 37). As can be seen from the time sequences, the thermocouple performed approximately equally well in all three forms of the signal conditioning and only for the first 4 or 5 seconds of test F-28-01. The cross-correlation was dominated by common mode 60 Hz noise all during tests F-29-01 and F-30-01 for the larger intersensor separations.

4.3.2 PAR Correlator Analyses and Results

In spite of its being considered inadequate to a transient situation, several attempts were made to process the recorded data with the PAR Model 101A Correlator. The correlation peak tracking circuit developed for G. D. Lassahn was connected to the output of the PAR Correlator. This instrument is fully described in TREE-NUREG-1011, Appendix B[2)]. Basically this instrument searches the PAR Correlator output for the correlation peak and outputs an analog signal proportional to the delay time of that correlation peak. This analog signal was then input to a

strip chart recorder. Thus, the output with this method was a plot of transit time versus time-into-blowdown, rather than a velocity versus time-into-blowdown plot as plotted from the computer.

Data from all of the tested sensor types were processed with this method. However, only the results for the single-beam gamma densitometer TTF channels will be presented since that channel pair was the only one for which comparable results were obtained from the computer analyses. The recorded signals were first processed with an exponential averaging time constant of 1 sec, but the correlator noise was so bad as to make the transit time graphs useless. The averaging time constant was changed to 3 sec and the densitometer signals were processed for all three full blowdowns with a 50 ms pre-computation delay and a 200 ms delay range selected. The results for test F-28-01, F-29-01 and F-30-01 are shown in Figures 38, 39 and 40, respectively. Furthermore, as a check on reproducibility, the data from test F-29-01 was processed twice. The results are both shown in Figure 39 and are designated Run 1 and Run 2.

4.4 Auto-Spectral Density Functions

Figures 41 through 45 show the auto-spectral density (ASD) graphs obtained using 40 frame data records and encompassing approximately 120 sec of recorded data. Both channels of each sensor type displayed very similar ASDs, so only one channel is shown.

The ASD typical of the gamma densitometer shown in Figure 41 was taken with the anti-aliasing filter set at 100 Hz. The ASD shows the roll-off in the frequency content of the signals to begin around 30 to 33 Hz.

The ASD from the conductivity probe is shown in Figure 42. The anti-aliasing filter was set at 100 Hz. This ASD also shows a roll-off in the frequency content to begin around 31 to 33 Hz.

Figures 43, 44, and 45 show the ASDs for the thermocouples with bandpass amplification, frequency compensation and signal compression,

respectively. The anti-aliasing filter was set at 100 Hz. It is noteworthy that in comparing Figures 43 and 44, the effect of the frequency compensation circuit can be easily observed. All these ASDs show a roll-off in the frequency content of the signals to begin around 13 Hz.

The 32 Hz break point indicated by the ASDs of the gamma densitometer and the conductivity probe might be interpreted as that of the fluid properties themselves since the frequency response of those sensor electronics are flat to a frequency well above that. However, this contention is only conjectural and additional data would be necessary to support this observation.

4.5 BF Full-Bore Turbine

The signals from the BF blowdown leg full-bore turbine were processed to obtain a volumetric flow rate as a function of time into blowdown. An average velocity was obtained by merely dividing by the cross-sectional area of the pipe. The results are shown in Figures 46, 47 and 48 for blowdowns F-28-01, F-29-01 and F-30-01, respectively. Due to the difficulty with the IRIG generator during the test the initial 2 seconds for test F-29-01 was skipped in the processing.

As can be seen from Figures 46 through 48, the average fluid velocity is relatively constant at about 2 to 2.5 m/s. During this time the gamma densitometer channels 11 and 13 indicated a void fraction between 0 and 80% with rather large fluctuations occurring often. Since the inertia of a full-bore turbine would result in its being most responsive to the higher density phase, it seems most probable that the turbine would be following the fluid phase flow rather than that of the gas steam phase.

4.6 Results Summation

Concerning the performance of the various TTF sensor types tested, the following statements can be made:

a) The single-beam gamma densitometer performed the best of the sensor types tested. A velocity 50% high compared to that of the BF full-bore turbine was obtained during the initial 16 to 18 seconds of a full blowdown. This may be seen by comparing Figures 21 and 26 to 46; 22, 27, 29 and 32 with 47; and 23 and 28 to 48.

After this initial time period the densitometer density channels (channels 11 and 13) indicate the flow to be mostly steam for which the density fluctuations might be expected to be small and undetectable among the statistical fluctuation noise of the gamma radiation sources themselves.

b) Cross-correlation of the conductivity probe signals resulted in a non-zero transit time during the same approximate time period (initial 20 seconds) of test F-28-01 as the gamma densitometer TTF. However, the correspondence between the BF turbine indicated velocity and the conductivity TTF velocity is not as good as for the gamma densitometer TTF, as may be seen from a comparison of Figures 33 and 34 to 46.

c) The thermocouples performed similarly for all three forms of signal conditioning performed before recording as shown in Figures 35, 36 and 37. There was no significant improvement in the cross-correlation results for either the frequency compensated signals or the compressed signals compared to those from the straight bandpass amplified signals. This agrees with the previously published results of Lassahn[2), 3)], but disagrees with the results of Ulber and Lubbesmeyer[4)].

The significant differences between the Ulber and Lubbesmeyer system and those of Lassahn and of this study are the use of an automatic gain control (AGC) circuit and an intentional location of the thermocouple tips at the center of the pipe. It is possible that these differences are indeed pertinent to a successful TC TTF but there is insufficient information to say definitely.

d) The thermocouples performed the worst of the three sensor types tested. A cross-correlation at other than zero transit time was obtained only during the initial 4 or 5 seconds of a blowdown as shown in Figures 35, 36, and 37. During this 4 or 5 second period there was good correspondence between the thermocouple TTF velocity and the BF turbine indicated velocity. After that period an examination of the thermocouple signals show them to be dominated by 60 Hz common mode noise.

e) There was good correspondence between the TTF velocities from the thermocouples (when they worked) and the single beam gamma densitometers.

f) The effect of intersensor separation was evident for the thermocouples and the conductivity probes, which gave poor correlations for other than their smallest separation of 279 mm.

This effect was not strongly evident, however, for the gamma densitometer which gave a TTF velocity for all three interbeam separations of 292, 441 and 513 mm. There appeared to be a slight adjustment of a time period for good TTF performance with the longest time (20 sec) observed for the minimum separation and the shortest time (16 sec) for the maximum separation. An examination of the average cross-correlation peak magnitudes for the three tests gave $\overline{C} \approx 0.52$ for test F-29-01 and $\overline{C} \approx 0.42$ for both F-28-01 and F-30-01. These apparent differences may not be statistically significant with respect to those differences between separate tests.

g) No comments can be made concerning the applicability of drag screen transducers as sensors for a TTF because this sensor type was not able to be tested.

h) It should always be borne in mind that the applicability of a TTF to single phase or homogeneous flow conditions is extremely limited. Under these conditions the random fluctuations in a

fluid parameter are very small in comparison to that parameter's absolute value, thus, requiring an extremely sensitive as well as high frequency response sensor.

5. CONCLUSIONS

A transient TTF using gamma densitometer sensors has been shown to work during the initial phase of a blowdown during which the void fraction varies from approximately 0.1 to 0.8. It functioned during this time for interbeam separations of 292, 441 and 513 mm with a slightly better performance demonstrated for the minimum separation.

The conductivity probe TTF functioned poorly at an intersensor separation of 279 mm and not at all for larger separations. It appears that it might show promise for yet smaller separations than the 279 mm.

The thermocouple TTF was shown to function almost not at all for any of the intersensor separations tested. Work by Hr. Dr. D. Lübbesmeyer at small separations (about 50 mm) reports success using thermocouples.

While a TTF was shown to work during part of a blowdown there does not yet exist sufficient data to engineer a system which will function during more of a blowdown. Further developmental efforts are recommended.

6. CONTINUED EFFORT

The results of this feasibility study are not conclusive. Those factors indicated for further investigations are:

a) Smaller intersensor separations.

b) Center-line location of sensors.

c) Utility of AGC amplification.

d) Level of inherent random fluctuations in fluid properties.

6.1 Intersensor Separation

All of the sensor types tested indicated improved performance using smaller intersensor separations. Extrapolation of these indications would predict further improved performance at separations less than those tested in this study.

6.2 Sensor Location

The sensor location for this study was not at all optimized because of the necessity of providing the ability to test a variety of sensor types. Closer attention ought to be paid to this aspect in future investigations.

6.3 AGC Amplification

This study has indicated a difficulty with the large dynamic range of the random fluctuation signals encountered during the entire course of a blowdown. Ulber and Lübbesmeyer[4] have reported successful TTF results employing an AGC circuit. Such a circuit should at least extend the period of applicability by a TTF by extending the dynamic response capabilities of the instrument signal conditioning.

6.4 Fluid Property Fluctuations

Very little is still presently known about the frequency content of random fluctuations in the fluid properties themselves upon which a TTF is fundamentally dependent. The ASDs of the densitometer and the conductivity probe shown in Section 4.4 might indicate that the frequency content of the fluid might be starting to roll-off starting at about 32 Hz. One might expect this roll-off to be a function of the system dimensions and its initial conditions before blowdown.

An effect folded into this is the frequency response of the sensor itself besides that of its signal conditioning electronics. This frequency response must be a function of the geometrical size or configuration of the sensor.

7. REFERENCES

1) Julius S. Bendat and Allan G. Piersol, "Random Data: Analysis and Measurement Procedures". Wiley-Interscience (New York 1971).

2) Gordon D. Lassahn, "Feasibility Study of Thermocouple Correlation Type Transit Time Flowmeter in Transient Steam-Water Flow". TREE-NUREG-1011 (March 1977).

3) Gordon D. Lassahn, "Thermocouple Correlation Transit Time Flowmeter Tests at WCL". TREE-NUREG-1007 (November 1971).

4) M. Ulber and D. Lübbesmeyer, "Erfassung und Arbeitung von Temperatursignalen bei Blowdown-Versuchen" ("The Detection and Processing of Temperature Signals for Blowdown - Experiments"). Lecture No. 2 at the KTG Technical Convention on Experimental Techniques in the Field of Fluid Thermodynamics (Hanover, U. K., 1977).

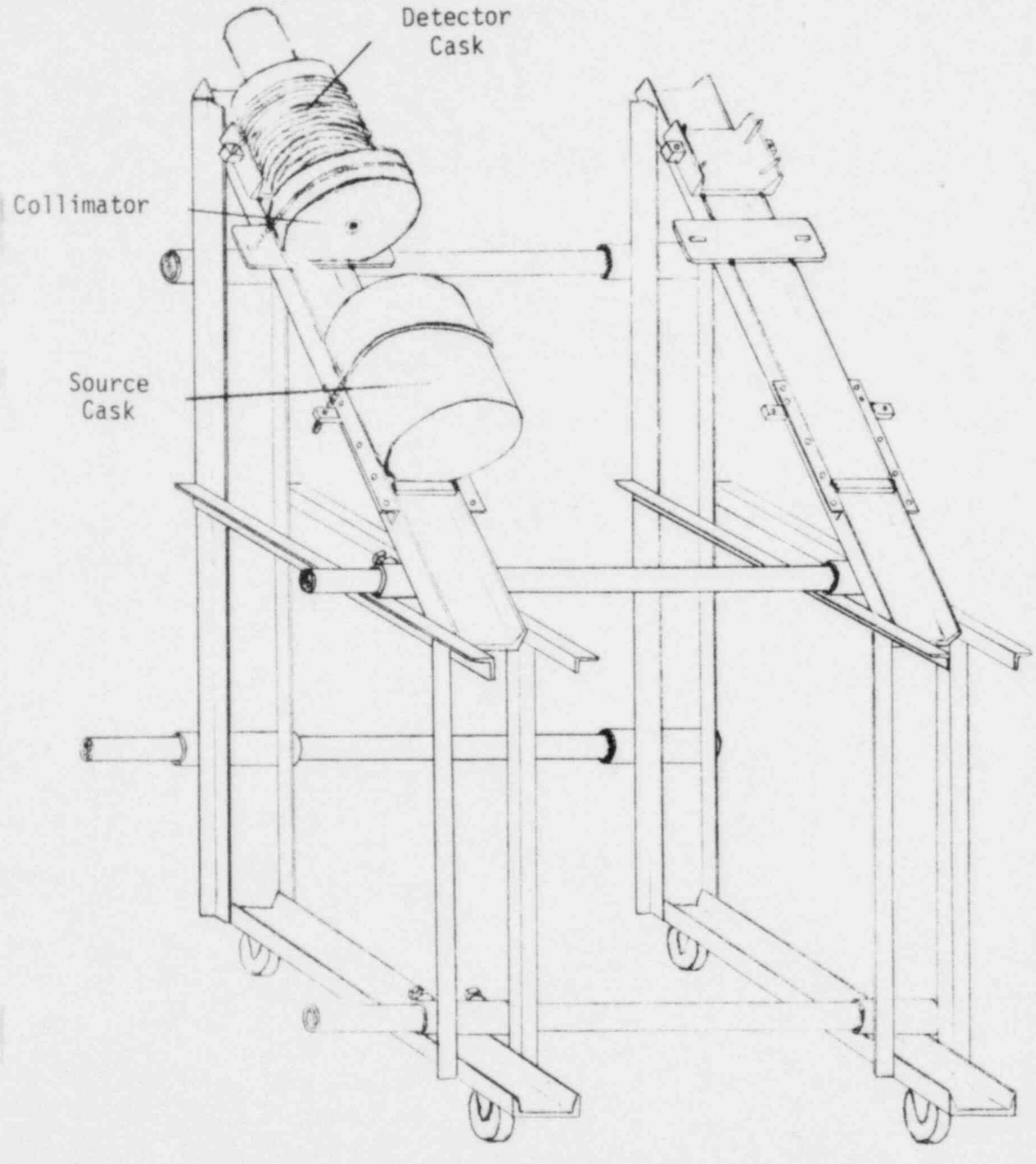

Figure 1 Gamma Densitometer Transducer Frame

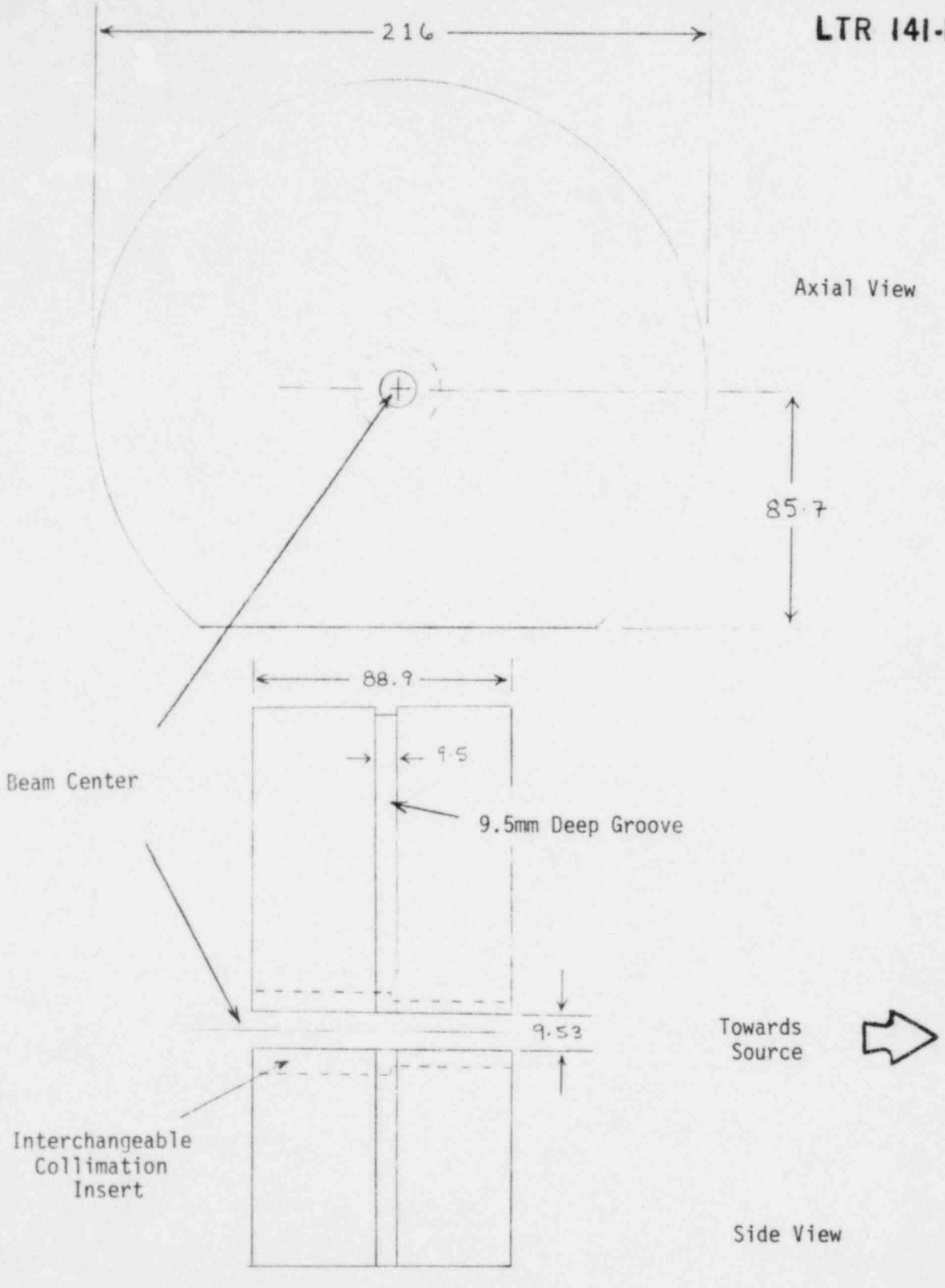

Figure 2 Gamma Densitometer Collimator

All Dimensions in mm

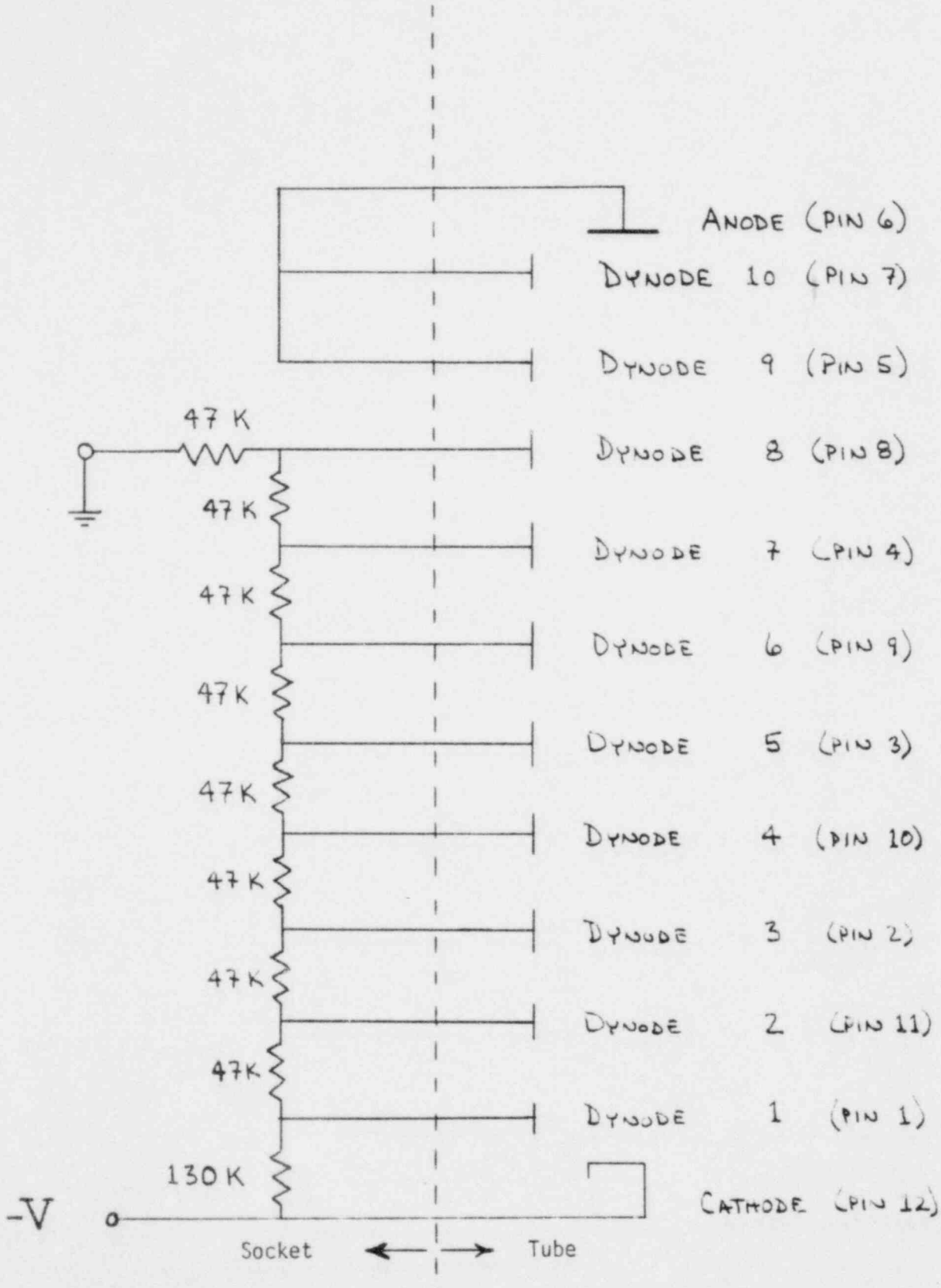

Figure 3 Photomultiplier Tube Socket Schematic

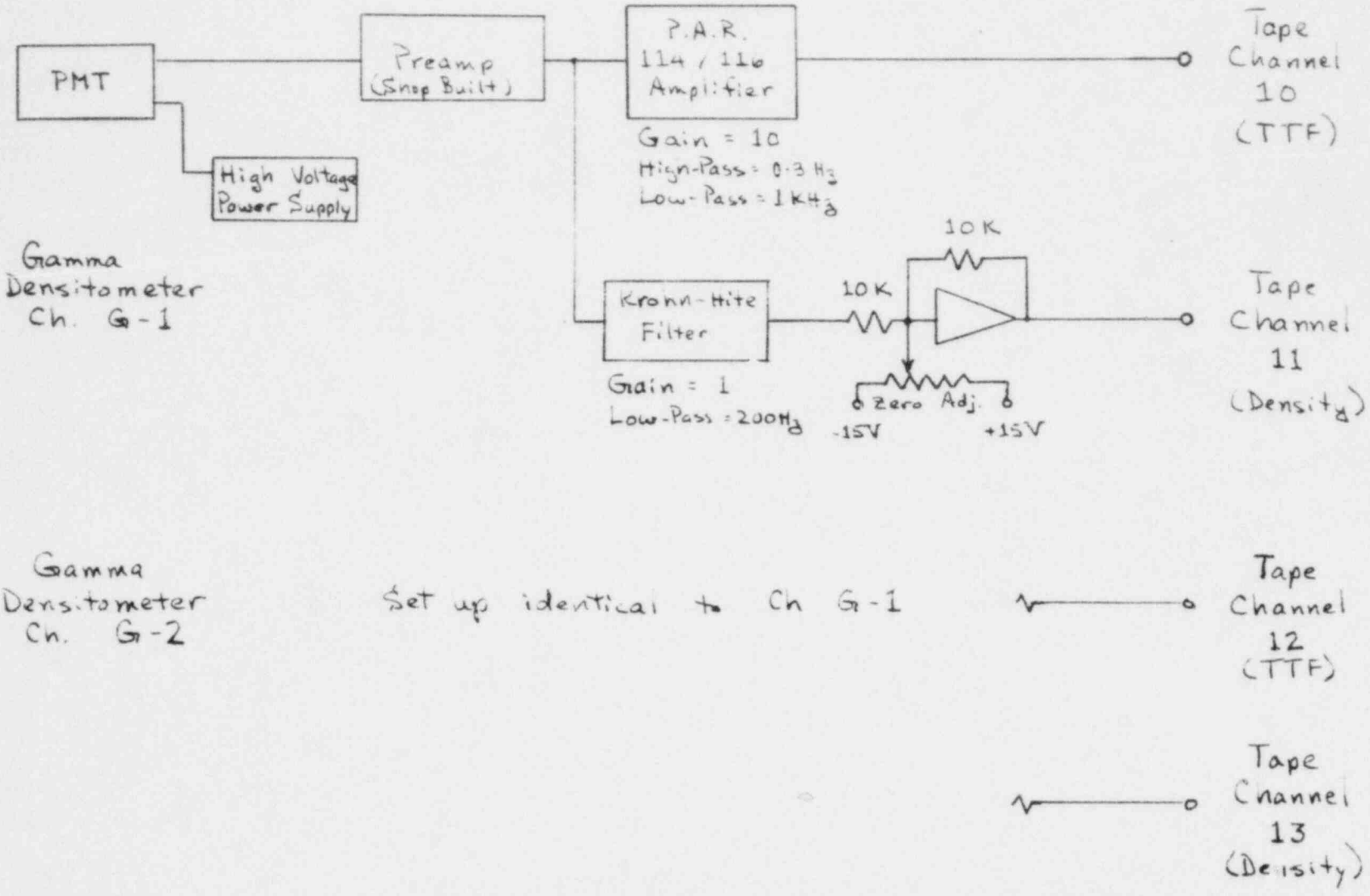

Figure 4 Gamma Densitometer Electronics Configuration

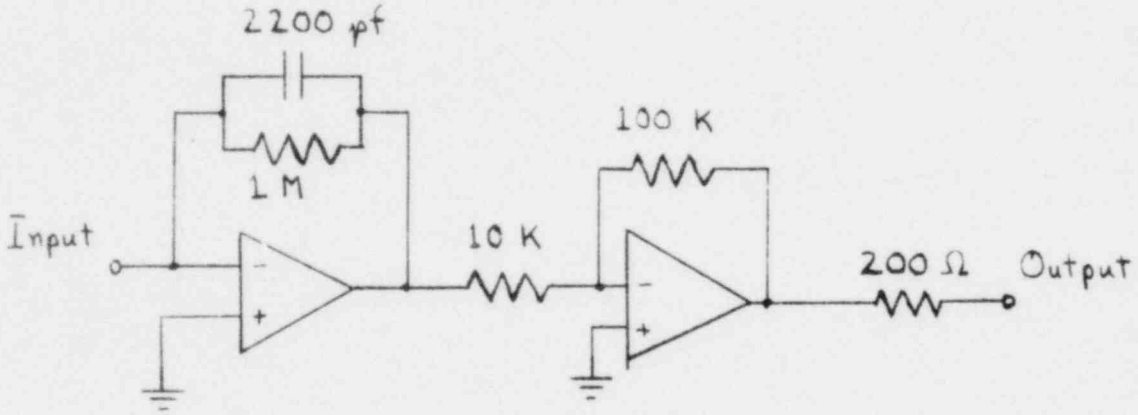

Figure 5 Gamma Densitometer Preamplifier Circuit Schematic

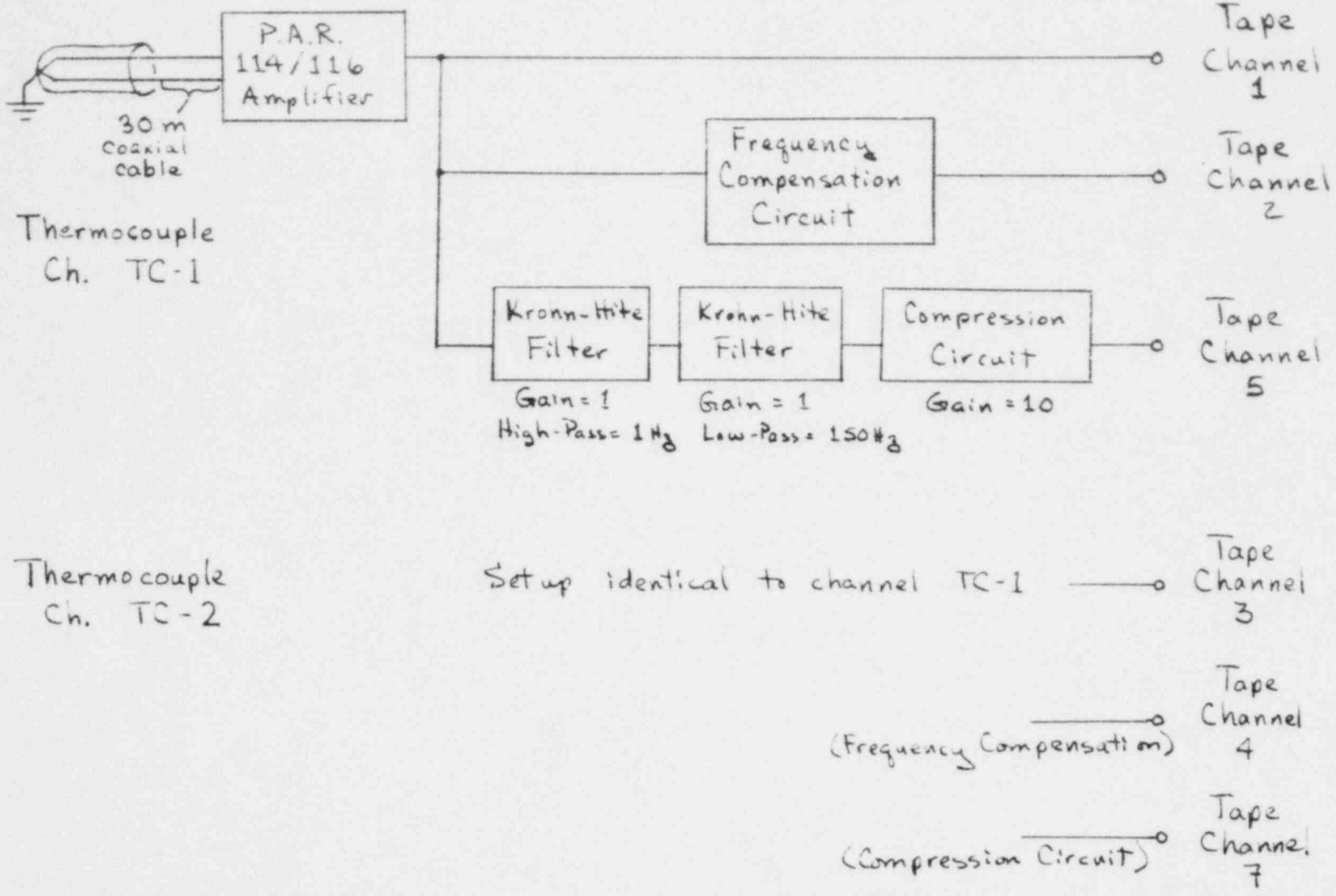

Figure 6 Thermocouple Electronics Configuration

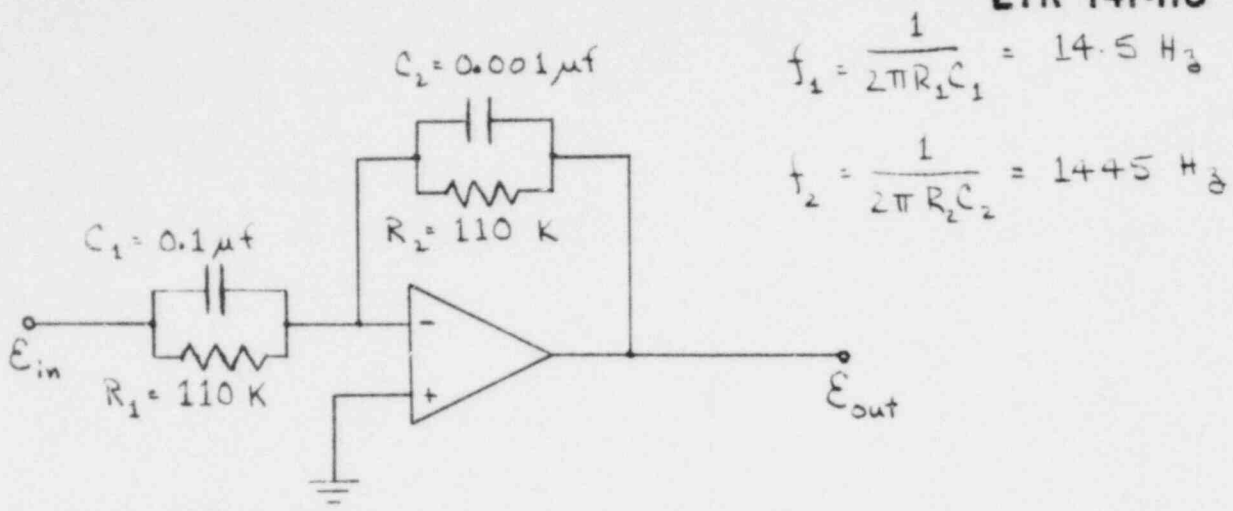

7a Frequency Compensation Circuit Schematic

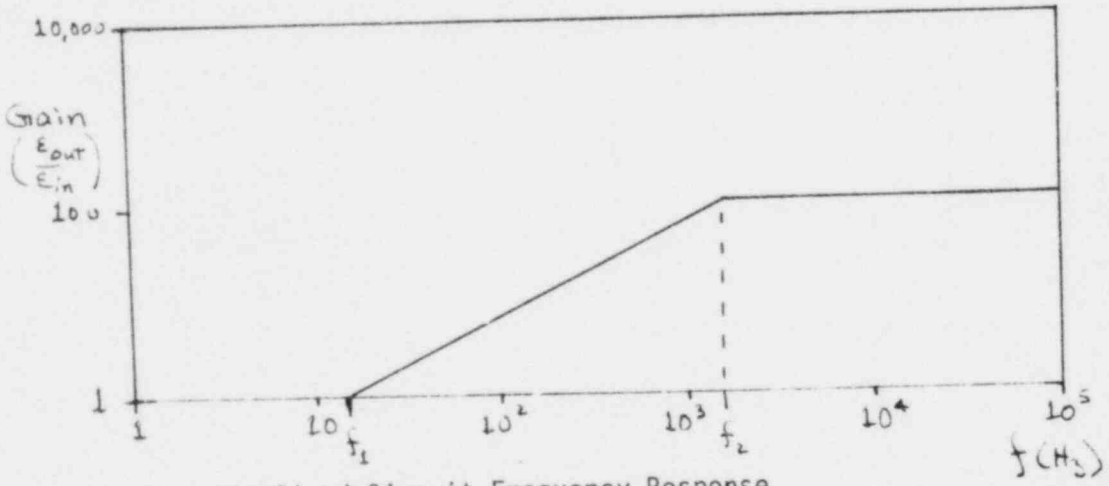

7b Idealized Circuit Frequency Response

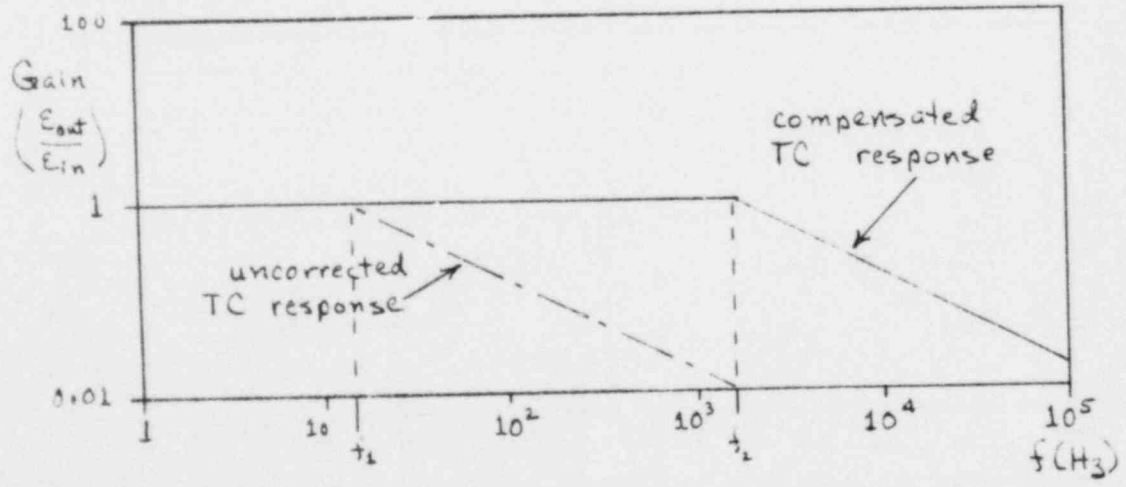

7c Idealized Overall Thermocouple Frequency Response

Figure 7 Thermocouple Frequency Compensation Circuit Schematic

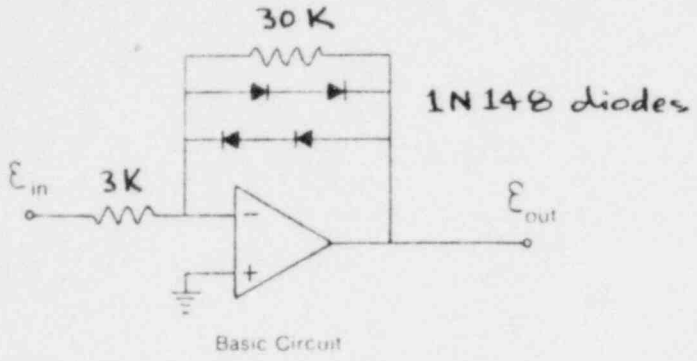

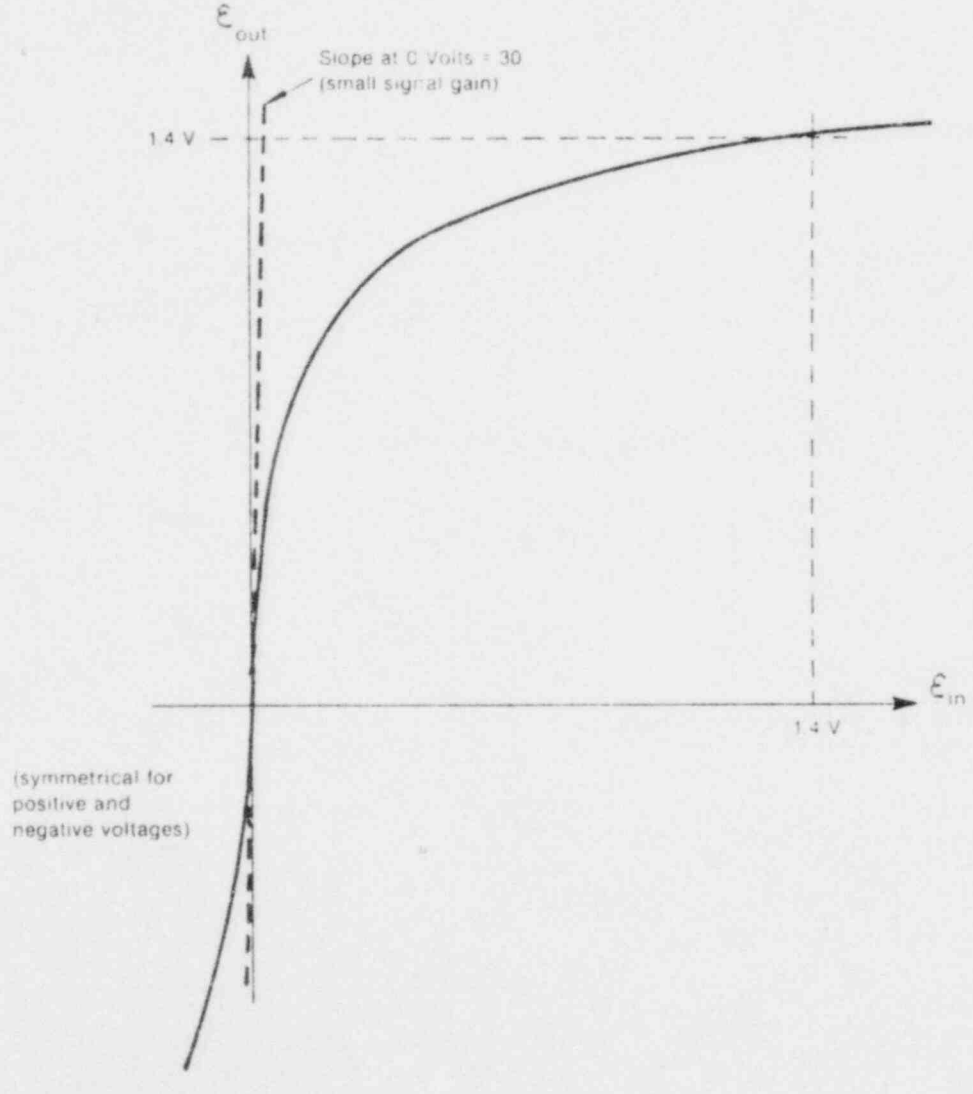

Figure 8 Signal Compression Circuit Schematic

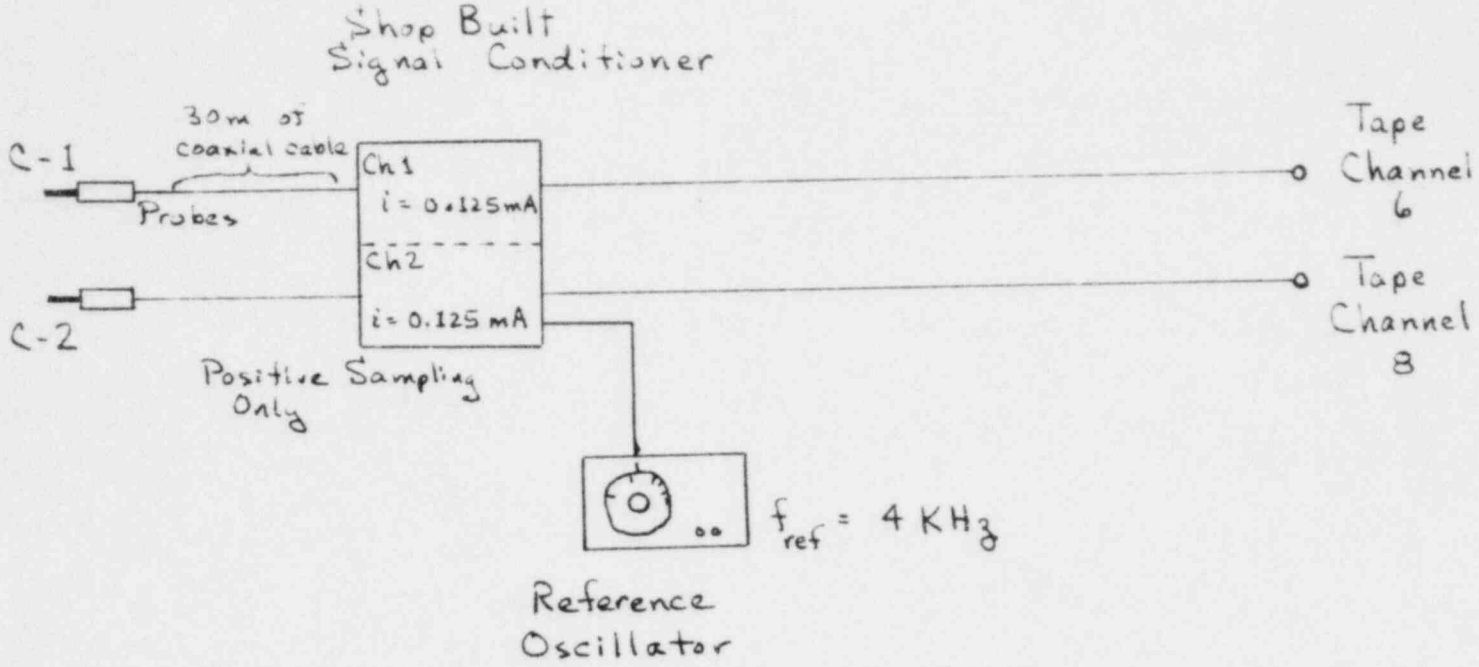

Figure 9 Conductivity Probe Electronics Configuration

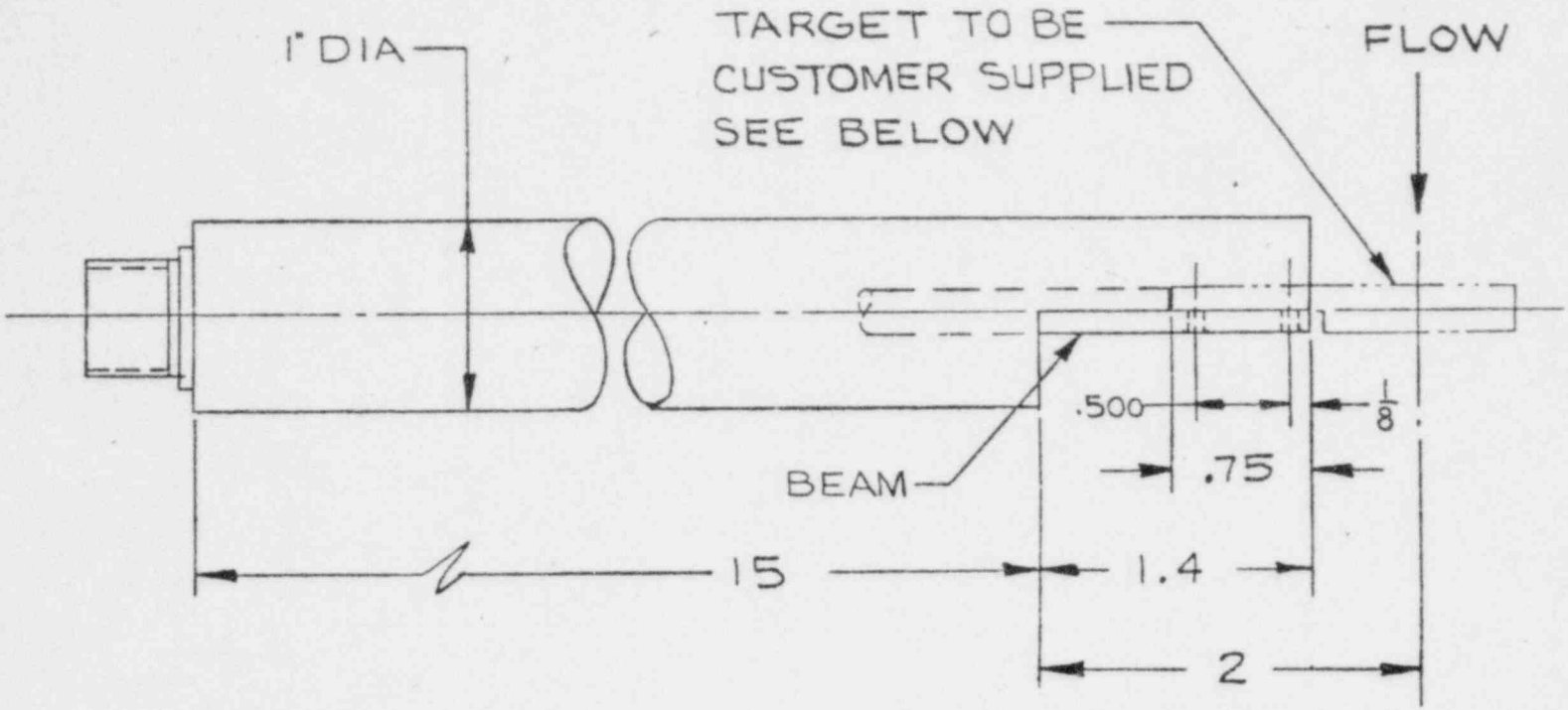

Figure 10
RAMAPO Transducer
Modification

RANGE: 2×10^3 TO 2×10^5 $lb/Ft\,SEC^2$

SIZE FOR EQUIVALENT TARGET
WITH DIA .422in TO .451in

MINIMUM SIGNAL 1.2 $\frac{MV}{V}$ @ FS

LTR. 141-118

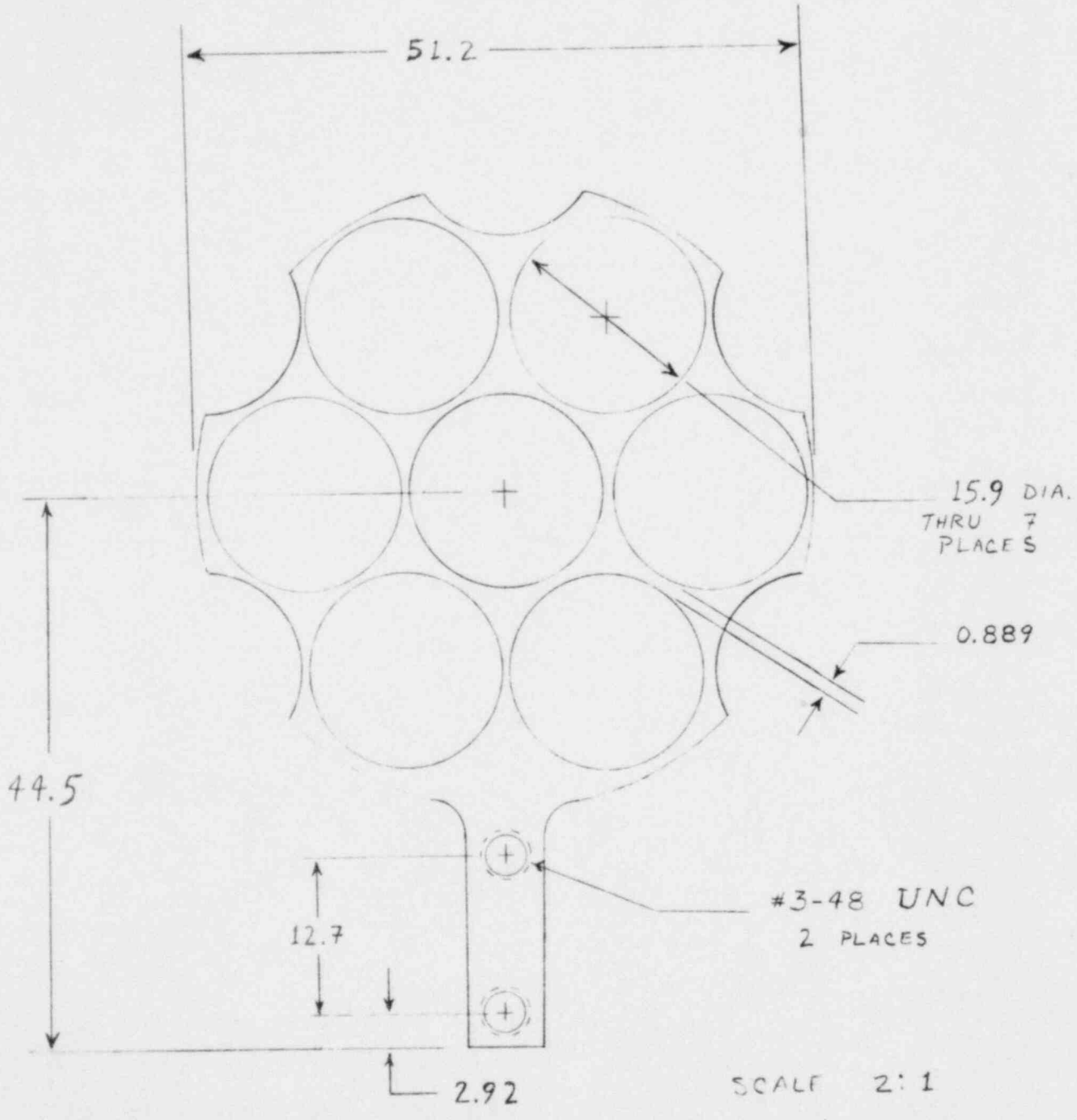

Figure 11 Drag Screen

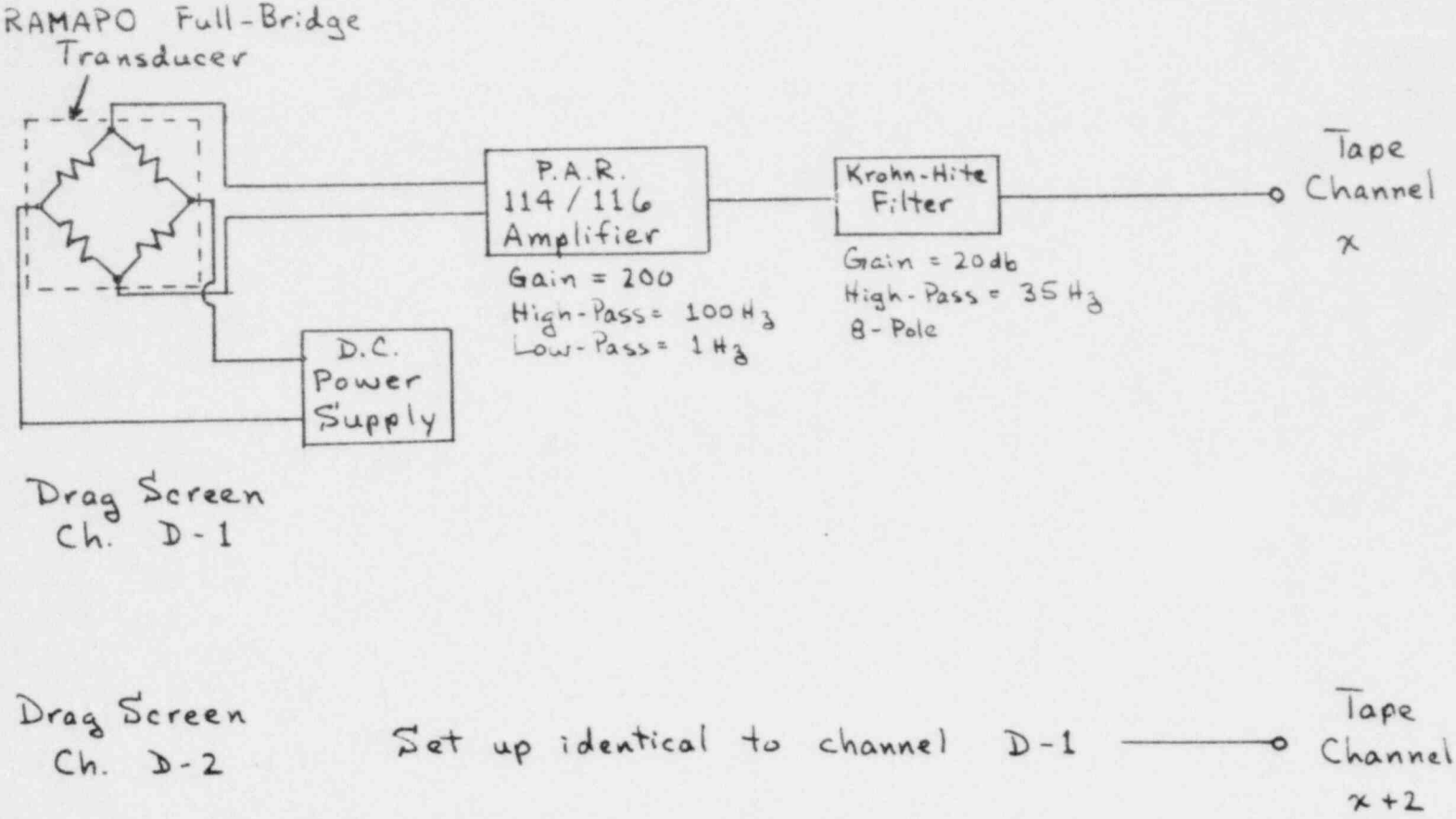

Figure 12 Drag Screen Signal Conditioning Configuration

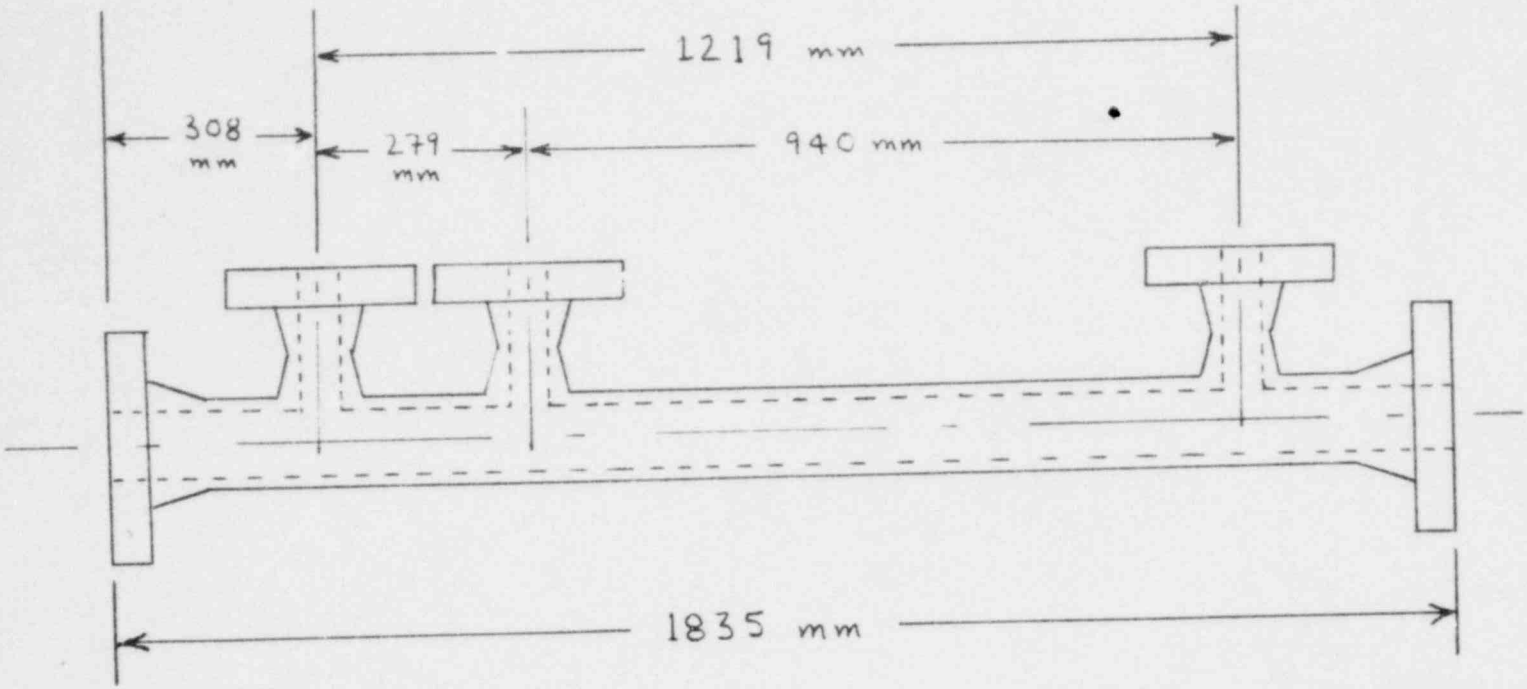

Plan View

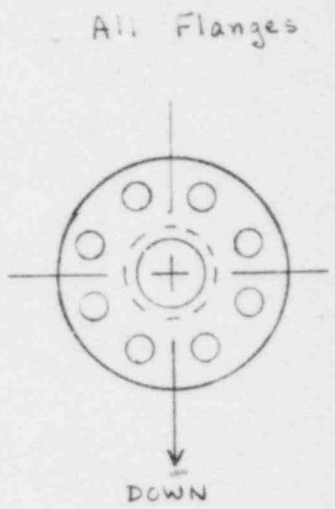

Bolt Hole Orientation

Figure 13 Test Spool Piece

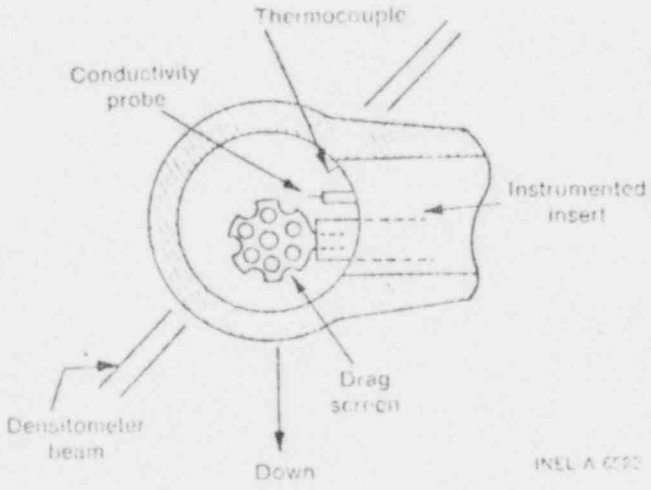

Figure 14 Instrumented Insert Sensor Configuration

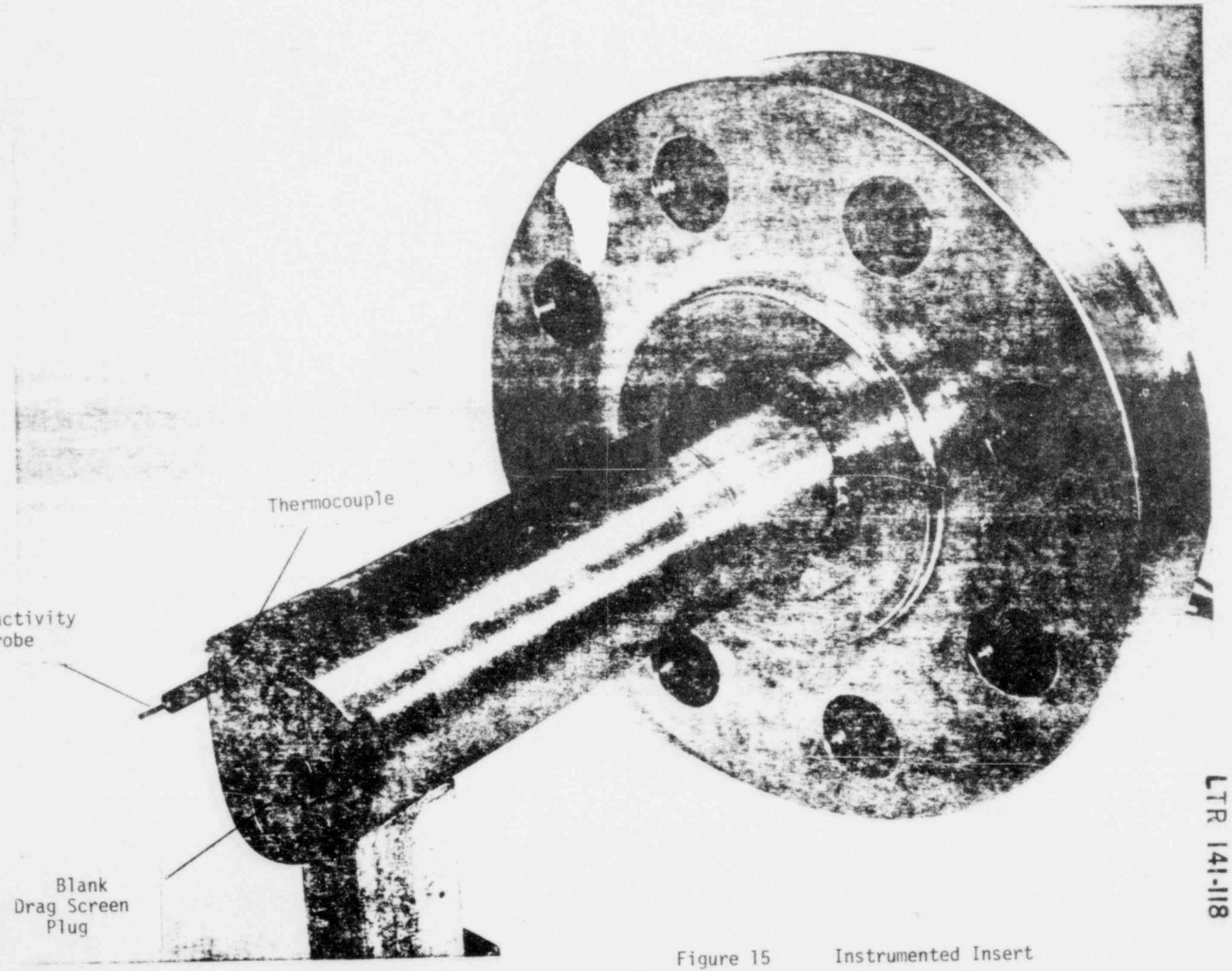

Figure 15 Instrumented Insert

LTR 141-118

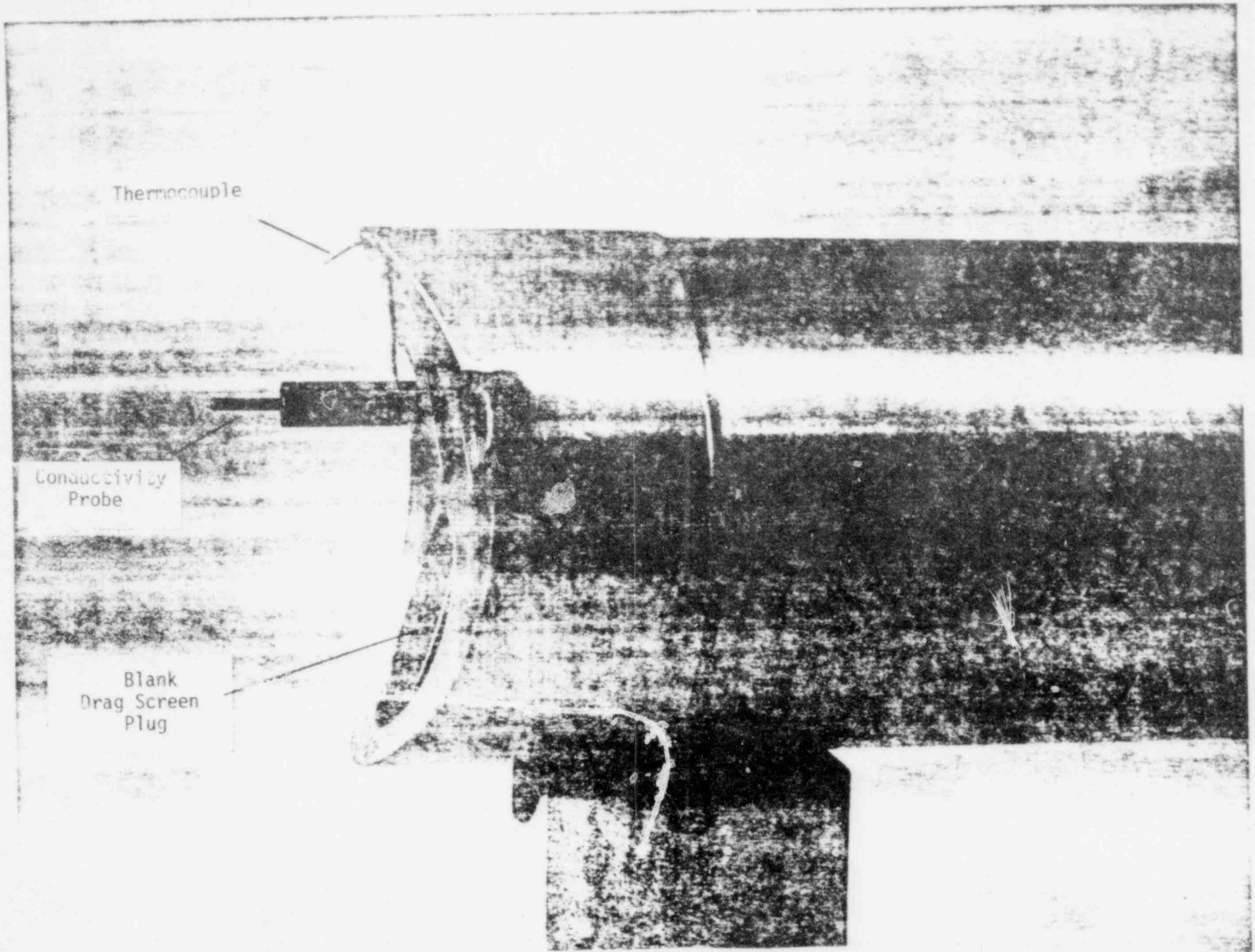

Figure 16 Close-up of Instrumented Insert

LTR 141-118

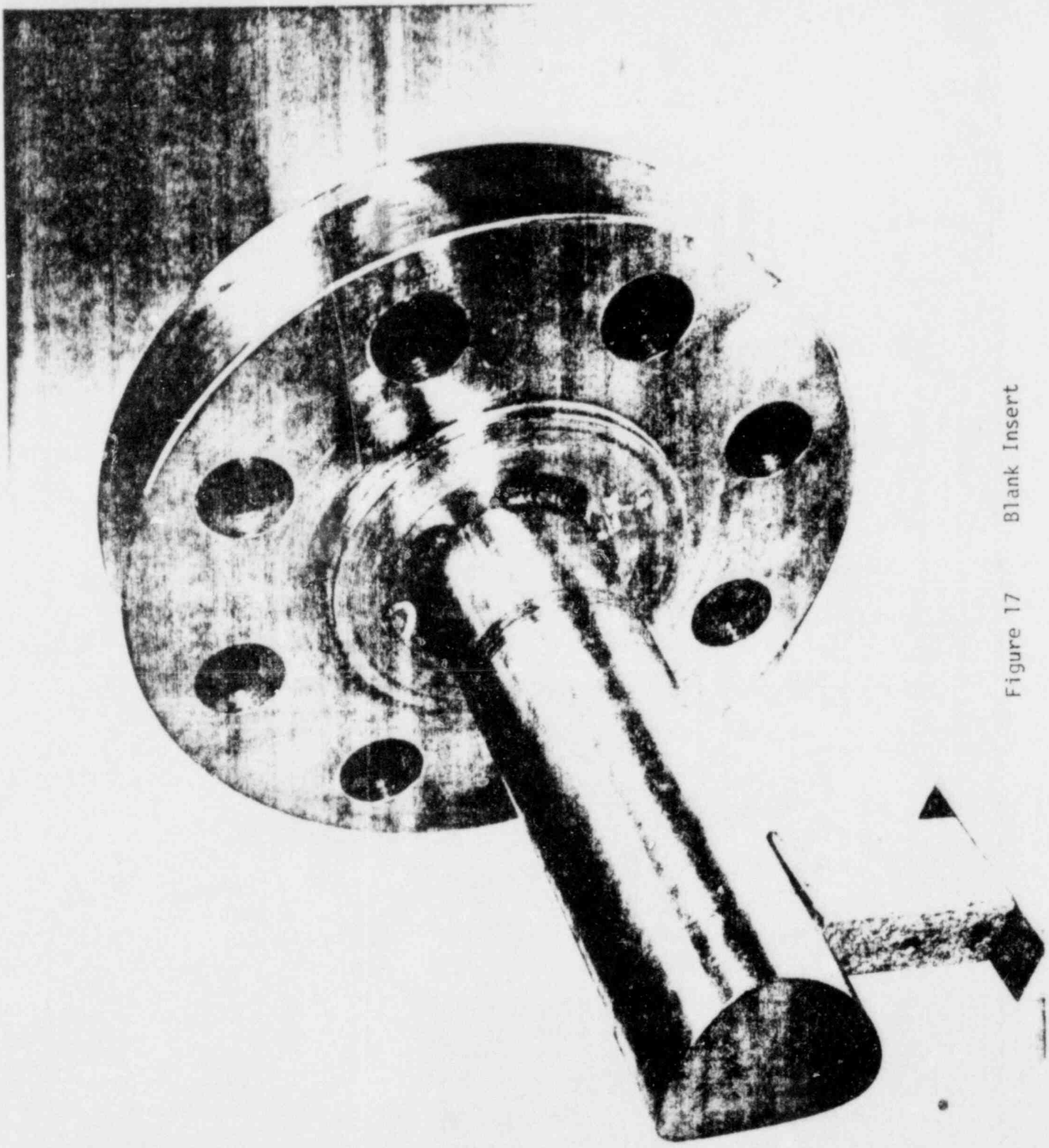

Figure 17 Blank Insert

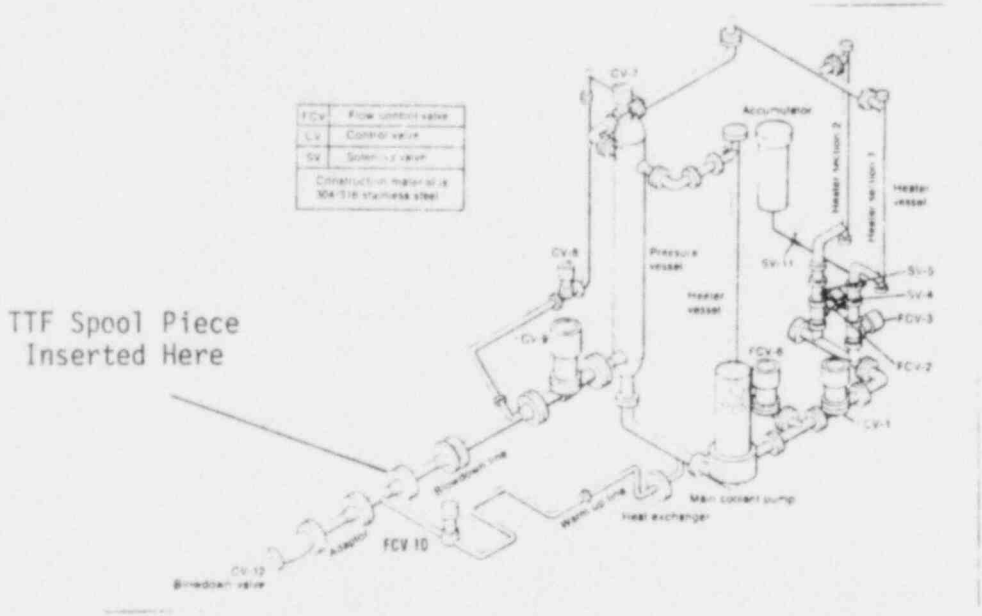

Figure 18 LTSF Blowdown Facility

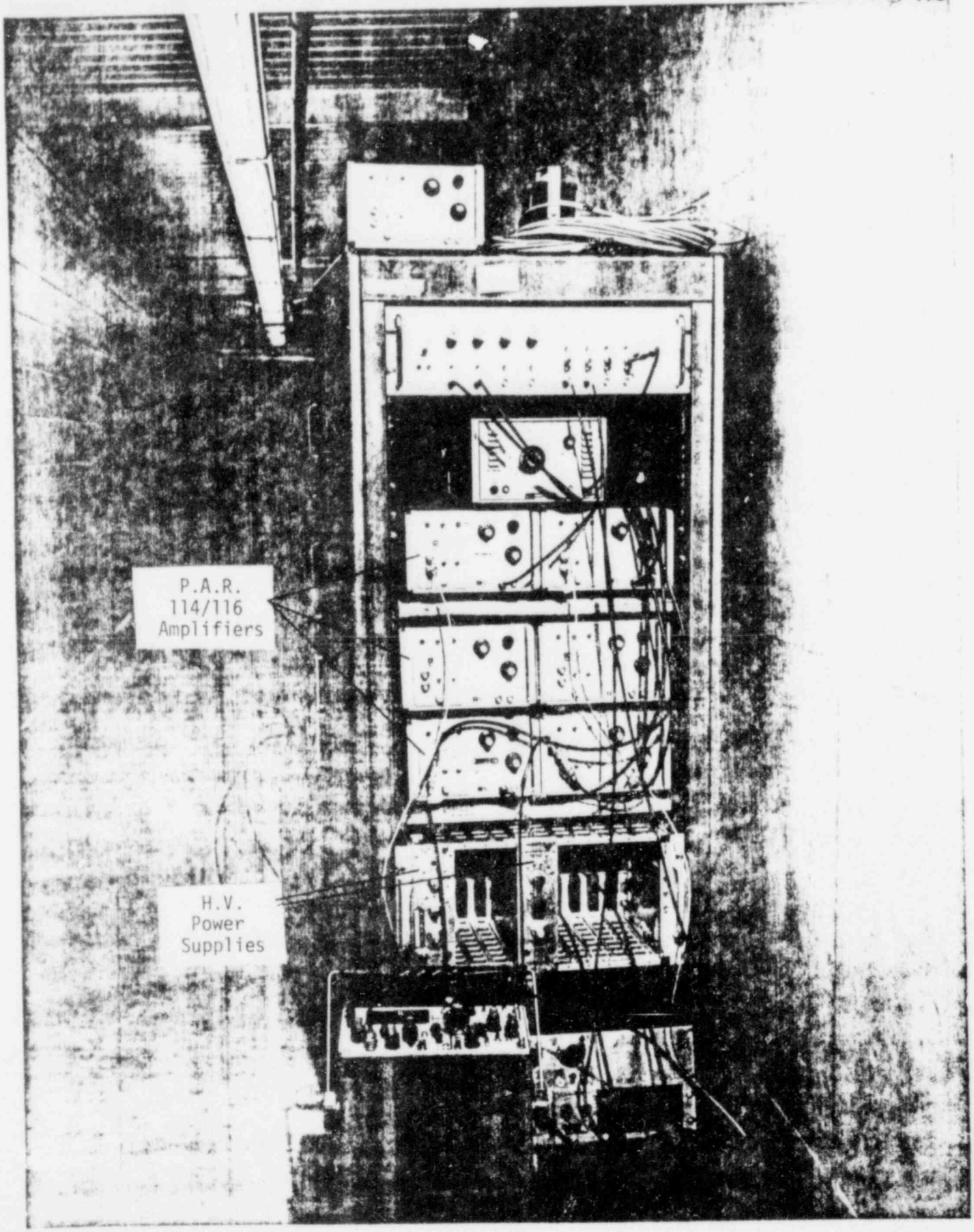

Figure 19 Data Acquisition and Signal Conditioning System

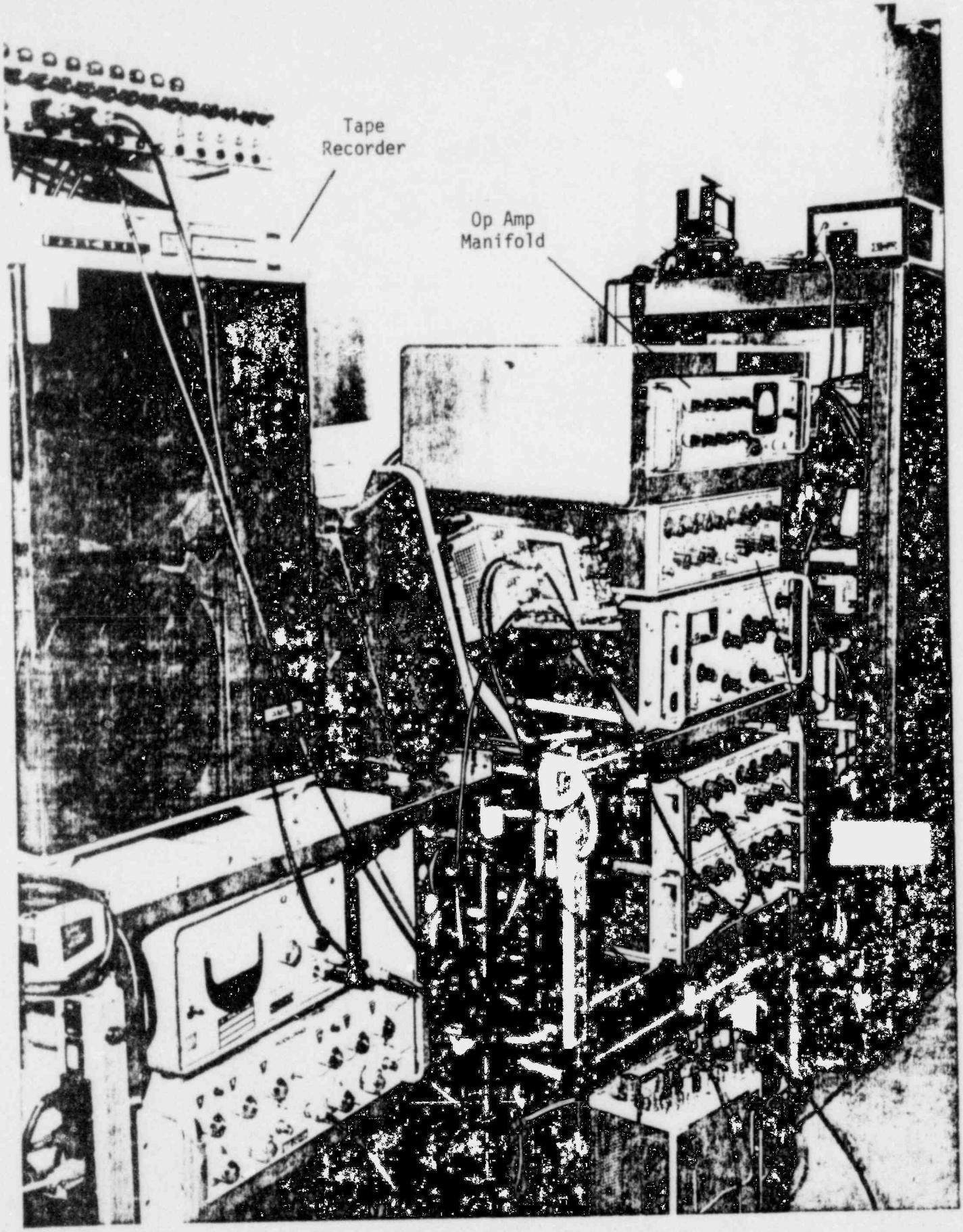

Figure 20 Data Acquisition and Signal Conditioning Sustem

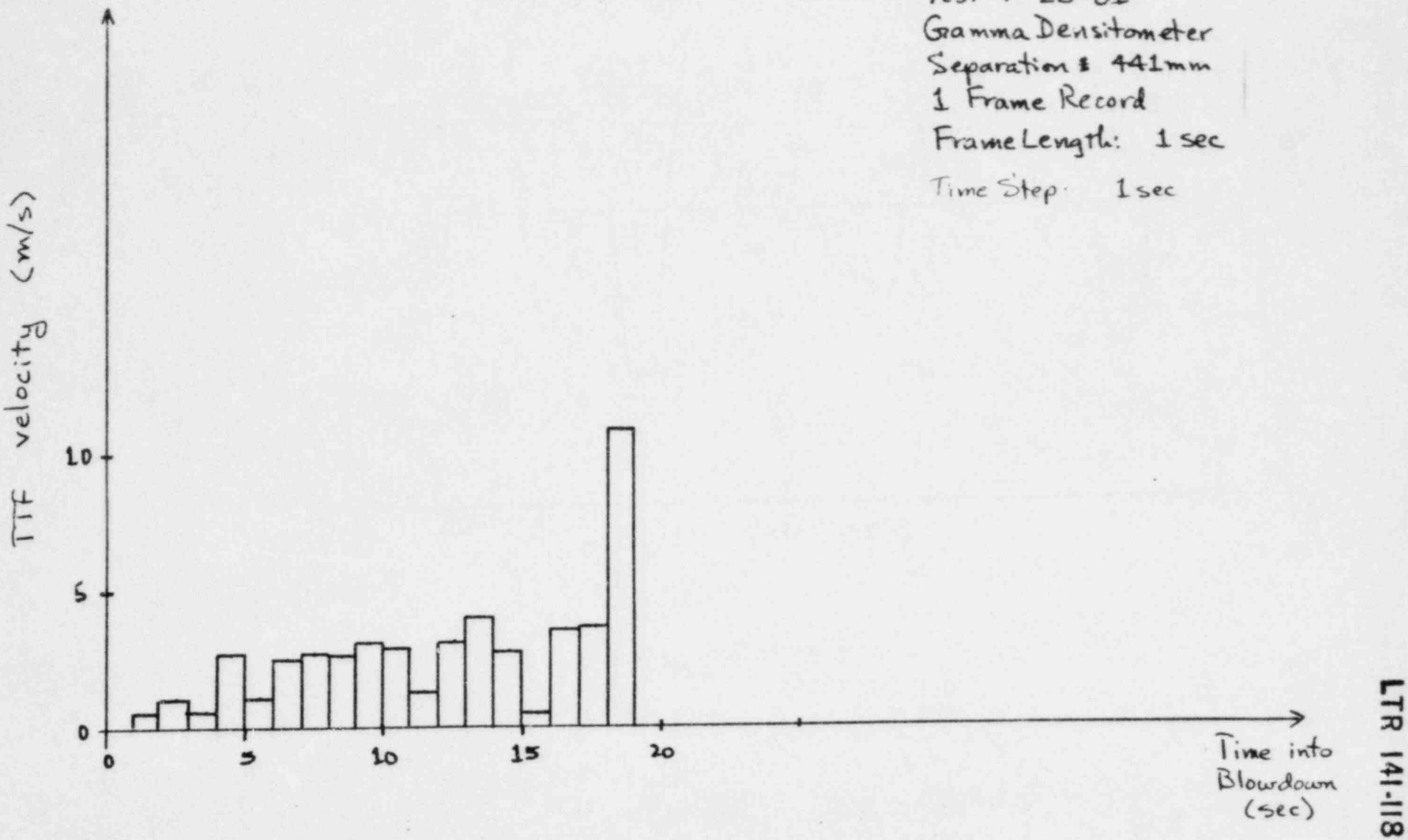

Figure 21 Time Sequence No. 1, Gamma Densitometer, F-28-01

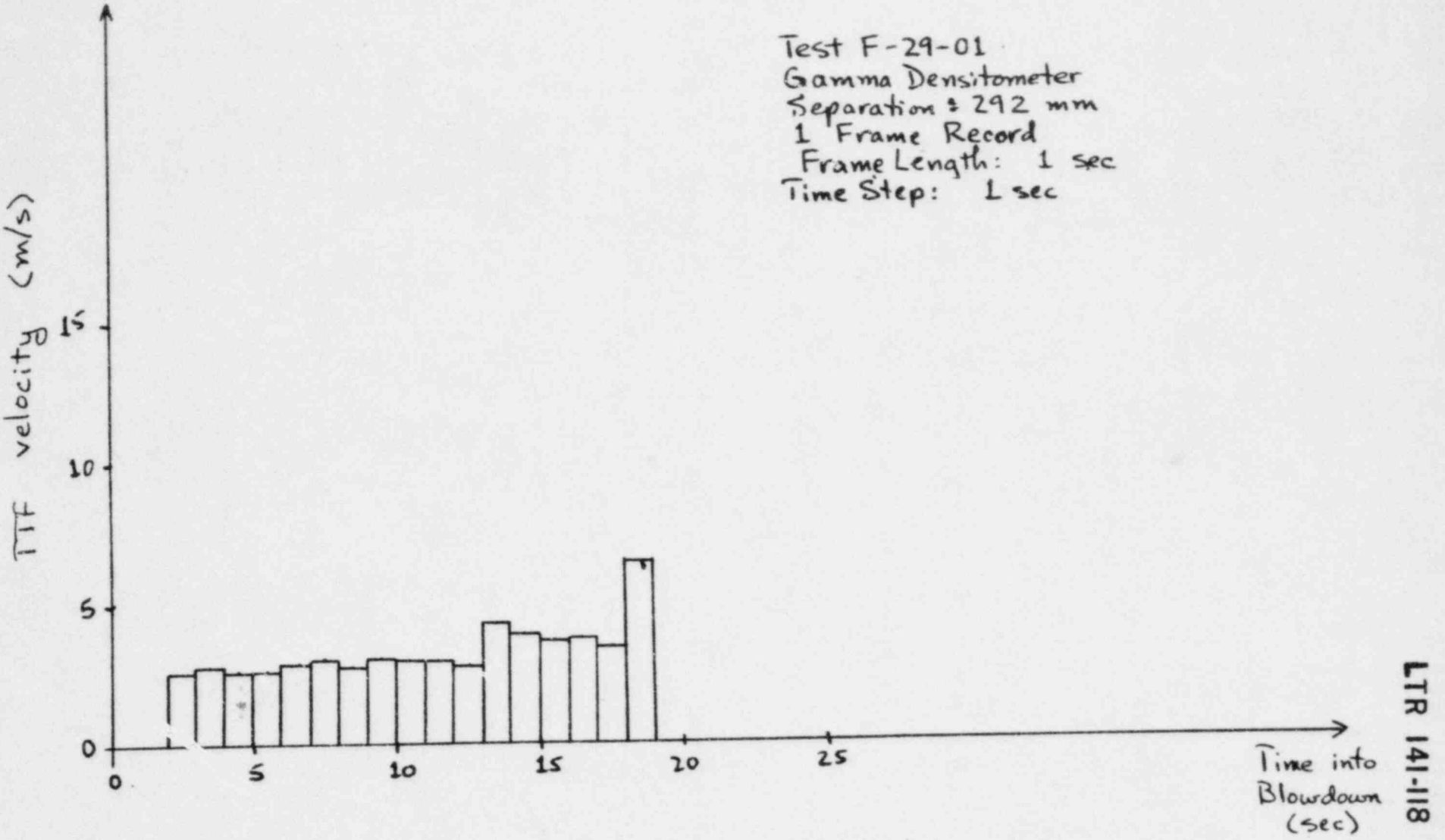

Figure 22 Time Sequence No. 2, Gamma Densitometer, F-29-01

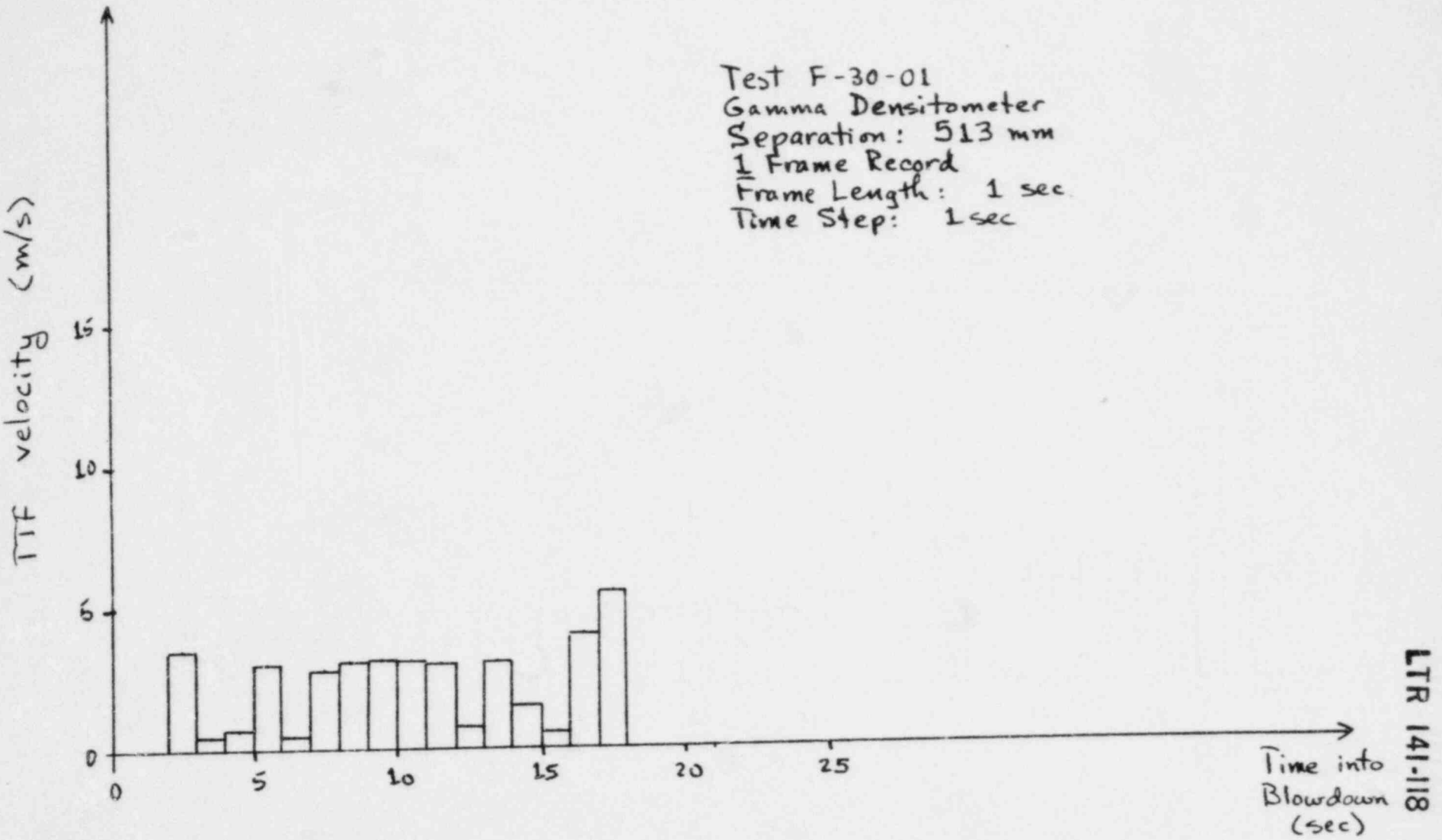

Figure 23 Time Sequence No. 3, Gamma Densitometer, F-30-01

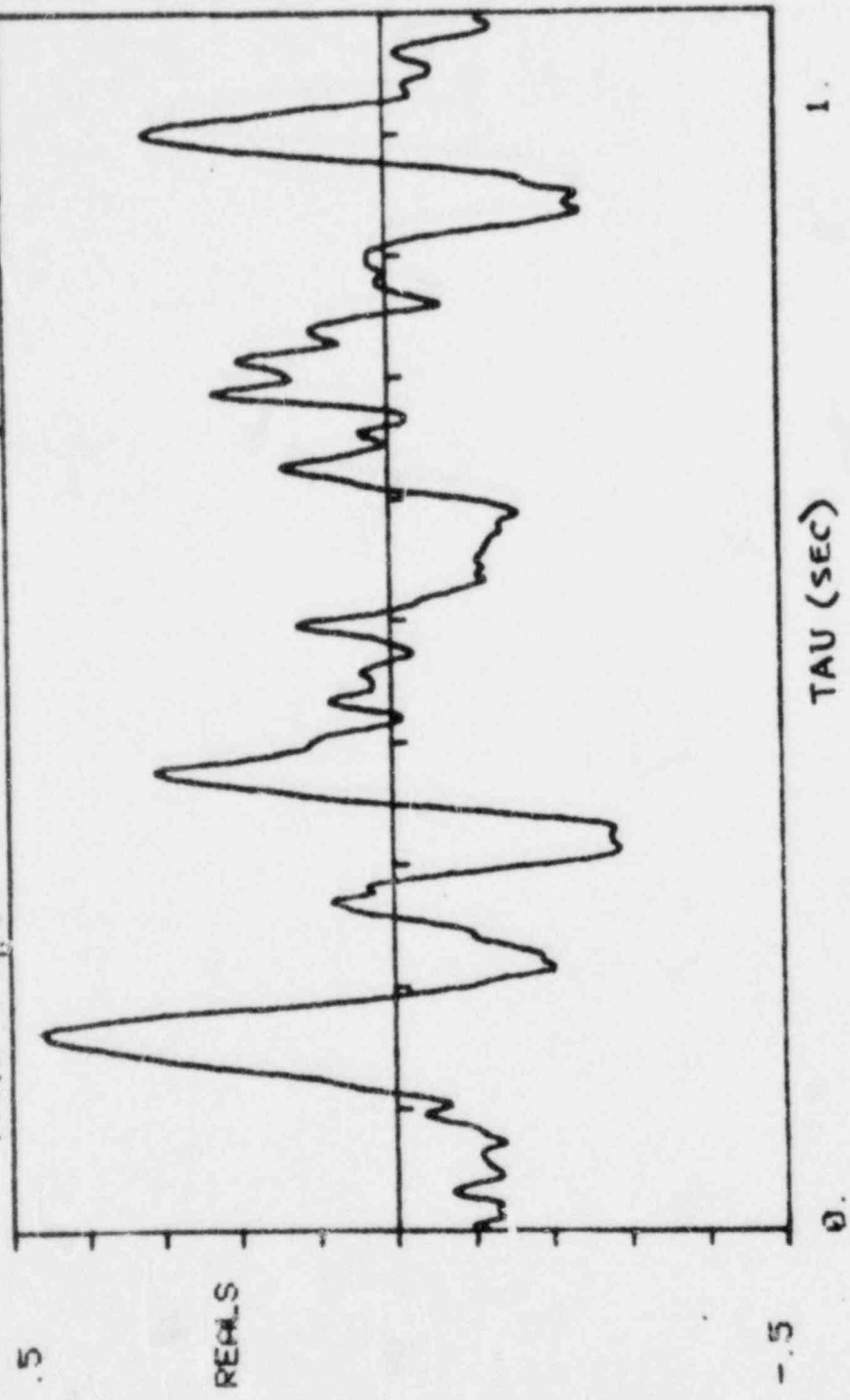

Figure 24 Cross-Correlogram, Time Sequence No. 1

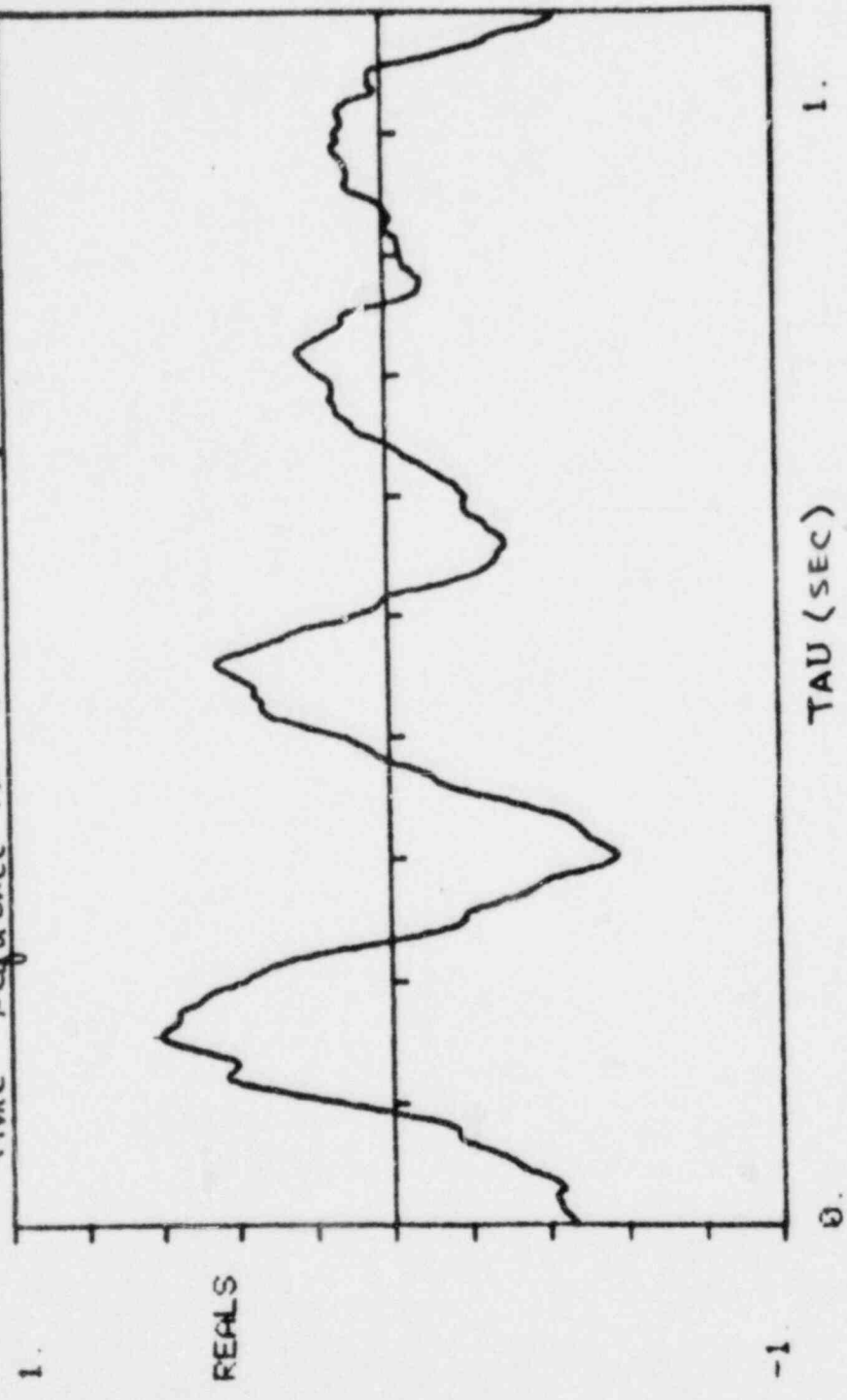

Figure 25 Cross-Correlogram, Time Sequence No. 1

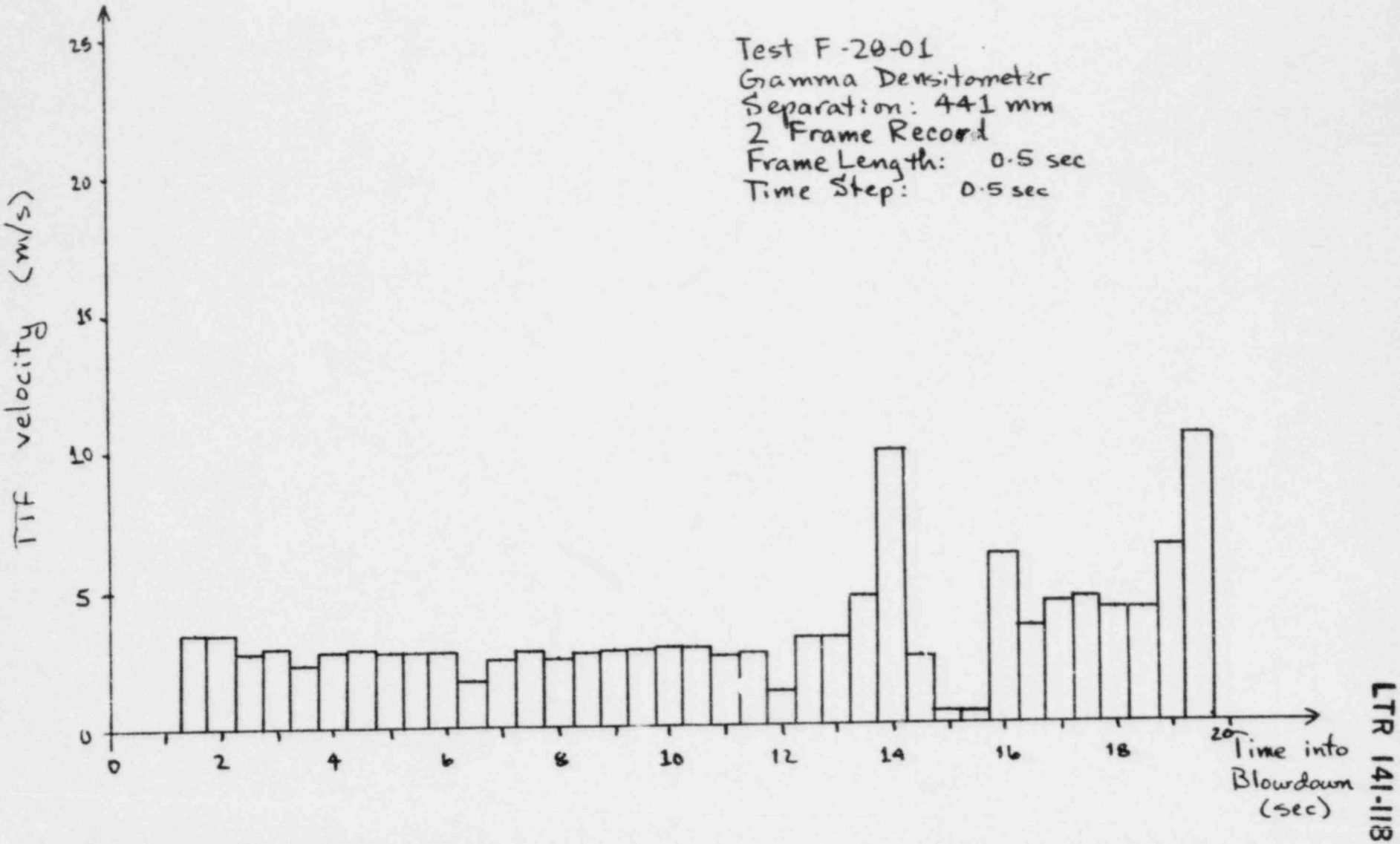

Figure 26 Time Sequence No. 4, Gamma Densitometer, F-28-01

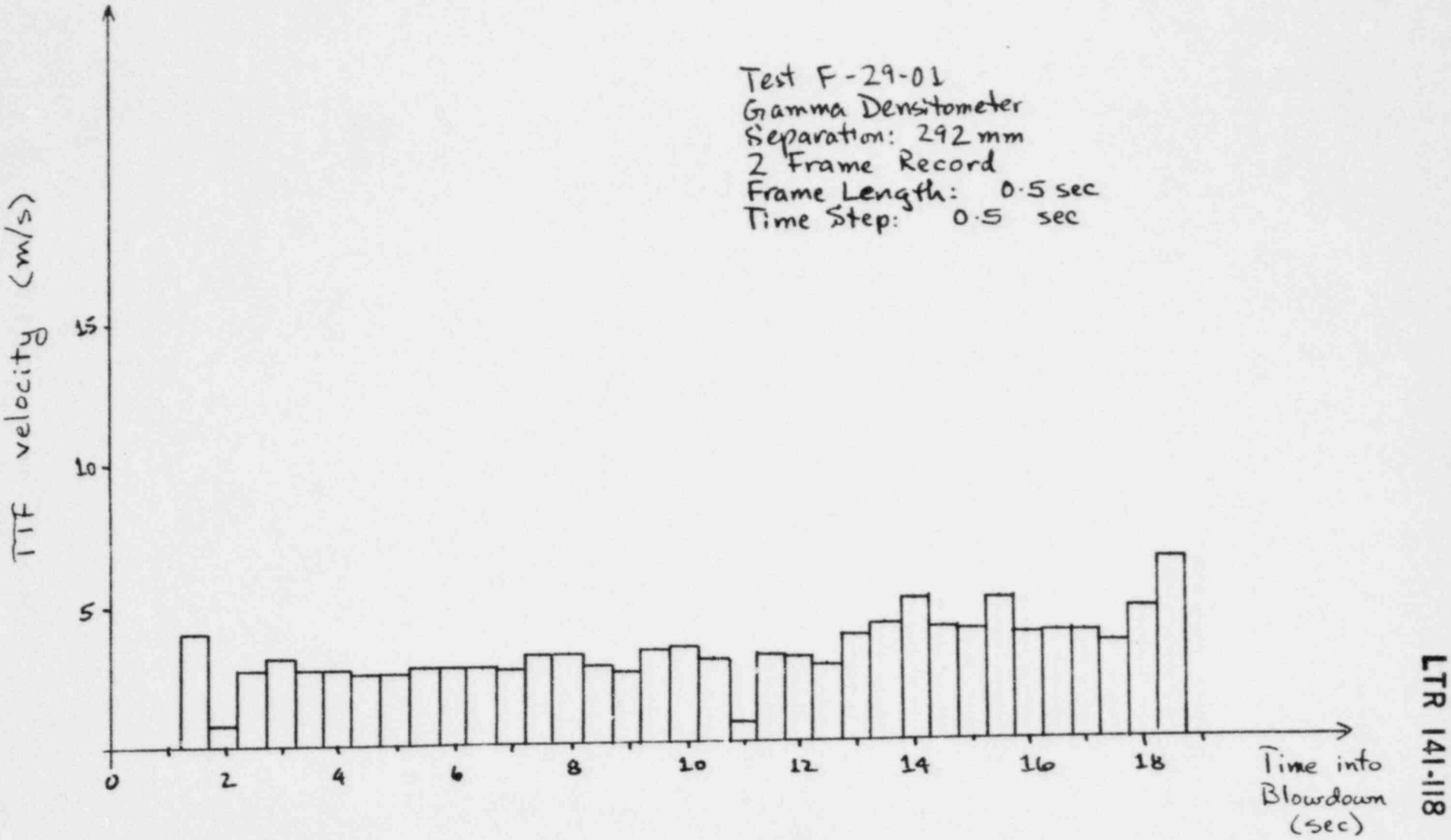

Figure 27 Time Sequence No. 5, Gamma Densitometer, F-29-01

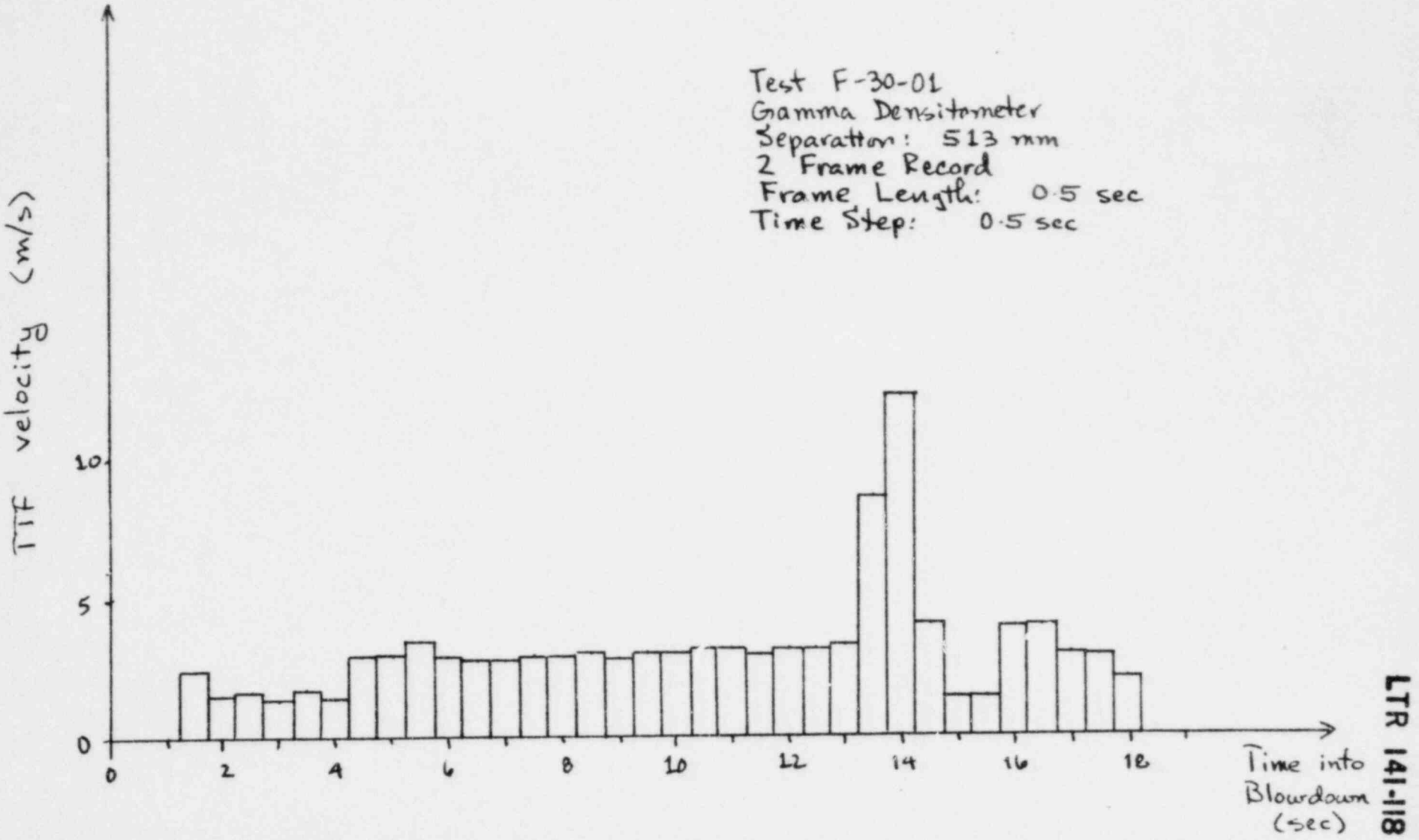

Figure 28 Time Sequence No. 6, Gamma Densitometer, F-30-01

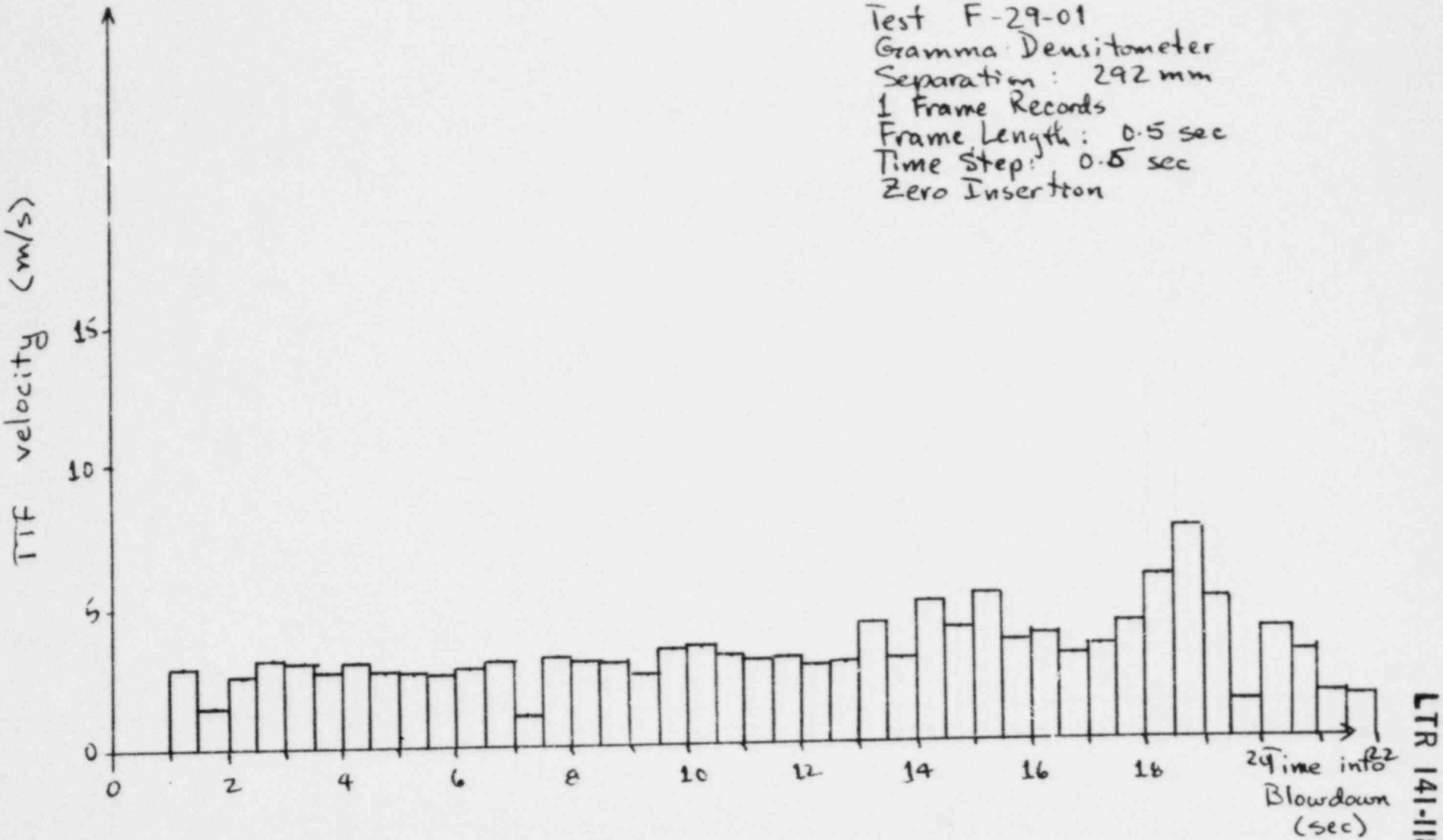

Figure 29 Time Sequence No. 7, Gamma Densitometer, F-29-01, Zero-Insertion

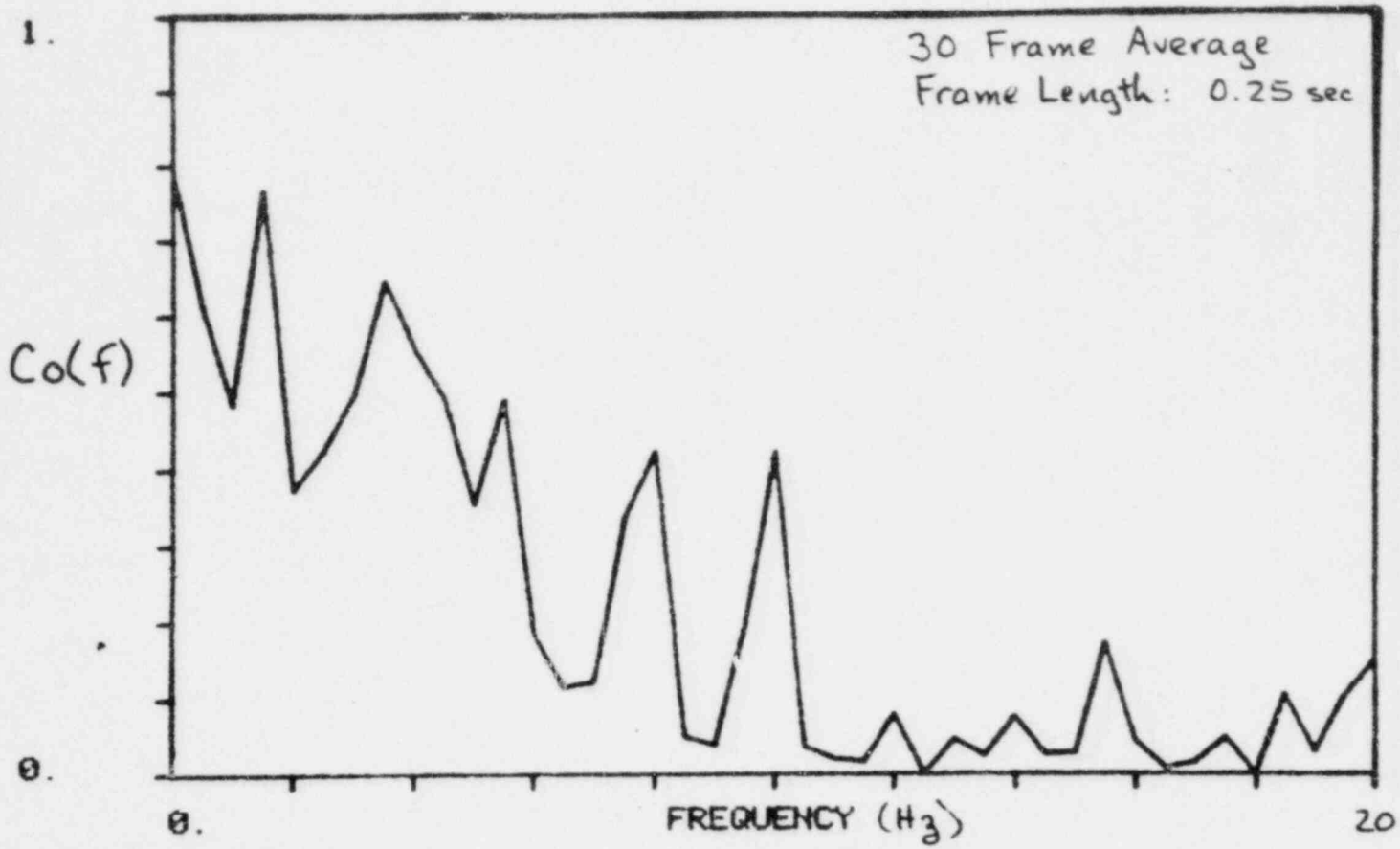

Figure 30 Coherence Function, F-28-01

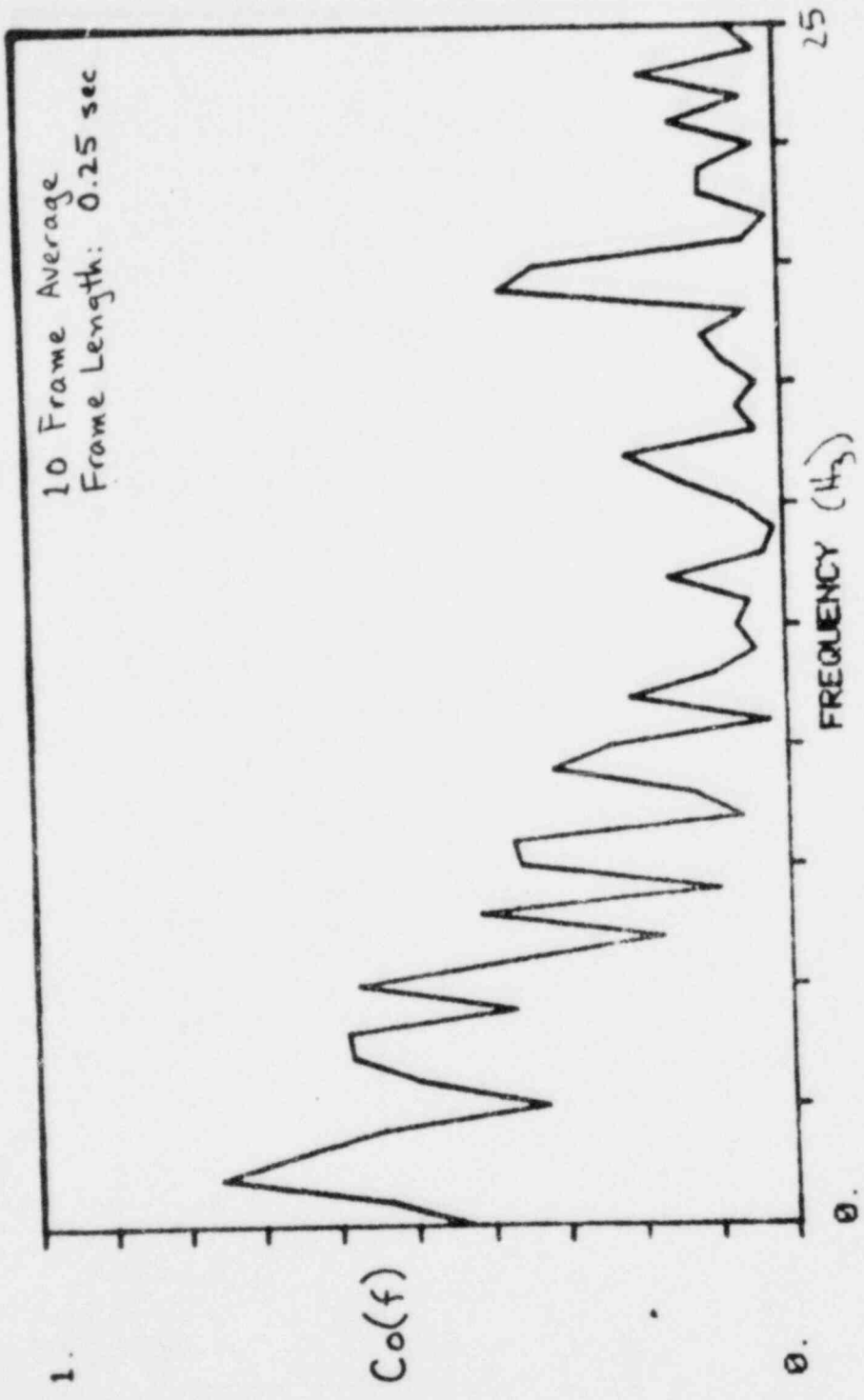

Figure 31 Coherence Function, F-28-01

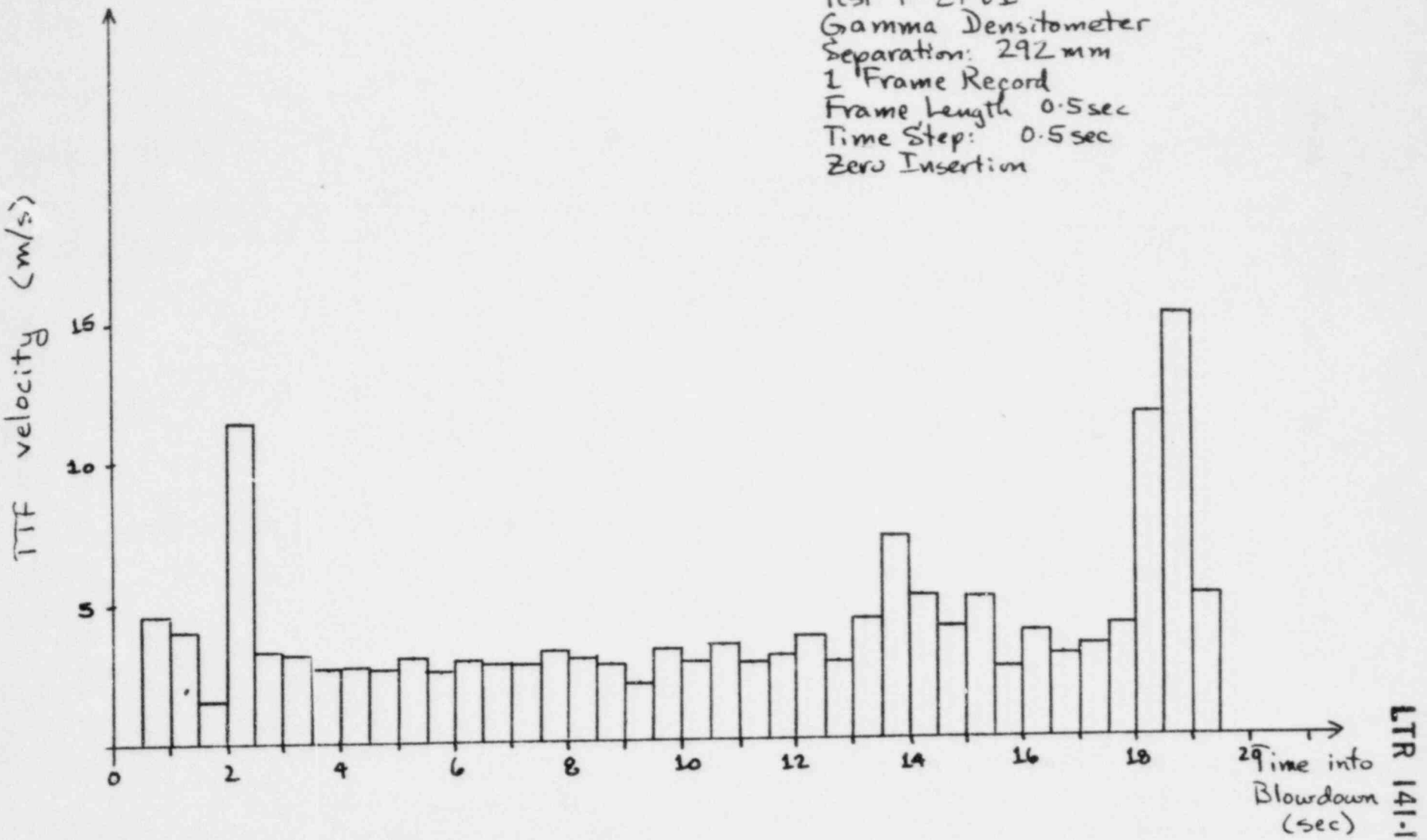

Figure 32 Time Sequence No. 8, Gamma Densitometer, F-29-01

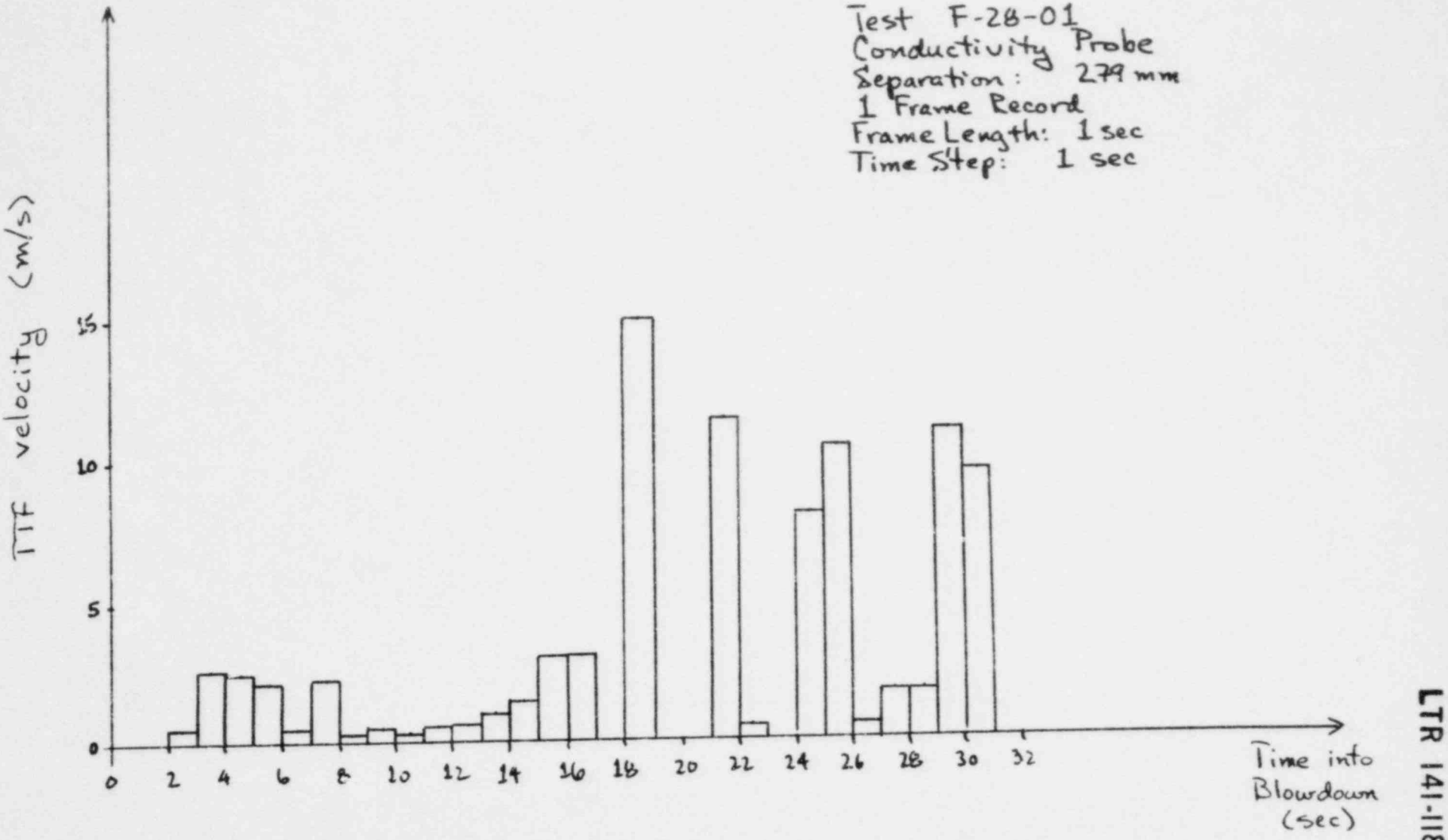

LTR 141-118

Figure 33 Time Sequence No. 9, Conductivity Probe, F-28-01

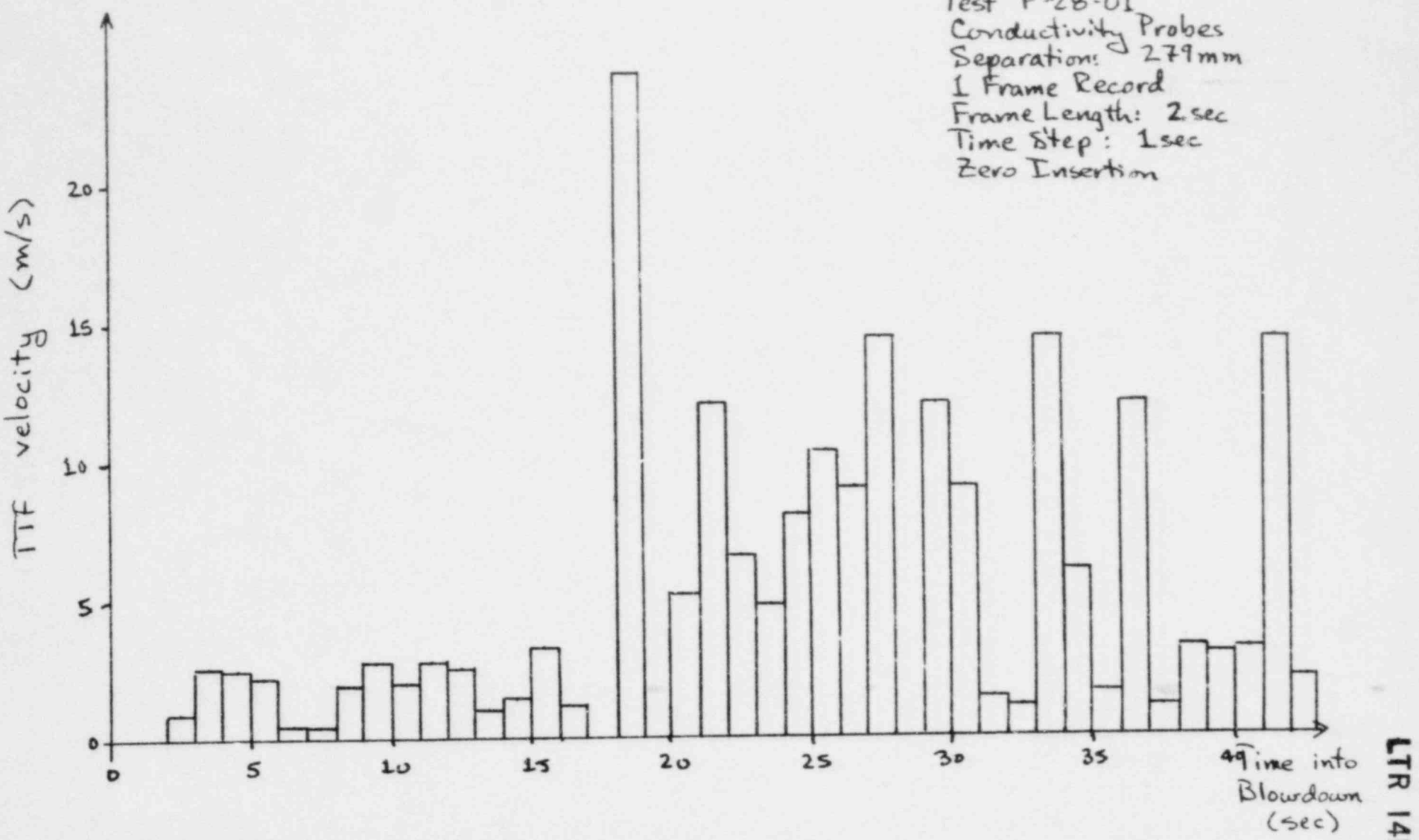

Figure 34 Time Sequence No. 10, Conductivity Probe, F-28-01

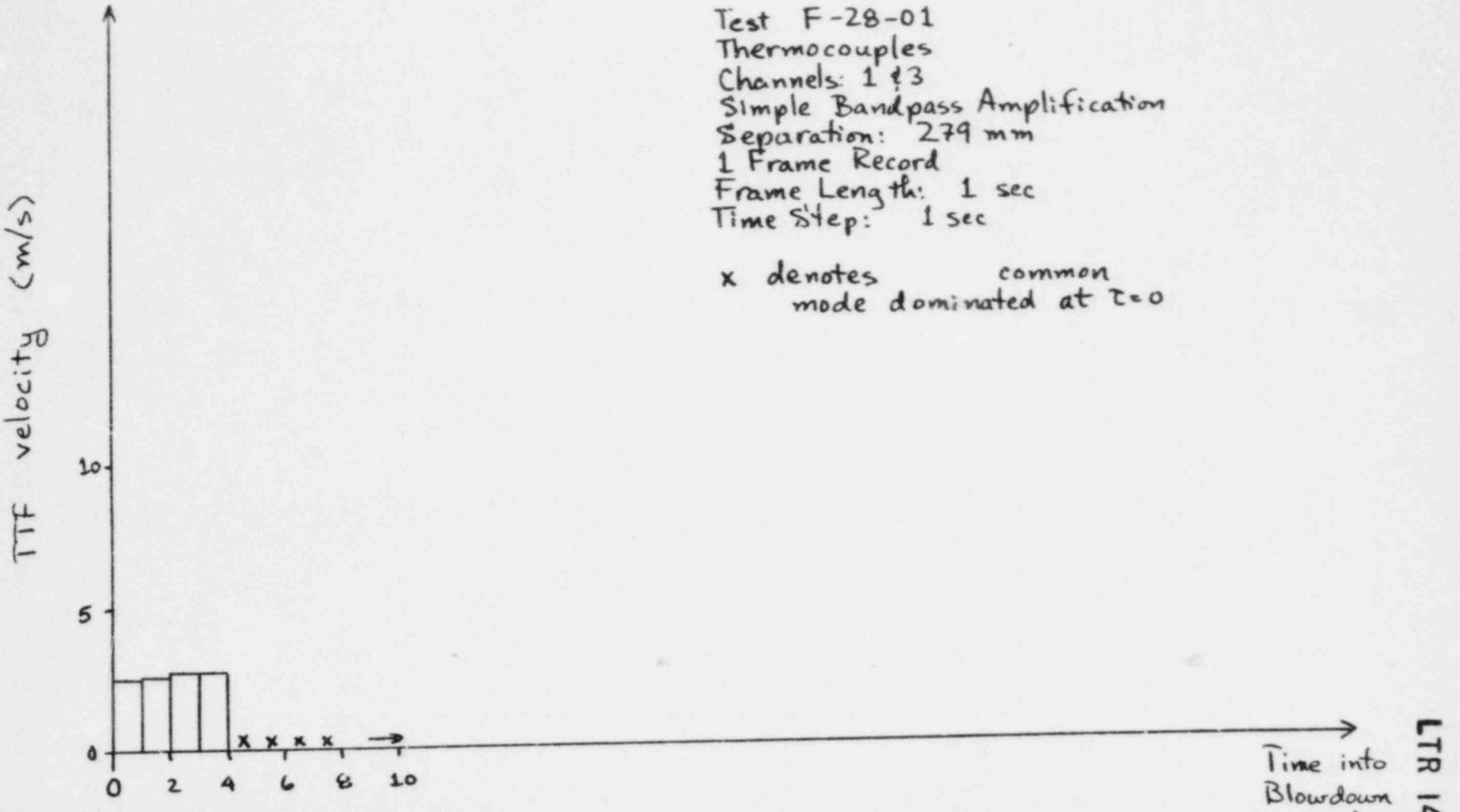

Figure 35 Time Sequence No. 11, Thermocouple, F-28-01, Straight Amplification

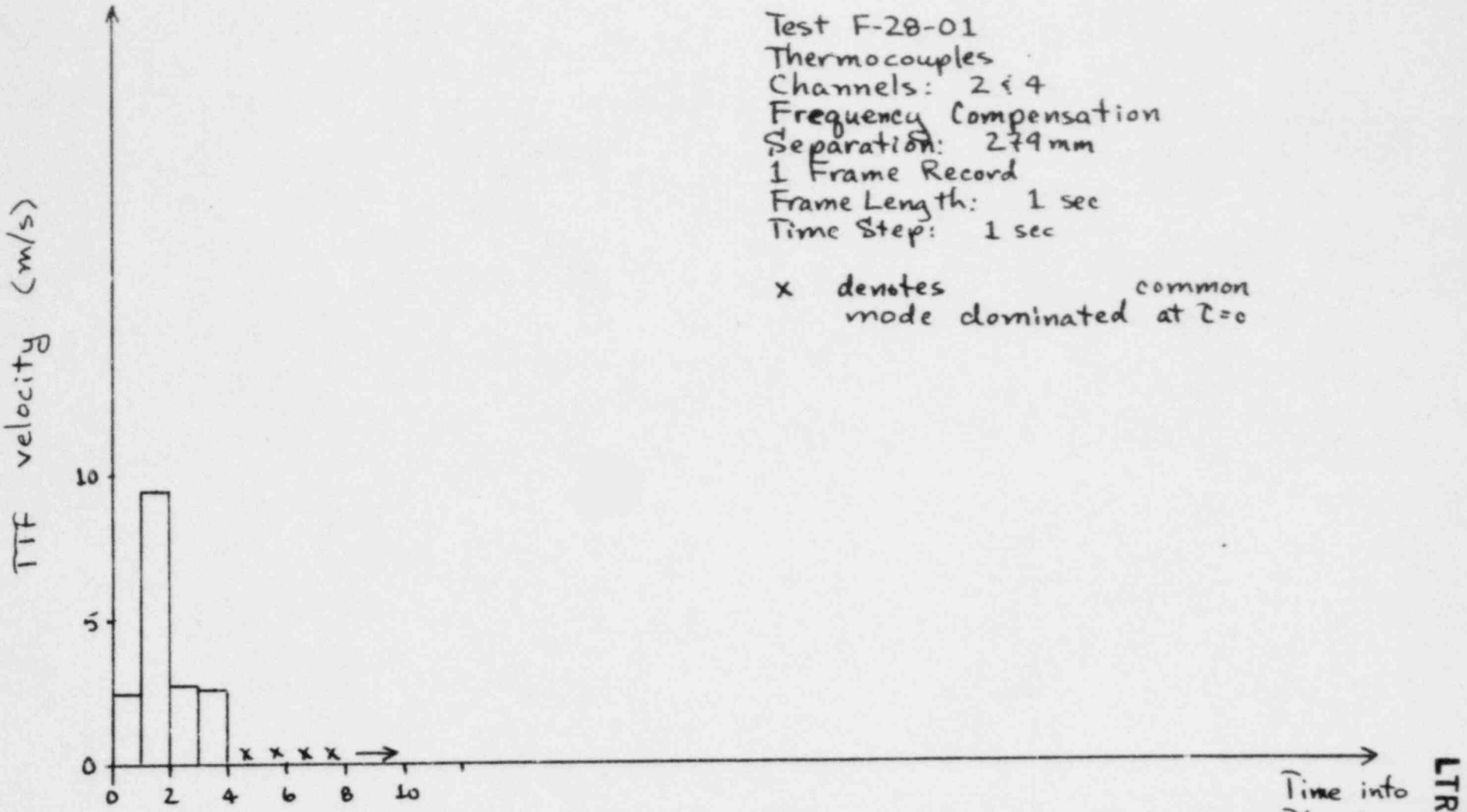

Figure 36 Time Sequence No. 12, Thermocouple, F-28-01, Frequency Compensation

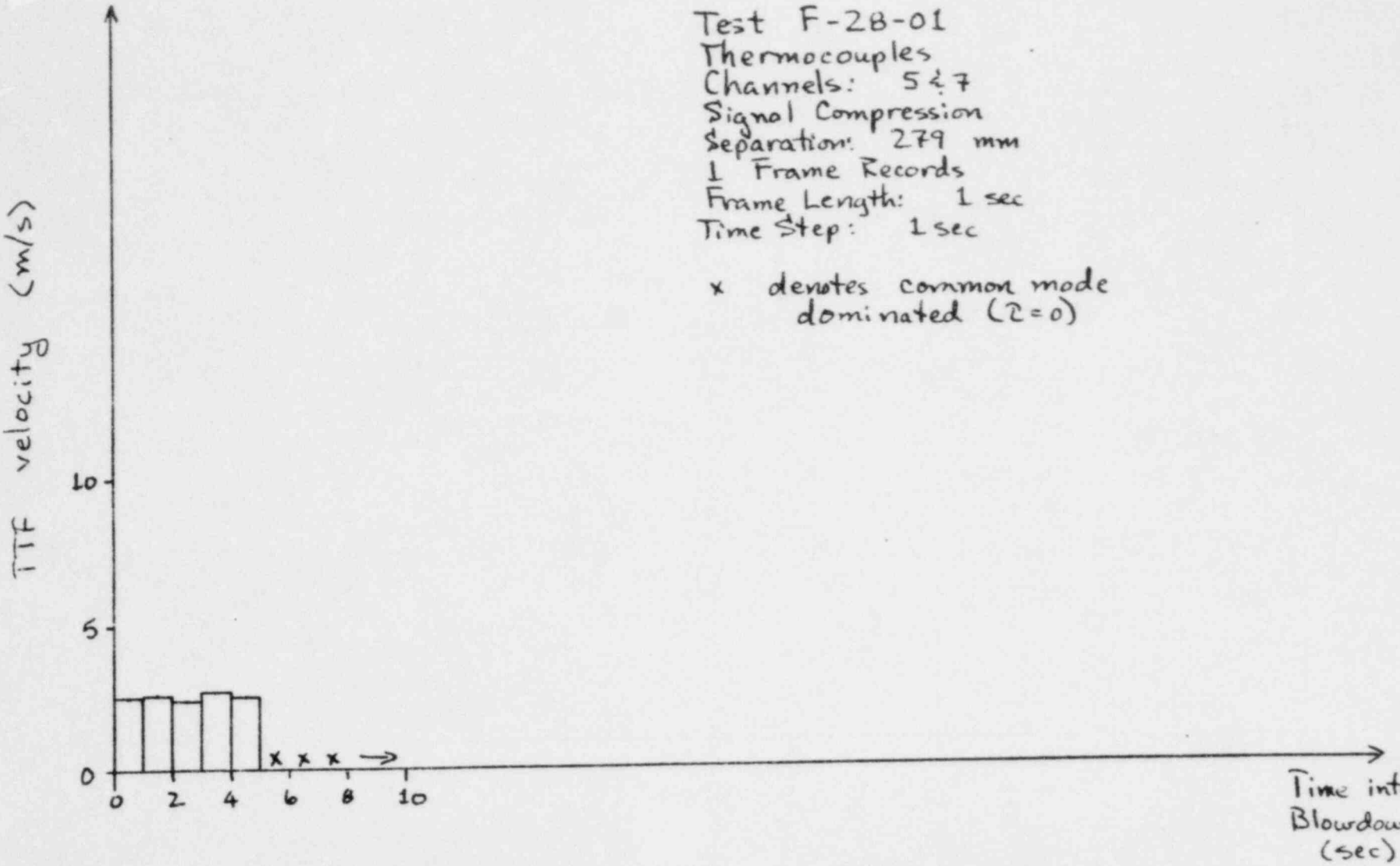

Figure 37 Time Sequence No. 13, Thermocouple, F-28-01, Signal Compression

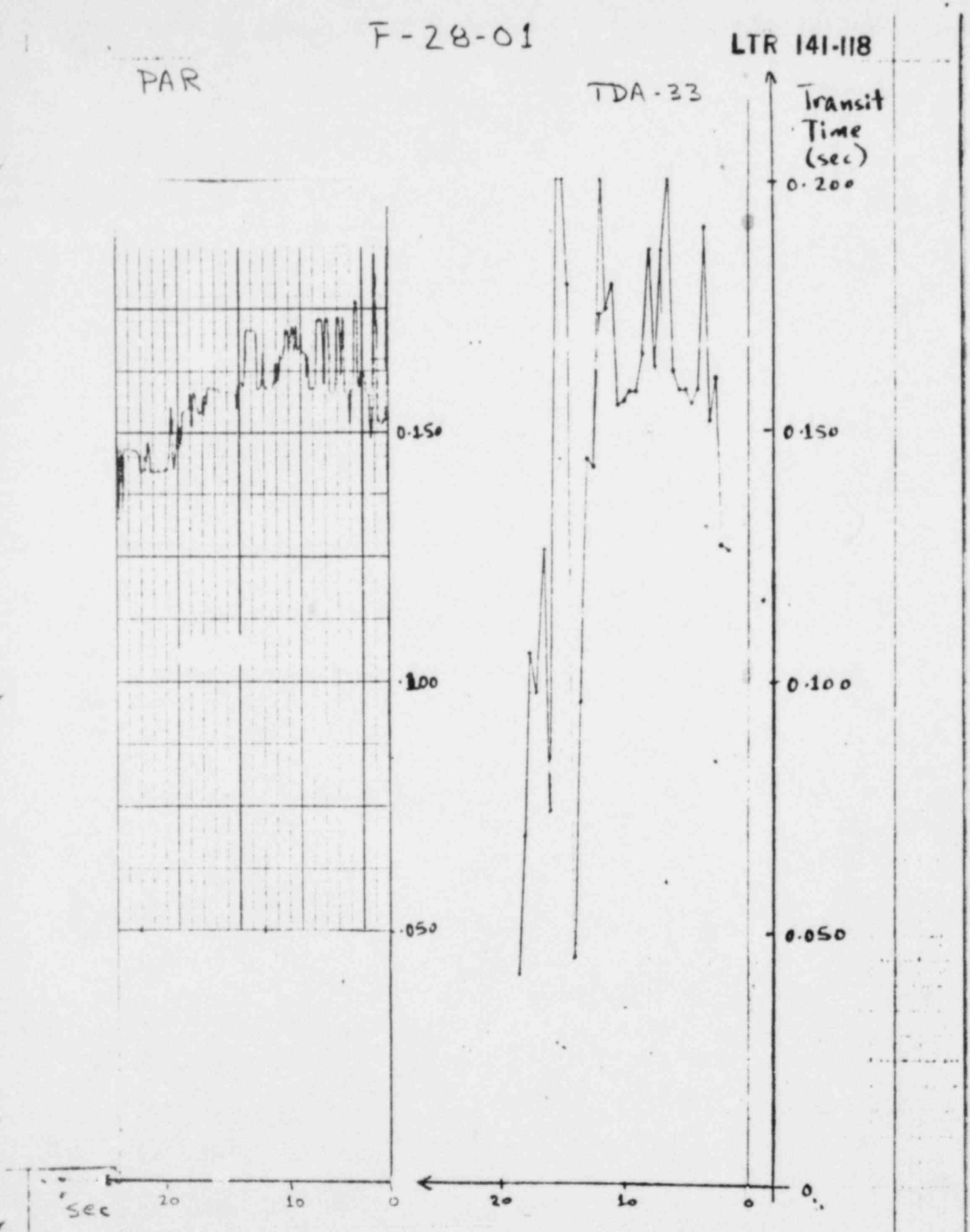

Figure 38 Transit Time Graph, F-28-01

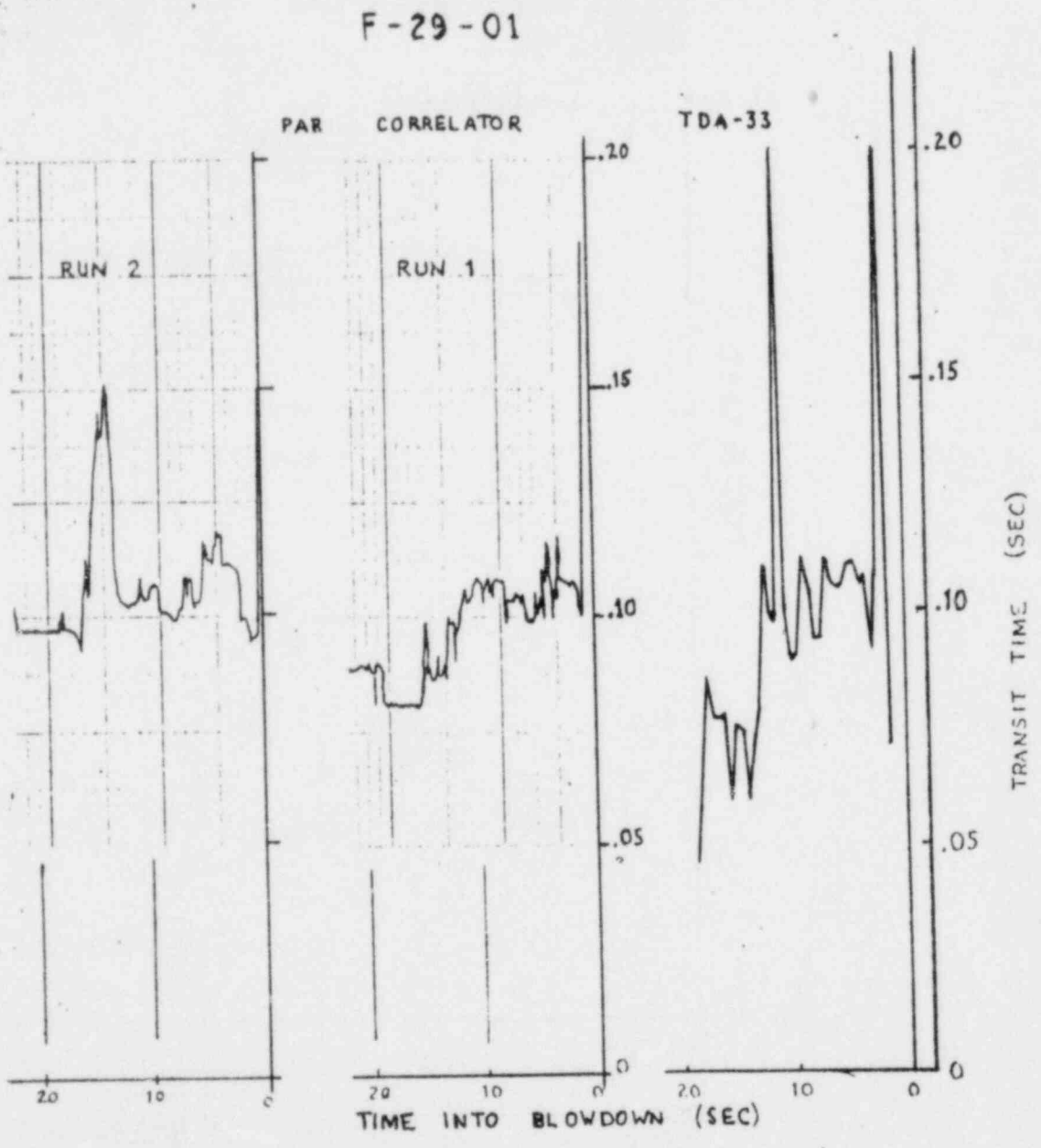

Figure 39 Transit Time Graph, F-29-01

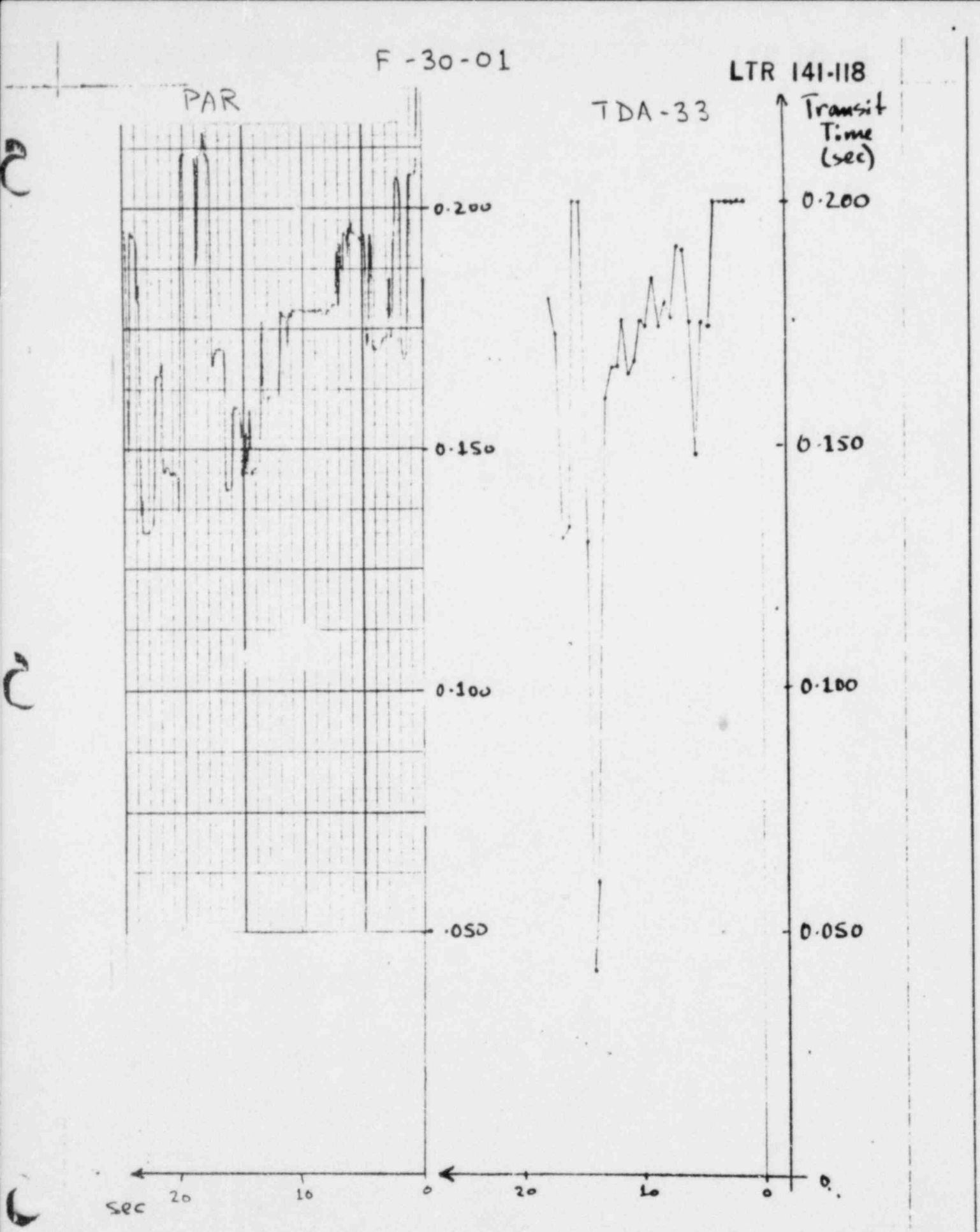

Figure 40 Transit Time Graph, F-30-01

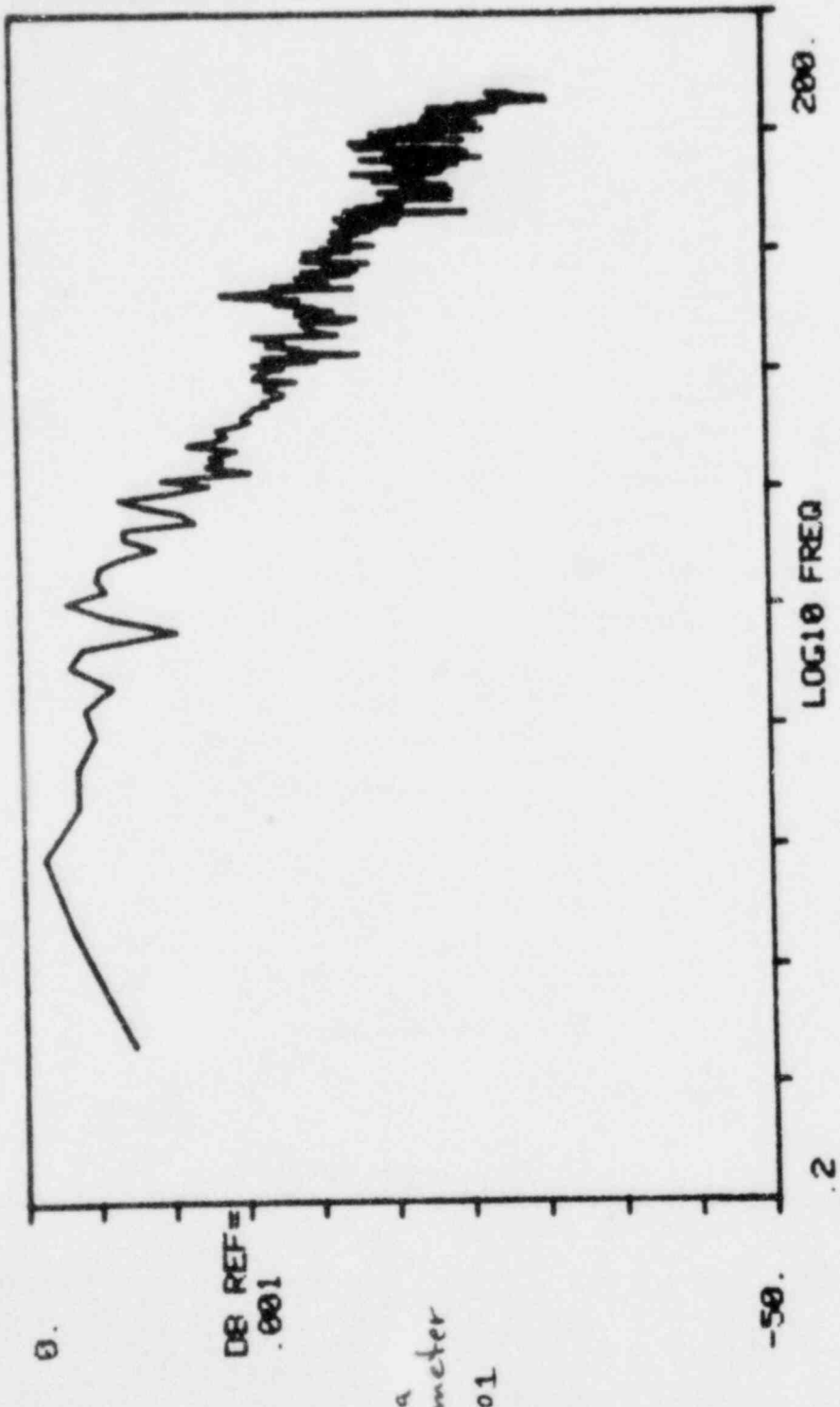

Figure 41 Auto-Spectral Density, Gamma Densitometer, F-29-01

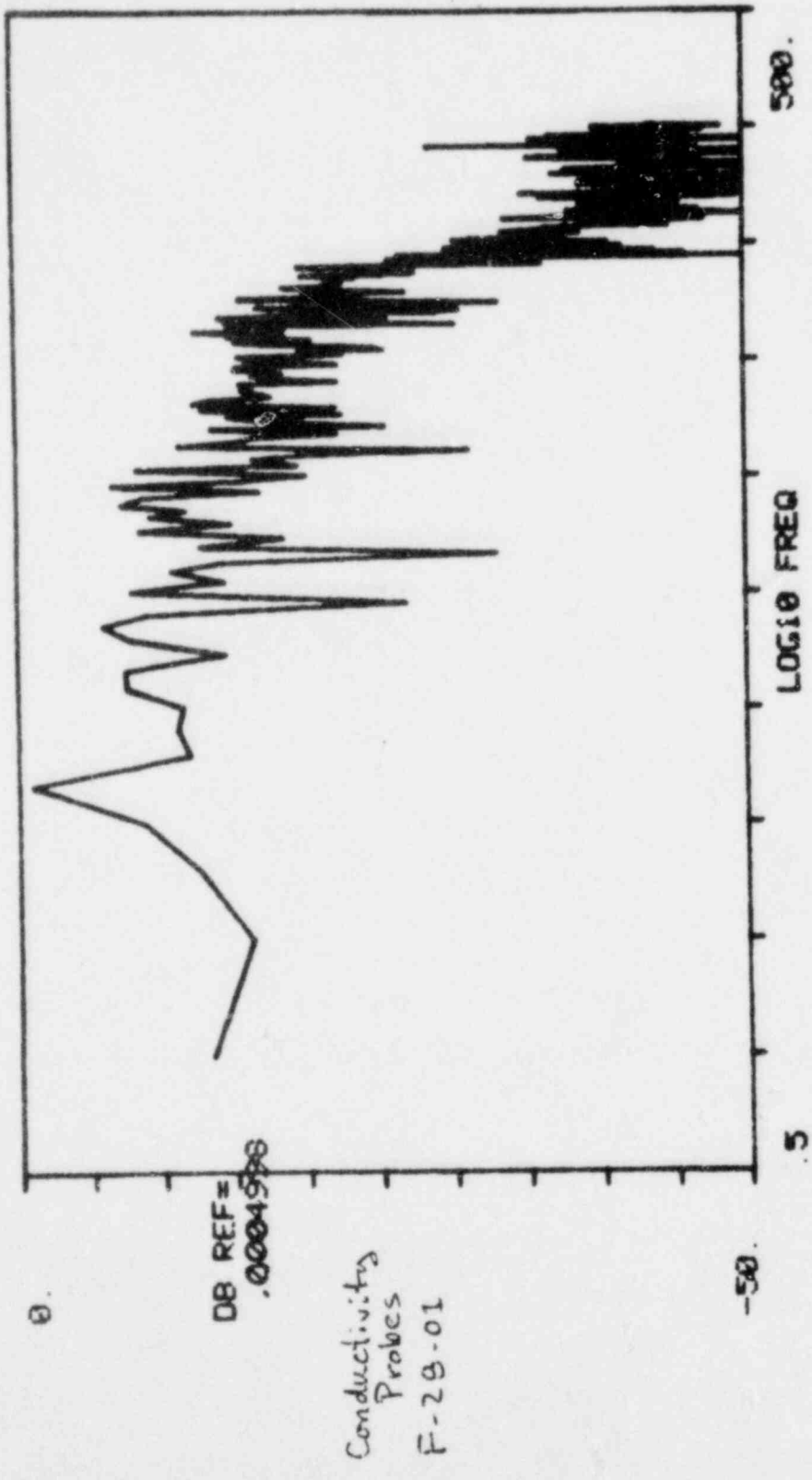

Figure 42 Auto-Spectral Density, Conductivity Probe, F-28-01

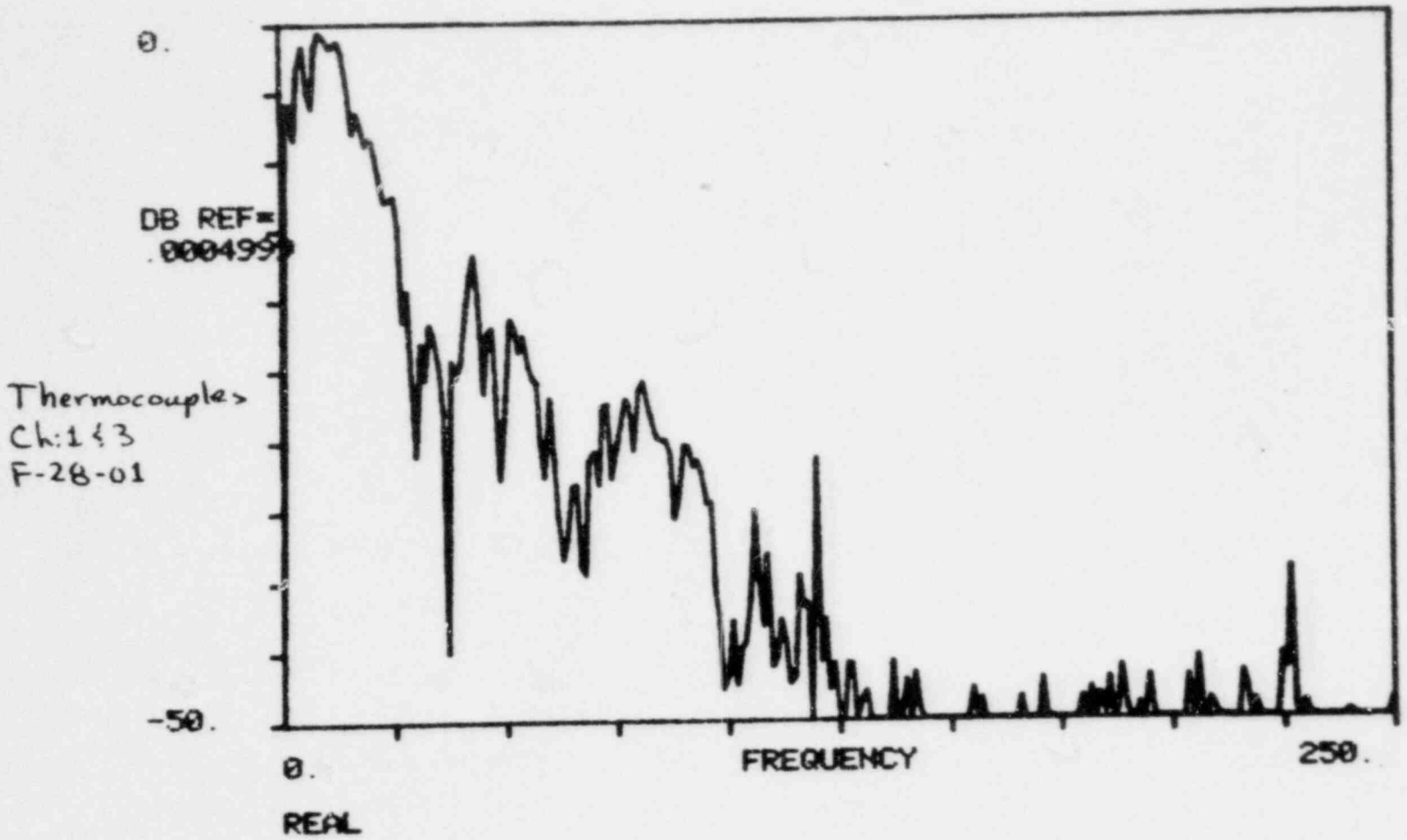

Figure 43 Auto-Spectral Density, Thermocouple, F-28-01, Straight Amplification

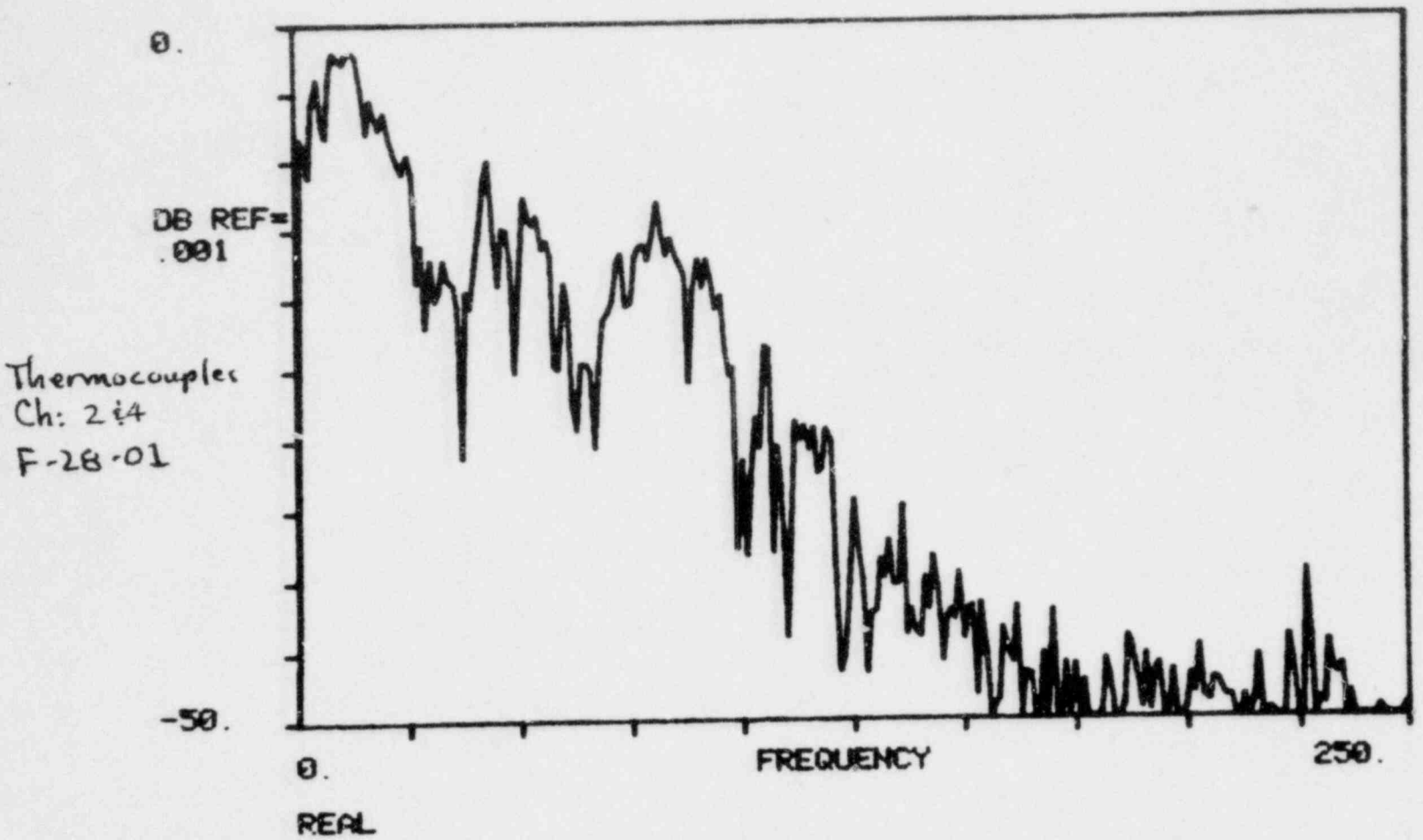

Figure 44 Auto-Spectral Density, Thermocouple, F-28-01, Frequency Compensation

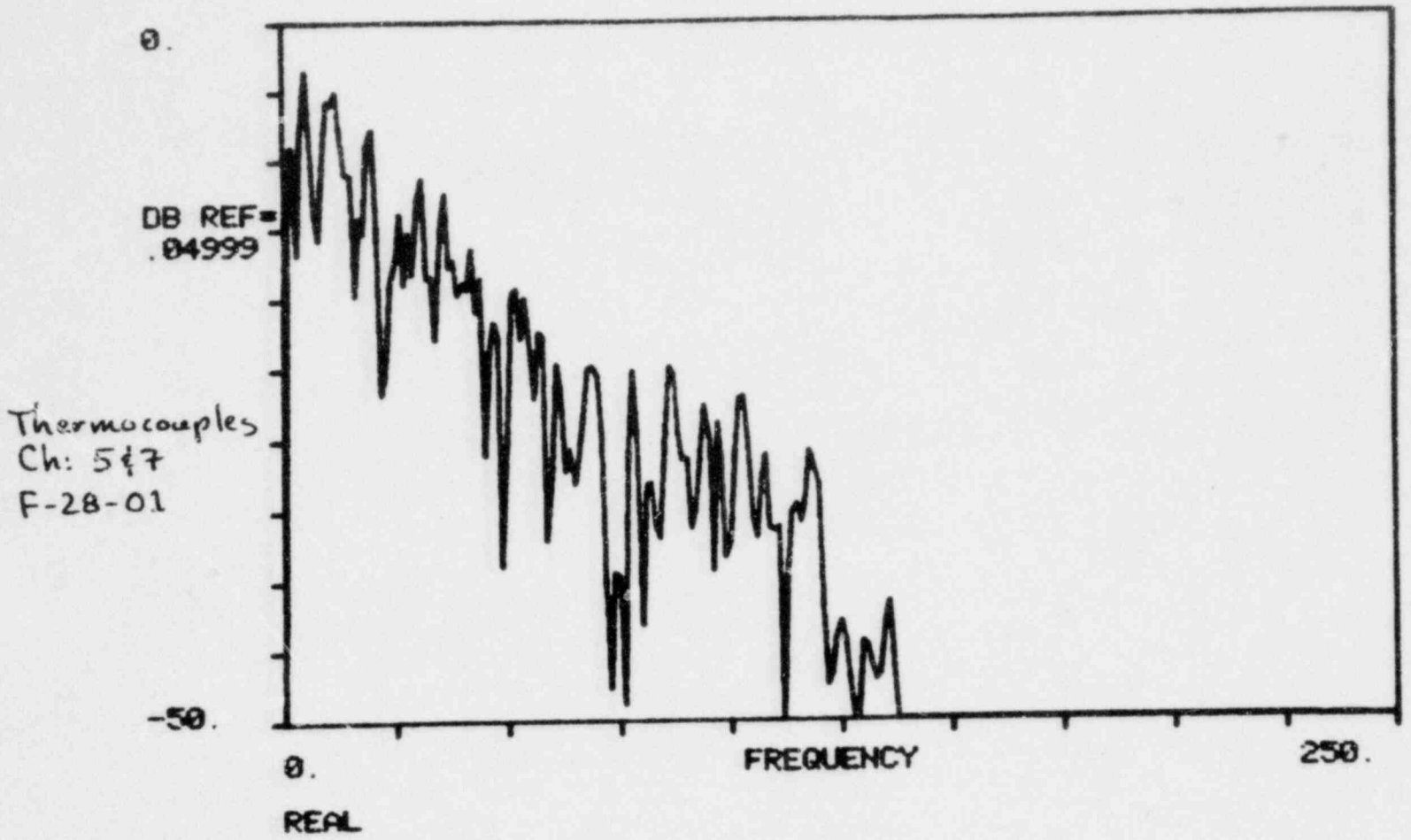

Figure 45 Auto-Spectral Density, Thermocouple, F-28-01, Signal Compression

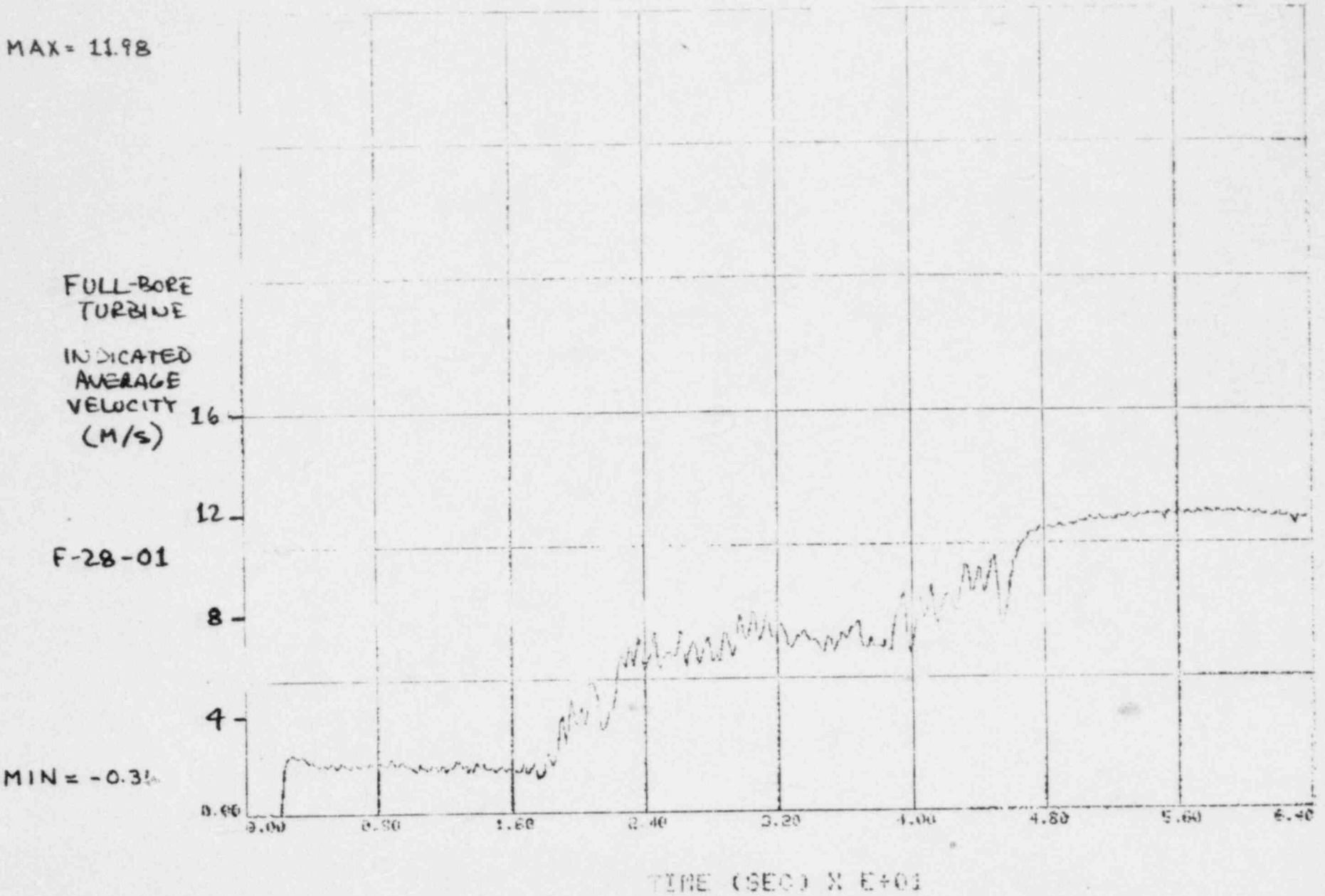

Figure 46 BF Turbine Indicated Velocity, F-28-01

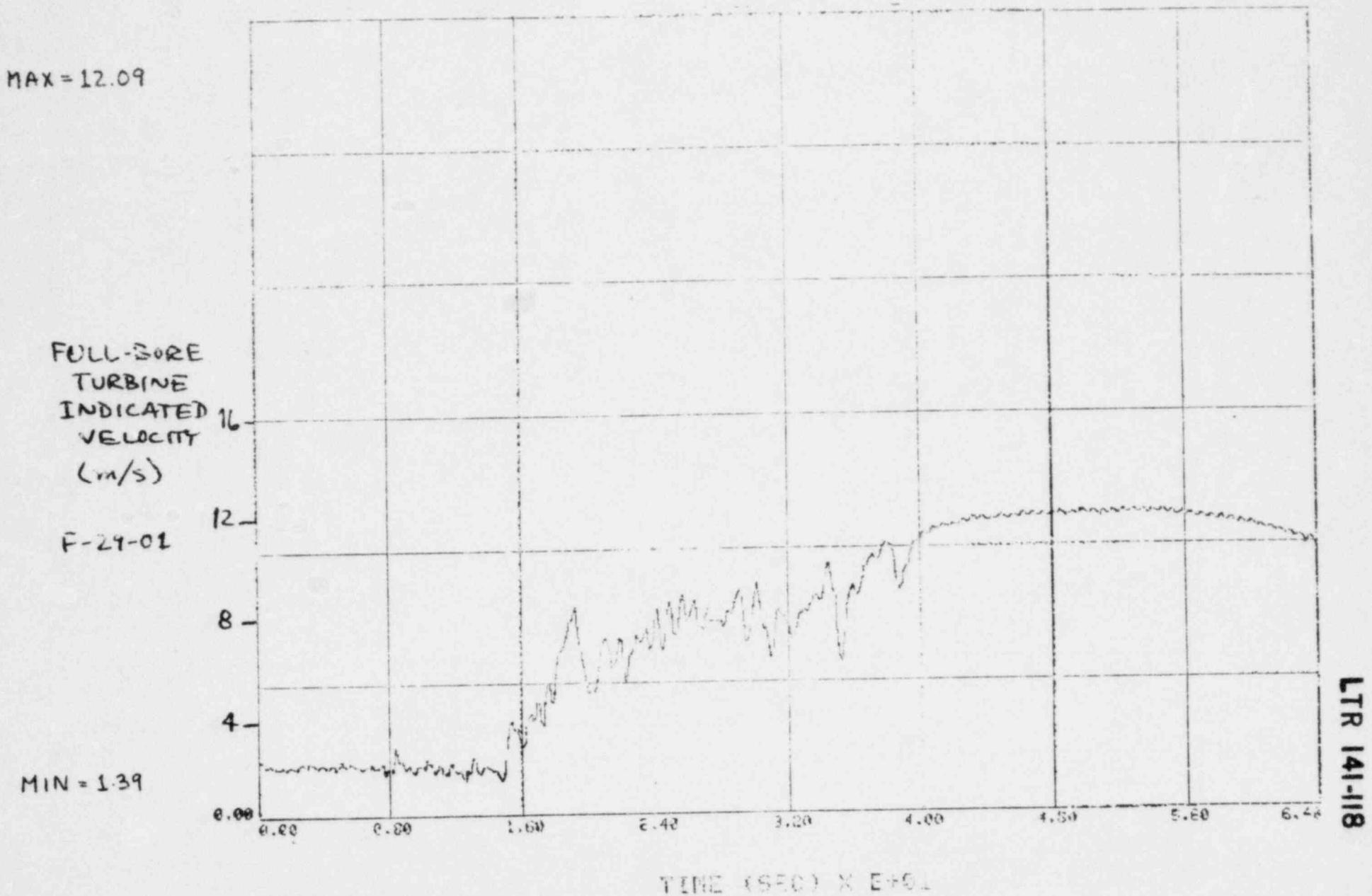

Figure 47 BF Turbine Indicated Velocity F-29-01

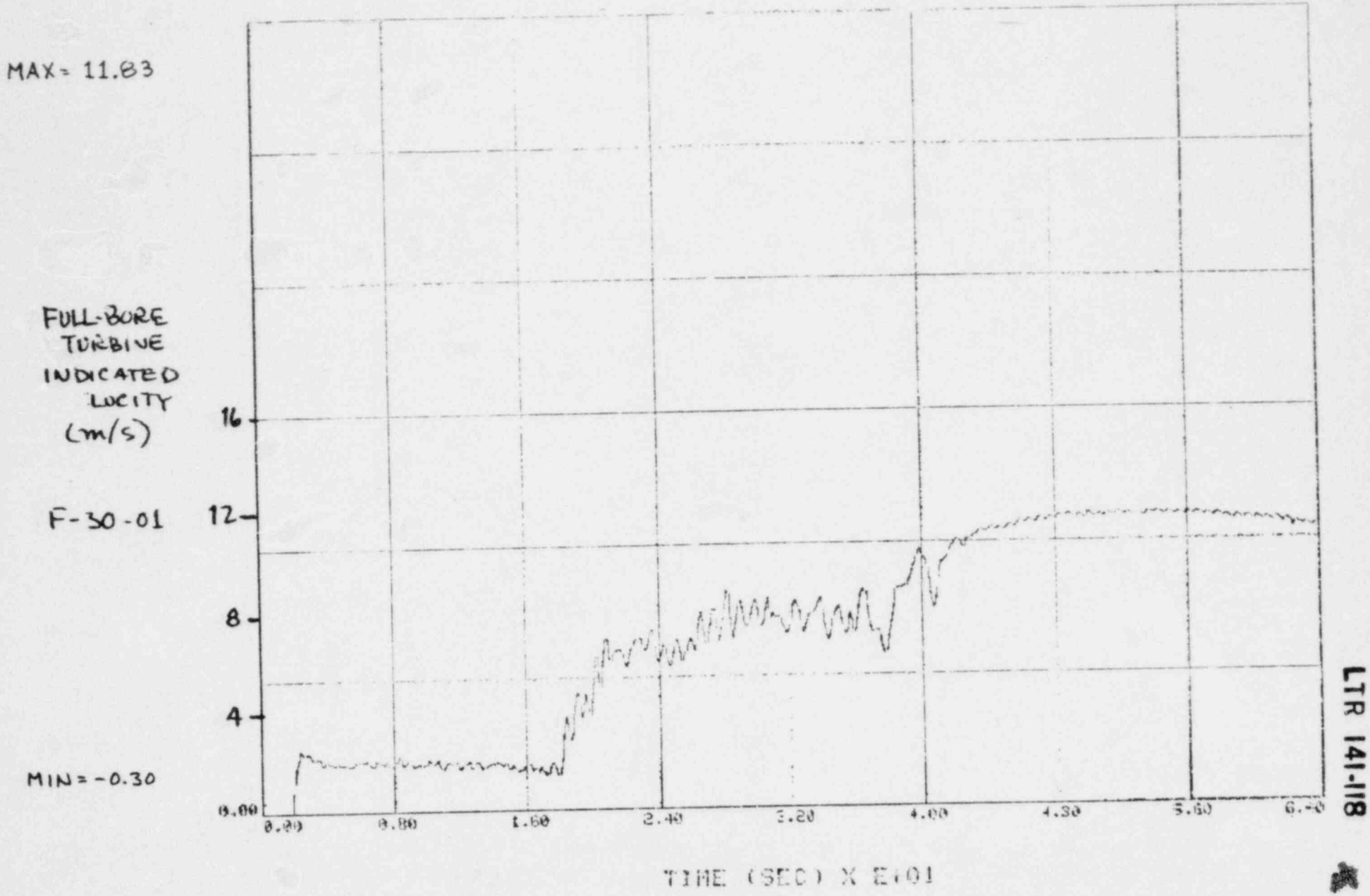

Figure 48 BF Turbine Indicated Velocity, F-30-01

TABLE I

INTERSENSOR SEPARATIONS

Test	Sensor	Separation (mm)	Insert
P-28-01 P-28-02	Thermocouple Conductivity	279 279	A,B
F-28-01	Densitometer	441	N/A
P-29-01 F-29-01	Thermocouple Conductivity	940 940	B,C
	Densitometer	292	N/A
P-30-01 F-30-01	Thermocouple Conductivity	1219 1219	A,C
	Densitometer	513	N/A

TABLE II

SIGNAL CONDITIONING DESCRIPTION AND REMARKS

U=Upstream Sensor
D=Downstream Sensor

Sensor Type and Channel Designation	Tape Channel No.	Remarks	Test number						
			P-28-01	P-28-02	F-28-01	P-29-01	F-29-01	P-30-01	F-30-01
C-1 Conductivity Probe	6	Shop built electronics; 0.125 mA drive current; 4 KHz reference oscillator frequency	U	U	U	D	D	D	D
C-2 Conductivity Probe	8	Shop built electronics; 0.125 mA drive current; same 4 KHz reference oscillator frequency as Channel 6	D	D	D	U	U	U	U
Thermocouple TC-1	1	Bandpass amplification 0.03 to 300 Hz Gain = 1000	U	U	U	D	D	D	D
	2	Bandpass amplification 0.03 to 300 Hz with Gain = 1000. Frequency compensation circuit.							
	5	Bandpass amplification 0.03 to 300 Hz with Gain = 1000. Additional Krohn-Hite 8-pole bandpass filtering: High-pass = 0.1 Hz; Low-pass = 150 Hz and +20 db gain. Signal compression circuit.							
Thermocouple TC-2	3	Bandpass amplification only 0.03 to 300 Hz with gain = 1000	D	D	D	U	U	U	U
	4	Bandpass amplification 0.03 to 300 Hz with gain = 1000. Frequency compensation circuit.							
	7	Bandpass amplification 0.03 to 300 Hz with gain = 1000. Additional Krohn-Hite 8-pole bandpass filtering: High-pass = 0.1 Hz; Low-pass = 150 Hz and +20 db gain. Signal compression circuit.							
Gamma Densitometer G-1	10	Shop built current-to-voltage preamplifier. Bandpass amplification 0.3 to 1000 Hz with gain = 10. 1/5 attenuation op-amp circuit. (TTF Channel)	U	U	U	U	U	U	U
	11	Shop built current-to-voltage preamplifier. Krohn-Hite 8-Pole low-pass filter to 200 Hz at gain of 0 db. Zero offset compensation op-amp circuit. (Density Channel)							
Gamma Densitometer G-2	12	Shop built current-to-voltage converting preamplifier. Bandpass amplification 0.3 to 1000 Hz with gain = 10. 1/5 attenuation op-amp circuit. (TTF Channel)	D	D	D	D	D	D	D
	13	Shop built current-to-voltage converting preamplifier. Krohn-Hite 8-Pole low-pass filter to 200 Hz at gain of 0 db. Zero offset compensation op-amp circuit. (Density Channel)							
IRIG-A	14	Time Reference: Type A, IRIG	NOT APPLICABLE						

APPENDIX A

Conductivity Probe Electronics

The conductivity probe driving source, signal detector and signal conditioner are constructed as a single self-contained unit according to the schematic in Figure A-1. A block diagram (see Figure A-2) illustrates the basic internal features of the unit. The unit is capable of servicing up to four individual probes simultaneously.

The conductivity probe electronics employs a alternating dual-polarity square-wave current to stimulate the probes. The voltage developed at a probe is a function of the conductivity of the two-phase fluid present at the probe. This voltage is then synchronously detected and rectified, sample and finally amplified before being presented to the channel output.

The frequency of all the internal synchronized process is derived from that an external reference oscillator connected to the internal master control clock through an interface unit. This oscillator interface is merely a zero-crossing detector so that the unit will accept reference oscillator waveforms of different types if necessary. The master control clock serves to divide the external reference frequency, f_{ref}, by 10 to obtain a very stable internal control frequency, f_c, that is,

$$f_c = f_{ref}/10 \qquad \text{(A1)}$$

The probe drive frequency is equal to that of the internal control frequency. The probe drive current is a dual-polarity current whose magnitude is selectable over five octaves from a minimum of 0.125 mA to a maximum of 2.0 mA.

The signal sampling portion of the electronics is connected to the probe through a high input-impedance voltage follower in order to prevent its loading the probe. The synchronous inverter functions basically as a

rectifier. It is an amplifier which has a gain of +1 during the positive half-period of the drive current and a gain of -1 during the negative half-period. The gain reversal is accomplished by means of an analog switch referenced to the probe drive frequency. A balance control is included to compensate for any baseline offset between the positive and negative gain half-periods.

The timing of the sample-and-hold operation is governed by the master control clock. The master control clock divides the period of the internal control frequency into ten equal segments, five in the positive half-period of a cycle and five in the negative half-period. Sampling during any half-period takes place at the start of the fifth segment of the half-period. The activated sampling window can be varied between 15 and 20μs wide. Two single-pole switches permit the selection of sampling during either the positive or negative half-period only, or during both the positive and negative half-periods. In any case the sampled value is held until its next update.

The sampled signal is either ac coupled through a high-pass filter with a 0.25 Hz cut-off or dc coupled to a final adjustable gain amplifier. The output of this stage is finally low-pass filtered with a 1.7 KHz cut-off before being presented at the output connection.

The relationship between the output sampling frequency, f_s, and the frequency of the external reference oscillator is

$$f_s = \begin{cases} 0.2\ f_{ref}, & \text{for both positive and negative sampling} \\ 0.1\ f_{ref} & \text{for either positive or negative sampling alone} \end{cases}$$

The maximum resolvable frequency according to the Nyquist sampling theorem is one-half of the sampling frequency. Thus, the maximum resolvable frequency is

$$f_{max} = \begin{cases} 0.1\ f_{ref}, & \text{both positive and negative sampling} \\ 0.05\ f_{ref}, & \text{either positive or negative sampling alone.} \end{cases}$$

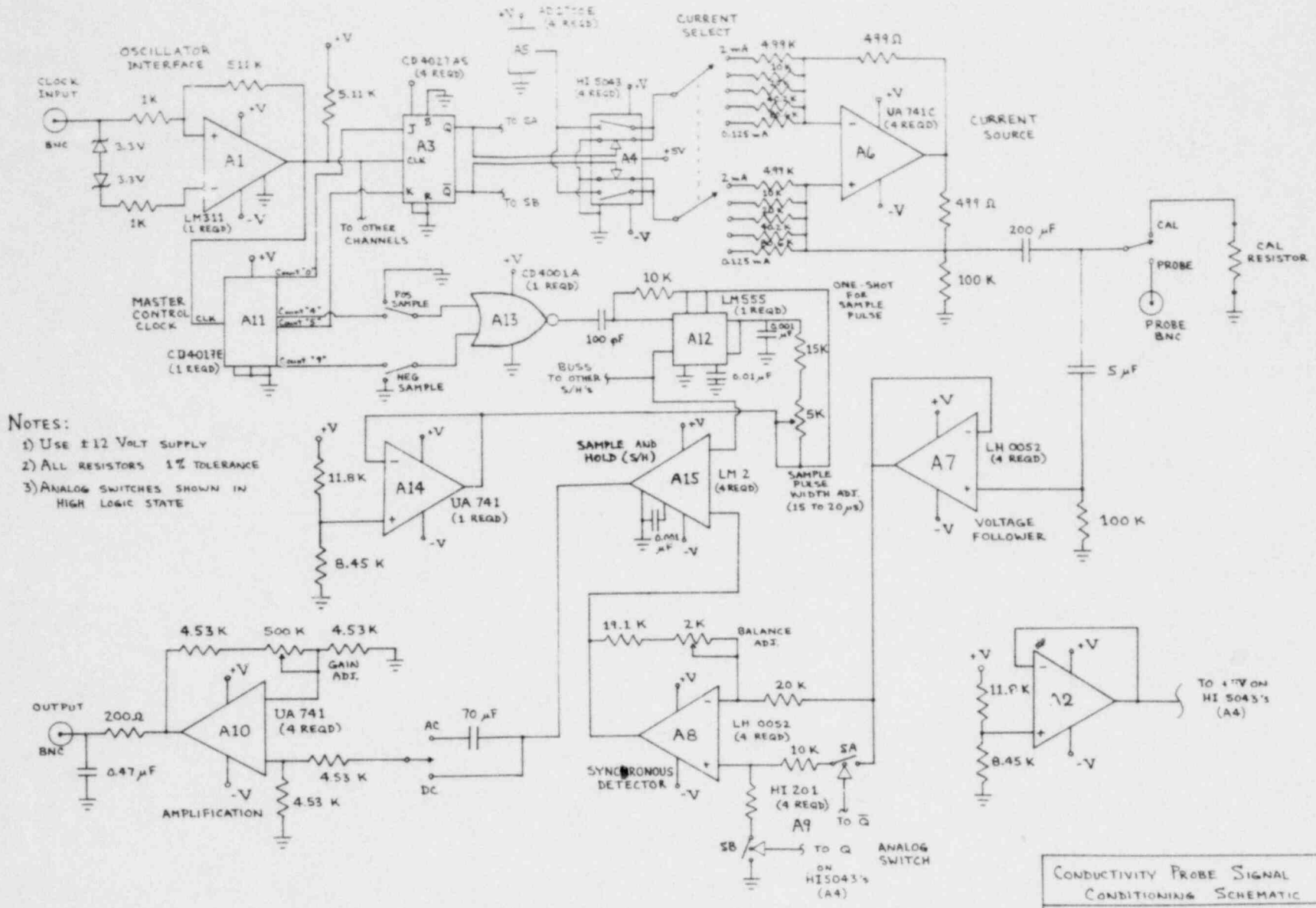

NOTES:

1) USE ±12 VOLT SUPPLY
2) ALL RESISTORS 1% TOLERANCE
3) ANALOG SWITCHES SHOWN IN HIGH LOGIC STATE

CONDUCTIVITY PROBE SIGNAL CONDITIONING SCHEMATIC	
FOR: A. G. BAKER	
DRAWN BY: JIM LEE	DATE: 8/23/77
PROJECT: TRANSIT TIME FLOWMETER	

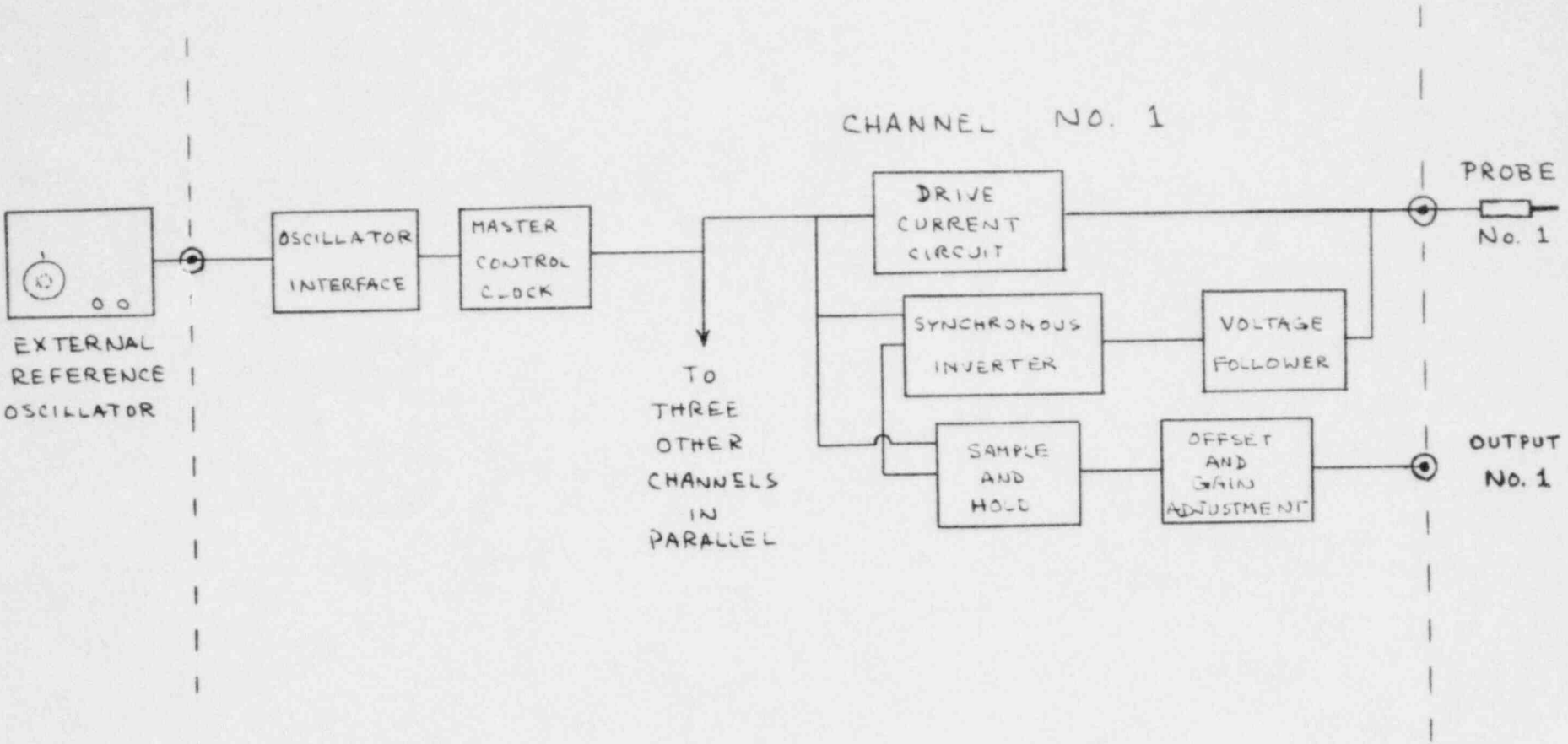

Figure A-2 Conductivity Probe Signal Conditioner, Block Diagram